PhD thesis

Modelling grey-level intensities for smart phones to view medical images

Soni, M.

Modelling Grey-level Intensities for Smart Phones to View Medical Images

A Doctoral Thesis

submitted in partial fulfilment of the requirement for the award of Doctor of Philosophy

from Middlesex University

by

Monalisa Soni

School of Computer Science

Middlesex University

June 2023

Abstract

This research concerns with the modelling of grey level intensities for mobile phones in order to view medical images in greyscale using different mobile phones.

While medical image format of DICOM employs a Greyscale Standard Display Function (GSDF) that describes the relationship between luminance level and display intensity values, medical images that have high contrast depicted in a computer monitor may not present as clearly in a smart phone. This is because a smart phone has a limitation of resolution with a small screen and cannot be calibrated to a specified grey level setting. This research is to investigate the difference between a computer monitor and a mobile phone with regard to depicting medical images.

The International Commission on Illumination (CIE) has recommended a colour appearance model CIECAM16 that can predict a colour appearance under many viewing conditions, e.g. an LCD display, as accurate as an average observer from human colour vision point of view. In this research, this colour appearance model is applied and enhanced in an attempt to predict grey-level intensity for mobile phones so that an image will appear near the same as it appears on an LCD monitor. Towards this end, more than ten psychophysical experiments are conducted by 14 observers with normal colour vision to study human perception on both an LCD monitor and mobile phones. It has found that for iPhone6S, middle range grey samples appear much brighter than on the LCD display that is calibrated to D65. The enhancement hence takes by modifying c value of CIECAM16, representing ambient colour compensation. It appears that when $c = 0.59$, the model of CIECAM16 correlates the best with observers' estimations. Then experiments on visual estimation are carried out to match the original x-ray chest images with COVID19 displayed on the LCD with those displayed on a phone before and after enhancement. The results show that the enhanced images by CIECAM16 with $c = 0.59$ appear to be much closer to the original in terms of COVID19 specific features, implying the importance of this work. Future work includes containing colour images (e.g. oesophagus videos, retinal images, etc.), more mobile phones in additional of iPhones and more test samples (currently with 20 grey samples). It is concluded that iPhones can be applied to view medical images without compromising key features.

Acknowledgements

I am in debt to my supervisor Prof. Xiaohong Gao for her constant guidance, support and encouragement throughout this project, in particular her constructive criticism and assistance in writing of this thesis, which otherwise would be impossible. Her way of understanding the need of students and fulfilling with vital involvement is appreciated.

I would like to express deepest appreciation to my second supervisor, Dr Shahedur Rahman. His extensive knowledge and understanding nature inspired me in whole tenure of this research and I have always been enjoying discussing all scenarios with him. His invaluable suggestions are always inspiring and motivates to look forward.

Many thanks to other fallow researchers for sharing their experiencing and motivating each other constantly. I am so grateful to students who helped me in data gathering doing experiments and achieving the best results. The technician team of Middlesex University has always been helpful providing me peaceful location for performing experiments and equipment.

My sincere thanks and gratitude go to my pillars, my parents for their encouragement, love and support all time. All my love to my elder sister, Vidhi Soni who shared all my ups and down throughout whole PhD study.

This work is supported by the School of Computing Science, Middlesex University. Their support is gratefully acknowledged.

Abbreviations utilised in the thesis:

Abbreviation	Full name
CIE	Commission Internationale de l'Eclariage
DICOM	Digital Imaging and Communication in Medicine
GSDF	Grey Scale Display Function
JND	Just noticeable difference
LCD	Liquid crystal displays
ICC	international color consortium
PACS	picture archival and communications system
CIECAM	CIE Colour appearance model
CT	Computerised Tomography
MR	Magnetic Resonance
PET	Positron Emission Tomography
HSV	Human visual system
AAPM	American Association of Physicists in Medicine
IEC	International Electrotechnical Commission
FDA	US Food and Drug Administration
ACR	American Carbon Registry
ISO	International Organization for Standardization
SPD	Spectral Power Distribution

List of publication:

1. Soni M., Raman S., Gao, X., Medical image enhancement for mobile phone viewing by applying colour appearance model CIECAM, 15th Congress of the International Colour Association (AIC2023), Chiang Rai Thailand, 28Nov - 2Dec 2023 (*to present*).

Captions of Figures

Captions of Tables

Table of Contents

Chapter 1. Introduction

In 2022, US Food and Drug Administration (FDA) (FDA (2022)) has issued its policy for device software functions an mobile medical applications, paving the way to apply smart phone viewing medical images (FDA (2011)). A smartphone is a mobile device with more advanced computing capability and connectivity than what basic telephone features, offering functionalities of typical personal assistance, digital camera, GPS navigation, media player in addition to calling and receiving services. It has become commonplace since the late 2000s. For example, in the UK, at the start of 2022, there were 71.8 million mobile connections, 4.2 million more than the UK population with a prediction that 95% will be using a smartphone by 2025 (Hiley, 2023).

One of the by-products of smart phone remains in the field of digital photography. It appears that more photographs are taken by using smartphones than normal cameras these days. For example, among few other phones which are being used in this study, the Apple iPhone 13, iPhone 10, iPhone 6S and iPhone 5S (in descending order of releasing dates) are with the most popular camera (Gottsegen, 2017). As a direct result, large amount of money is being invested by mobile developers to create photo apps in an attempt to satisfy the demands of colour satisfaction and accuracy. This easily indicates that colour is a key factor in mobile phones. A digital image is represented in a RGB colour space when it is being displayed on a monitor or a mobile phone screen. In an 8-bit form, the maximum range of RGB are within 0 and 255 regardless of physical natures of a displaying device. Hence the same Red, Green and Blue values in one device usually do not present the same appearance on another device, which is the dependency characters of RGB colour space. While a colour monitor is usually equipped with a calibration feature to set the colour range under a specific light condition, e.g. D65 (average daylight), a mobile phone does not have the light function, which casts a doubt that if an image displayed on a phone presents all the needed

information the image carries. This research investigates this important viewpoint with the application to medical images.

Although mobile phone is not the standard device to view medical images, in some cases, e.g. in an emergency situation in an ambulance, there is a need to obtain all related information, including imaging before a clinical decision is made. Hence displaying medical images correctly plays a vital role in real life.

In medical field, recent advancement in imaging tools have revolutionized modern medicine by assisting clinicians in decision making on diagnosis, treatment, and prognosis. To ensure that acquired images are providing consistent, repeatable, and interpretable information, a standard format, DICOM, standing for Digital Imaging and Communications in Medicine, is used for communication and management of medical imaging information and related data.

In addition, a DICOM Grey-scale Standard Display Function (GSDF) is introduced to safeguard image displaying monitors, having the correct resolution and proper colour contrast for human eyes to interpret image accurately. GSDF introduces a unit of just noticeable difference (JND) to measure contrast sensitivity of the human visual system (HVS) (Webster, 2022) by specifying the precise display luminance that should be produced for a given input value. The practical result of using the GSDF is that different displays can be set to have the same Grey-scale response (for consistent presentation of images), which may enhance the improvement of the perceptual linearity of a display over other calibration settings and thus better match the capabilities of the HVS, resulting in consistent diagnostic performance across varying display devices. GSDF is mainly for calibrating black and white devices for viewing grey-level medical images. In practice, grey level are employed (to be details in Chapter 4) to ensure that each shade can be visible to the human eye when a device is at DICOM GSDF standard. For a colour device, all devices should be calibrated

into the same viewing environment, e.g. D65 (average daylight) in addition to view DICOM grey-level patterns. This is to ensure the consistence cross all colour monitors. To calibrate a colour monitor (to be detailed in Chapter 5) environment, all the displays can be set into the same luminance levels (e.g. D65) by adjusting the level of Red (R), Green (G) and Blue (B) colour levels using a software and a sensor, in this study, ColorMunki. As a result, these adjustable displays are classified as Primary displays that can be applied for clinical decision-making processes.

Because of the prevalence of smart phones, mobile platforms, usually referred to as secondary displays for medical images as approved by the U.S. Food and Drug Administration (FDA) (FDA, 2022), can provide ease of access in distributing images and constructing reports to be sent to related clinicians. In particular, mobiles tend to be more useful when communicating with patients at their bedsides to provide non-diagnostic consultations.

While all the current colour monitors can be calibrated into any desired luminance levels, most smart phones do not facilitate this function, i.e. their R, G, B levels cannot be adjusted apart from the level of brightness. Hence, a software system is in need to manually enhance the concerned images to a certain contrast level should a phone miss any brightness range.

Hence the **aim** of this project is to investigate the feasibility of using mobile phones to view medical images without losing key features. Towards this goal, the following **objectives** are to be met:

- Studying human perception perceiving grey-level samples under D65 on an LCD monitor
- Studying human perception perceiving the same group of grey-level samples on mobile phones

- Determining the difference between monitor and phones based on CIE tristimulus values of (x,y,Y).
- Determine the difference of subject estimations between monitor and phones
- Modelling mobile phones to enhance lightness contrast for viewing grey-level medical images built upon CIE colour appearance model CIECAM16
- Evaluating developed lightness model for viewing x-ray images with COVID-19 disease.

The structure of the report is organized as follows. Chapter 2 highlights of contribution of this study. Literature Review and previous work is given in Chapter 3, which details the background, standard and the current progress in the field of colour science and monitor calibration. Chapter 4 introduces the international standards with regard to viewing medical images on various displays.. In Chapter 5, methodology employed in this studied is described, including conducting psychophysical experiments on both a colour monitor and mobile phones. Data Evaluation and Observation study is also mentioned in this chapter 5. Chapter 6 describes the experimental results obtained on the LCD monitor, whereas Chapter 7 details the similar results conducted on mobile phones. Modelling these data for mobile phones takes place and is addressed in Chapter 8. Finally the work is discussed, concluded and in Chapter 9 together with future work directions.

Chapter 2. Overview of the Study and Highlight of Contributions

While a colour monitor can be calibrated to any specified viewing condition, e.g. D65 (average daylight), smart phones don't support this function. Due to the nature of widespread usage, portable and convenience, it is ideal to apply mobiles to view medical images, especially in an emergency situation (e.g. in an ambulance). Hence the **aim** of this project is to investigate the feasibility of using mobile phones to view medical images without losing key features. Towards this goal, the following **contributions** have been made:

- Establishment of a lightness model for iPhones built upon CIECAM16
- Conduction of visual estimation experiments confirming chest x-ray images appear clearer when viewing on a phone with enhanced with this developed model than without
- Confirmation of feasibility of using iPhones to view chest x-ray images for inspecting COVID19 features.

2.1 Overview of the project

The Figure 2.1 outlines the study conducted in this project. It starts with the subjective estimation of grey samples displayed on a LCD monitor and on mobile phones of varying models. Then modelling of lightness for mobile phones takes place to ensure the same image appears similar when viewed on both LCD and mobiles. Evaluation is conducted for chest x-ray images to see whether enhanced images on phone appear clearer than their counterparts without enhancement. The model for mobile phone lightness is established based on the standard colour appearance model by Commission Internationale de l'Eclariage (CIE), CIECAM16.

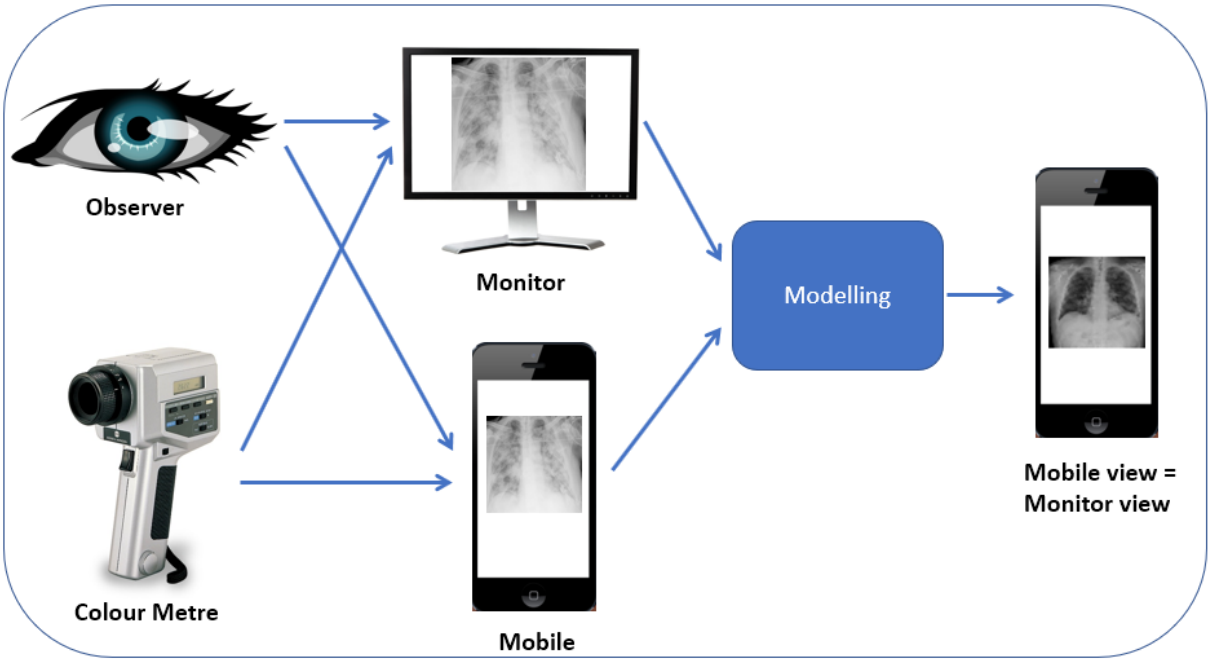

Figure 2.1. Overview of this study.

2.2 Overview of psychophysical experiments by observers

In total, over 90 psychophysical experiments are conducted by observer, generating 6210 data. They are performed by subjects with normal colour vision. In addition, 7110 colour measurements take place using a colorimeter of Minolta CS-100A as given in Table 2.1. Twenty grey samples are selected for experiments whereas 30 colour samples are for observer training.

Table 2.1. Summary of experiments and measurements conducted in this study, where $no = number$.

Display	**Monitor**	**iPhone6S**	**Motorola**	**Samsung**	**iPhoneX**	**iPhone 13 Pro**	**Total**
Observer	25	15	9	10	10	5	**74**
No experiments	30	15	10	15	10	10	**90**
No of test sample	30	30	30	30	30	30	**180**
Measurements (x,y,Y)	2700	1350	810	900	900	450	**7110**
Estimations obtained	1800	1350	810	900	900	450	**6210**

Chapter 3. Literature review

This Chapter reviews the general theory of colour science, background information of medical images and the role of colours in image.

3.1 Overview of Colour Science

Colour is a visual experience generated primarily by three components, a visual system, a colour object and a light (Sangwine (1998), Davis (1998), Roy (2000)). Such as an apple, a light that shines part of the apple and a human eye to visualise the object. The light source generates light illuminating an object, some part of the object to eye through which it helps brain to observe the colours.

As a part of the human vision system that involves a light source, an object and a brain processing system, colour vision is the ability of the eye to allow us to distinguish different colours (made of different colour waves) through three colour cells: Red, Green and Blue. Accurate colour measurement requires reliable light sources, in order to make objects react to the components of the spectrum, and therefore colour vision properties of human observers involved in the measurement process. In 1666, Newton found that white light consists of a visible spectrum which includes all the visible colours ranging from Red, Orange, Yellow, Green, Blue to Violet. These colours are parted in the electromagnetic spectrum with energy in the range of 380nm to 780nm. Human vision detection is also possible between this colour range which is also known as '*visible light*' (Lamb (1995), Hardin (1988), Nassau (1997), Falk (1986), Lee (2005), Wyszecki (1982), Webster (2000), Shevell (2003), Hunt (2004), Speranskaya (1959)).

3.2 Image Processing in Medical Images

Medical images are concerned with sensitive information related to patient disease. Normally medical digital images are converted into digital image from physical report (Kagadis (2013), Varma (2012)). A digital image (I) is described in a 2D discrete array and is divided into M rows and N columns. The intersection of a row and a column is termed as a pixel, i.e. **pi**cture **el**ement. Therefore, a whole image is represented by a rectangular array of picture elements called pixels. The pixel value assigned to the integer coordinates $[m, n]$ with $\{m = 0, 1, 2 \ldots M - 1\}$ and $\{n = 0, 1, 2 \ldots N - 1\}$ can be described as $I[m, n]$ and usually is digitized to [0, 255] for monochromatic images. An example of image is shown as below.

Figure 3.1 illustrates a Monochromatic Grey image. Value of pixel I $[m, n]$ is between $[0, 255]$. The whole image represents an array of pixel values.

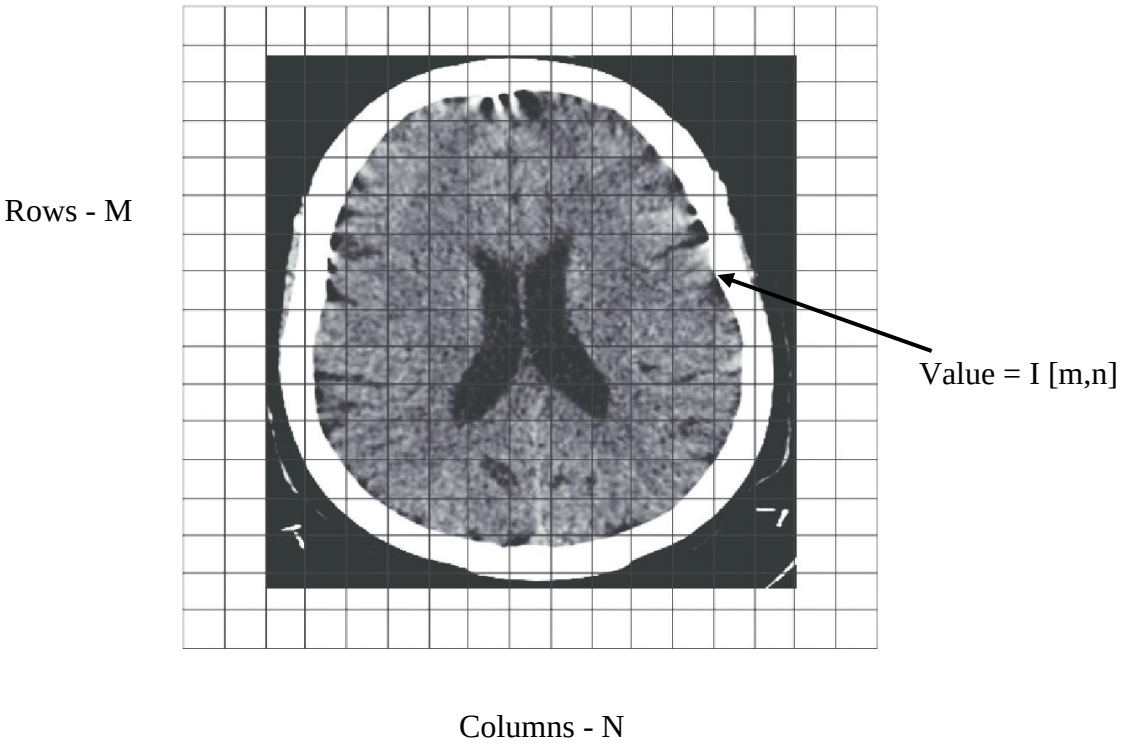

Figure 3.1. An illustration of the pixel concept of digital medical images (Ramakrishnan (2016)).

Radiologic images tend to be grey colours.

3.3 Colorimetry

In 1931, the International Commission on Illumination (CIE) adopted a system of colour specification which has lasted to the present time, known as the CIE system of colorimetry. In this system, a colour is defined by a set of X, Y, Z values, called tristimulus values. Two samples with identical material should be judged as a exact match when their tristimulus values are the same.

In colorimetry, a system of colour specification has been developed to relate certain stimulus characteristics to the calculated response of a standardised average observer. In any given set of

viewing conditions, a colour stimulus may be matched by a unique mixture of three appropriately different colour stimuli.

In 1666, Newton found that the white light consists of visible spectrum which includes all visible colours ranging from red, orange yellow, green and blue to violet. Based on the experimental facts of Newton's famous experiments, the road for colour investigation was open for progress. Now, scientists have found that colour is part of Electromagnetic spectrum with energy in the range of 380mm to 780mm wavelength as illustrated in Figure 3.2.

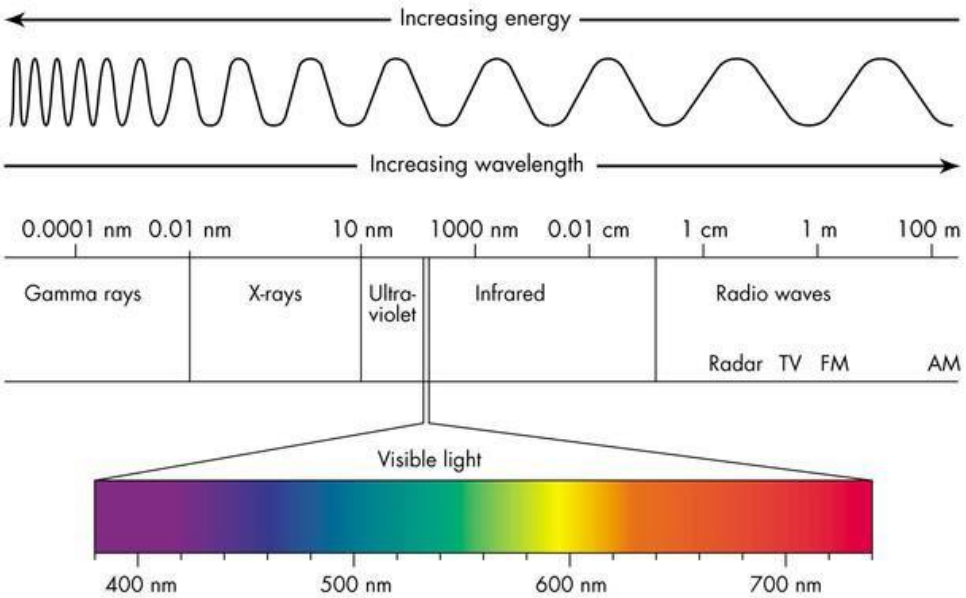

Figure 3.2. Electromagnetic Spectrum (Taylor (1962)).

Colour is the perceptual result of light, object and eyes, which is demonstrated in Figure 3.3. The light source generates light illuminating an object. Some part of the spectrum of the light is reflected from the object and is subsequently measured by an observer such as our light-sensitive

eyes or by a colour camera. The measured light is then sent to our brain where the colour of the light is observed. The description above shows that an observed colour contains three essential elements: Light, Object and Observer.

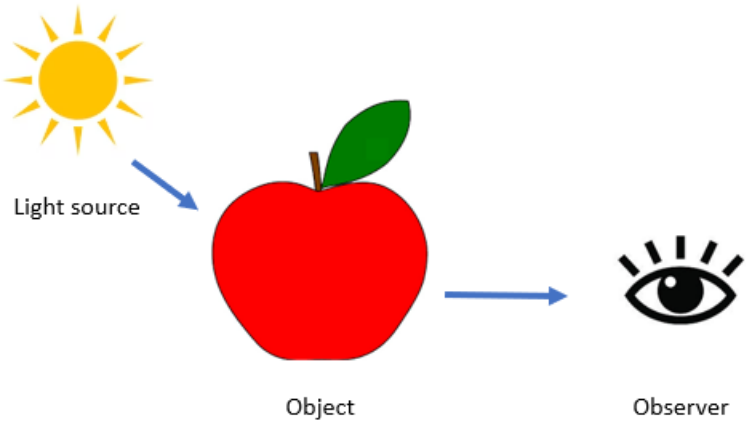

Figure 3.3. Essential elements for colour perception (Young (1802), Hering (1964)).

3.3.1 CIE Standard Sources and Illuminants

A light source is a real physical light, whose spectral power distribution can be experimentally measured. The main light source is the Sun. In addition, there are number of artificial light sources including fluorescent lamps, or by heating up materials. There are two ways to characterise a light source. One is to use a light SPD (Spectral Power Distribution). SPD is the amount of radiant power at each wavelength represented by λ of the visible spectrum and donated by P(λ). The other common term to characterise light sources is Colour temperature.

Colour temperature corresponds to the temperature of the heated blackbody radiator. The colour of the blackbody radiator changes with the change of temperature. The absolute temperature is measured using K standing for Kelvin. For example, the radiator changes from black to 0 K

(Kelvin) to reed at about 1000K, white at 4500K to bluish white at about 6500K. The colour temperature of the sun may vary during the day time (like reddish at sunrise and bluish at noon) and bases on the weather conditions (sky with or without clouds). The CIE recommended that the average daylight has the colour temperature of 6500K and is denoted by D65 (Judd (1964), Billmeyer (1981)).

Several standard light sources have been recommended by CIE for colour description (CIE (1971)).

One of these, CIE Source A, is a tungsten-filament lamp operating at a colour temperature of 2854 K, while CIE Sources B and C are derived from Source A by passing its light through special liquid filters (the Davis-Gibson filters). Source B, with a colour temperature of about 4870 K, is an approximation of noon sunlight. Source C, about 6770 K, is the light of average daylight. Other light sources widely used in colour matching are the xenon arc and Macbeth 7500 K Daylight, the latter obtained by modifying light from a tungsten-filament lamp with glass filters. The spectral power distribution curves for some of these sources are shown in Figure 3.4 (Hunter (1987)).

When the spectral power distributions were measured, the standard sources A, B, and C were soon defined as standard illuminants A, B, and C by CIE in 1931. An illuminant is defined by a spectral power distribution. It may or may not be possible to make a source to represent it. In 1965 the CIE recommended a series of illuminants to supplement illuminants A, B and C based on the experimental results from the spectral power distribution of natural daylight (Judd (1964)). They represent average daylight over the spectral range of 300 to 830 nm and have correlated colour temperatures between 4000 and 25,000 K. The most important ones are illuminants D65 and D50, having a correlated colour temperature of 6500 K and 5000 K respectively (Henderson (1970)).

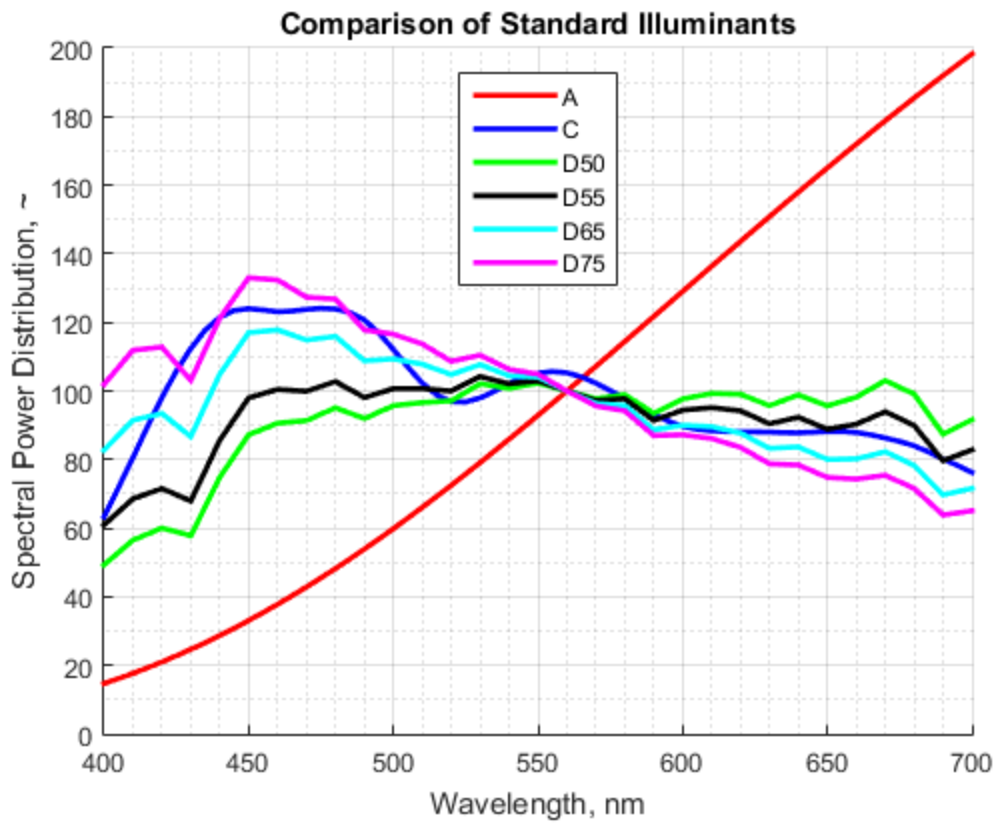

Figure 3.4 Correlation between colour temperature and spectral power distribution (Hunter (1987)).

3.3.2 The Object

Coloured materials are called objects. The colour of an object is defined by the reflectance or transmittance that is a function of wavelength. Reflectance is the ratio of the light reflected from a sample to that reflected from reference white board and is donated by R(λ). Usually, the colour reflected from or passed through an object is the product of the SPD of the illuminant (P(λ)) and spectral reflectance of the object (R(λ)) is computed by the formula of Eq. (3.1).

$$PR(\lambda) = P(\lambda)R(\lambda) \tag{3.1}$$

3.3.4 *CIE Standard Observers*

The scientific basis for measuring a colour is the existence of three different colour-response mechanisms in the human eye. These three responses come from the colour-receptors functions of visual wavelengths and were standardised and incorporated into the CIE standard observers. The observer measures light coming directly from a light source P(λ) or light which has been reflected from objects in the scene R(λ). The observer can be a colour camera or human eyes. For the human eye, the retina contains two different types of light sensitive receptors – Rods and Cones. Rods are more sensitive to monochromatic light and are responsible for vision in twilight. Cones are responsible for colour perception and consist of three types of receptors sensitive to Long (Red), Middle (Green) and Short (Blue) wavelengths. The response of these three cones with wavelength is shown in Figure 3.5 below (Badano (2015)).

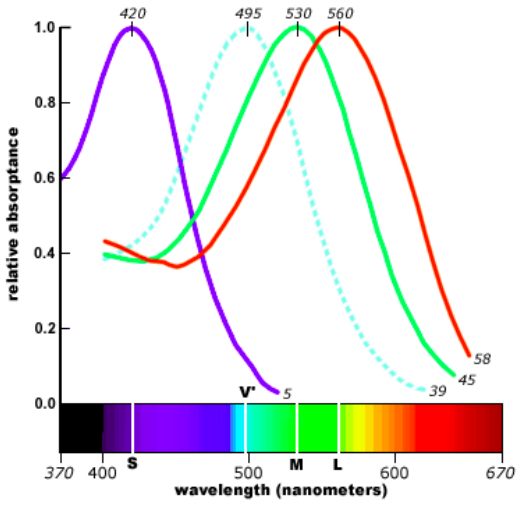

Figure 3.5. Colour cones with wavelength (Helmhotz (1924), Wright (1964)).

Since the sensation of a human observer cannot be measured by an objective instrument, experiments need to be conducted to measure human observers' spectral sensitives to colours. The

observers are asked to match a test light, made of one single wavelength, by adjusting the energy levels of three separate primary lights which are Red, Green and Blue recommended by CIE.

These functions were derived using the experimental results obtained by 10 and 7 observers in Wright's and Guild's investigations respectively. Wright's and Guild's results were in such a good agreement that the CIE (1931) was able to take the mean results as defining the response of an average observer. The experiments leading to the 1931 CIE standard observer were performed using only the fovea of human eye, which covers only about a 2^o angle of vision. Hence the CIE 1931 standard colorimetric observers are also referred to as 2^o CIE standard observer (CIE (1971)) which should be applied when an object subtends a viewing angle of less than 4^o.

At each wavelength the amount of energy was recorder for the three primary colours. The results of this matching are called *Colour matching functions*, usually denoted as $\bar{x}(\lambda)$, $\bar{y}(\lambda)$ and $\bar{z}(\lambda)$ as presented in Figure 3.6. Also these colour matching functions can be treated as colour response of the eye. The tabulated numerical values of these functions are known collectively as the CIE standard observer.

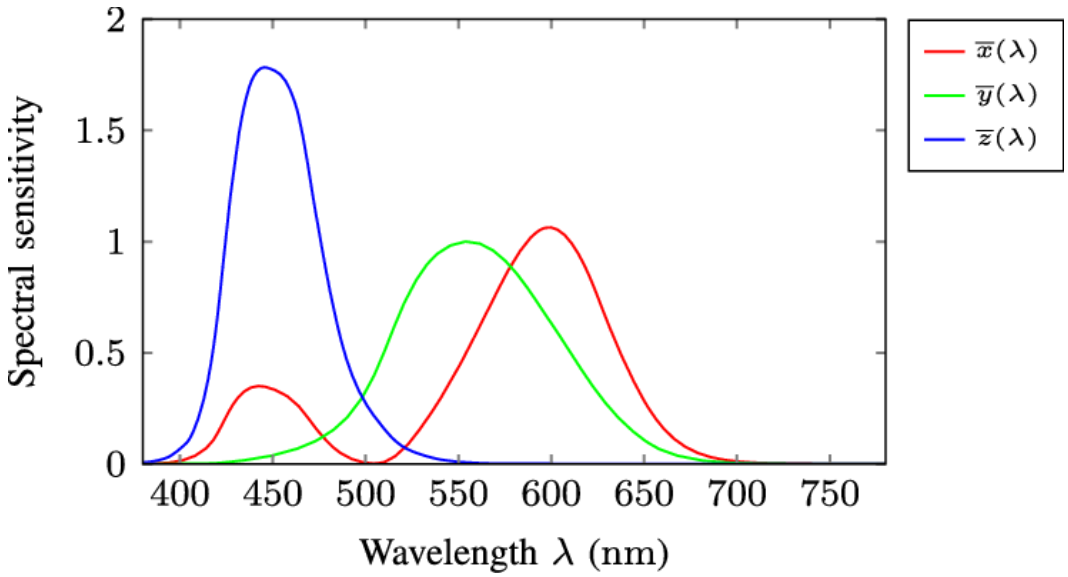

Figure 3.6. Colour matching function for human (Hunt (1987)).

In conclusion, the colour can be measured as a vector of three measurement $\rho = [X, Y, Z]$ given by Eqs. (3.2) to (3.4), which are defined as CIE tristimulus values.

$$X = \int_{\lambda} P(\lambda)\mathrm{R}(\lambda)\bar{\mathrm{x}}(\lambda)\mathrm{d}\,\lambda \tag{3.2}$$

$$Y = \int_{\lambda} P(\lambda)\mathrm{R}(\lambda)\bar{\mathrm{y}}(\lambda)\mathrm{d}\,\lambda \tag{3.3}$$

$$Z = \int_{\lambda} P(\lambda)\mathrm{R}(\lambda)\bar{\mathrm{z}}(\lambda)\mathrm{d}\,\lambda \tag{3.4}$$

Where λ denotes wavelength ranging from 380nm to 420nm, ρ (λ) is the spectral power disturbance of illuminant, R(λ) is the spectral reflectance or transmittance factor of the object depending on whether an object is reflective or transmissive medium and $\bar{x}(\lambda), \bar{y}(\lambda), \bar{z}(\lambda)$ are colour matching function of human eyes.

In some industry applications, colour matching functions for viewing large fields are required (Jacobson (1948)). In 1964 the CIE recommended a new standard observer to supplement the use of the 1931 observer in an effort to obtain better correlation with visual perception for large samples, covering an angle of viewing field of more than 4°. This is called the 1964 CIE supplementary standard observer or 10° CIE standard observer which was based on the experimental work conducted by Stiles and Burch (Stiles (1959)) and Speranskaya (Speranskaya (1959)) in 1959. Their experiment employed a total of 67 observers using mixtures of monochromatic lights, matched fields of 10° angular subtense. Figure 3.7 shows the actual sample size of a 2° field and a 10° field seen at a normal viewing distance of 50 cm (Billmeyer (1981)).

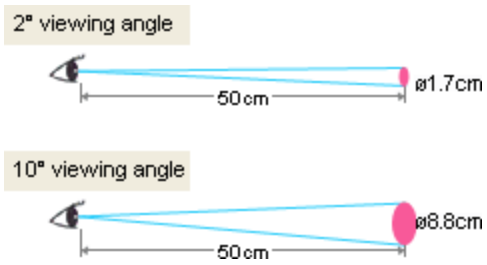

Figure 3.7 CIE 2^o and 10^o viewing angles.

3.4 Colour spaces

The previous section introduced the basic colour knowledge about physical colour properties, three basic elements of observed colours and colour matching functions. However, it is difficult to cope with those physical colour images. Therefore, science uses colour model and spaces to express colour so that digital images can be handled and understood in terms with colours.

The colour space is a mathematical representation, which is three-dimensional orthogonal co-ordinate system. Apart from RGB colour space, there are many ways to represent colours depending on application type. In different colour spaces, the three axes represent different meanings. The digital image can be treated within different colour spaces, which facilitates the operations. The colour spaces that are utilized in medical image representation are described in following sections.

3.4.1 RGB Colour

The RGB colour space is the most used colour space for image processing. This space is the basic one because colour scanners, displays and even cameras are most often provided with direct R (Red), G (Green), B (Blue) signal input and output.

To represent RGB colours, a cube can be defined on the R, G and B axes shown in Figure 3.8. Each colour being described by its components (R, G, B), is represented by a point and can be found either on the surface or inside the cube. All grey colours are placed on the main diagonal of the cube from black (R=G=B=0) to white (R=G=B=max).

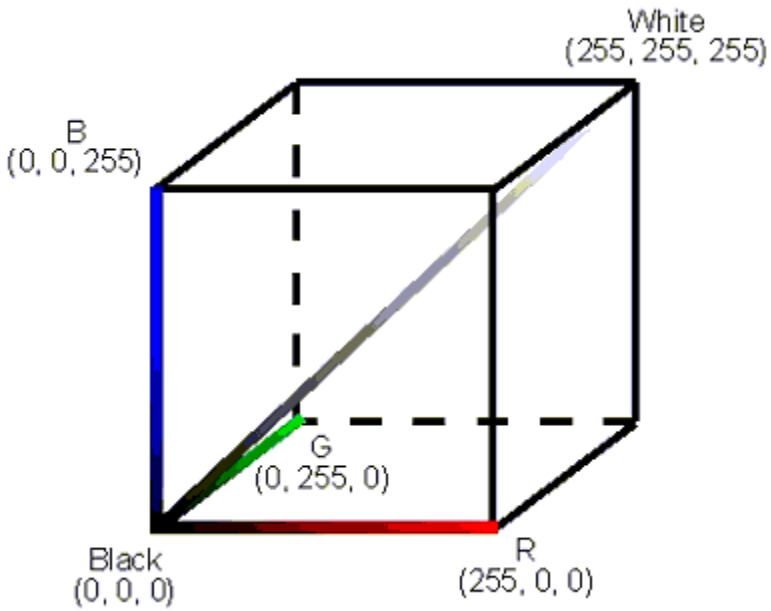

Figure 3.8. RGB Colour Space (Susstrunk (2018)).

It is hard to visualize colour based on R, G and B components. Also, three coordinates are highly correlated. As a consequence of this strong correlation, variation in ambient light intensity have a disastrous effect in RGB by shifting the clusters of colour pixels toward the white RGB = [255, 255, 255] or the black corner RGB = [0, 0, 0] of the cubic space. From a colour point of view, an abject can thus be unrecognizable if it is observed under different intensities of illumination.

RGB colour space is not directly related to the intuitive notion of Hue, Saturation and Brightness. For this reason, other colours have been developed which can be more intuitive, in manipulating colour and were designed to approximate the way human's perceive and interpret colour. They are the HIS, HSV and HSL colour spaces.

3.4.2 HIS, HSL and HSV colour spaces

HSI, HSL and HSV are perceptual colour spaces. In the perception process, a human can easily recognize attributes of colour: Intensity, Hue and Saturation. Hue represents the actual colour. Saturation indicates how deep or pure the colour is. Intensity is simply the amount of light. HIS colour space can be easily transformed from RGB colour space (Agoston (2005), Cheng (2001), Fairchild (2005), Foley (1995)). Figure 3.9 illustrates HIS colour space.

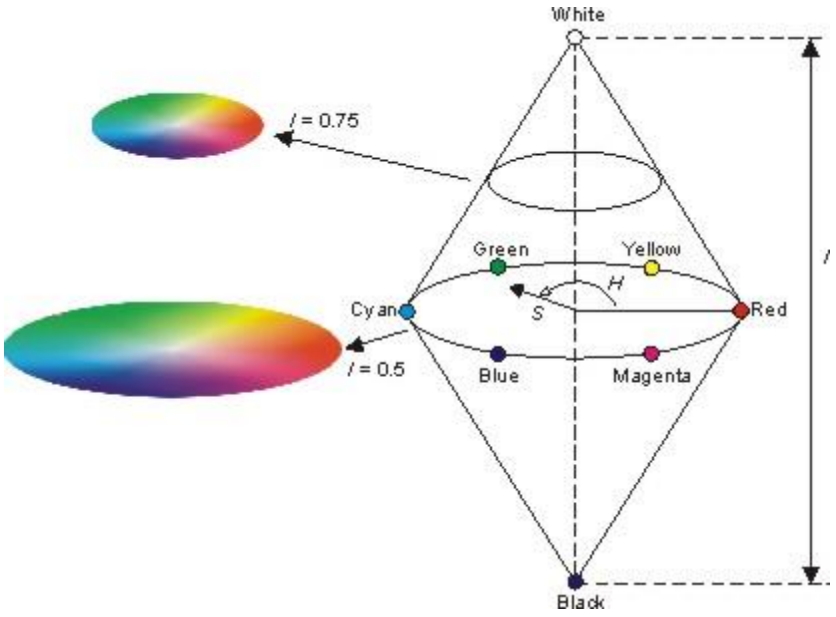

Figure 3.9. HSI colour space.

Figure 3.9 shows that intensity I is changing from 0 to max (usually is 255), saturation S is changing from center (0) increasing t max (1) or from 0 to 255, and hue H is changing from red as a circle ranging from 0 to 360. HSL and HSV colour space are similar to HSI colour space. These three colour spaces provide more intuitive description of colour. CIE introduce a colour space which is CIELUV colour space (Billmeyer (1981), Burnham (1963), Wright (1929), Guild (1931), Hering (1964)).

3.4.3 CIELUV

In 1976, the CIE defined a new colour space CIELUV to enable us to get more uniform and accurate models. Sometimes, it is also called universal colour space. This colour representation results from work carried out in 1931 by the Commission Internationale d'Eclairage (CIE). The CIE LUV colour space is a perceptually uniform derivation of a standard CIE space. Hence, it is essential to briefly introduce the CIEXYZ colour space and chromaticity colour space before giving more detail of CIELUV colour space.

- CIEXYZ and chromaticity colour spaces of xy and u'v' chromaticity diagrams

  Colour has commonly been measured by viewing combinations of three standard elements. CIE in 1931 has defined the CIEXYZ colour space which is relative to the standard observer and also is called the tristimulus colour space. The tristimulus values of them are not correlating. Hence, CIE has defined a colour space normalized from XYZ colour space as expressed in Eqs (3.2) to (3.4). The relative values of x, y and z are defined as Eqs. (3.5) to (3.7).

$$x = \frac{X}{X+Y+Z} \tag{3.5}$$

$$y = \frac{Y}{X+Y+Z} \tag{3.6}$$

$$z = \frac{Z}{X+Y+Z} \tag{3.7}$$

As $x + y + z = 1$, x and y can be used to describe the colour, which is called xy chromaticity co-ordinates colour space. The example of x, y chromaticity diagram (left) and $u'v'$ chromaticity (right) is shown in Figure 3.10.

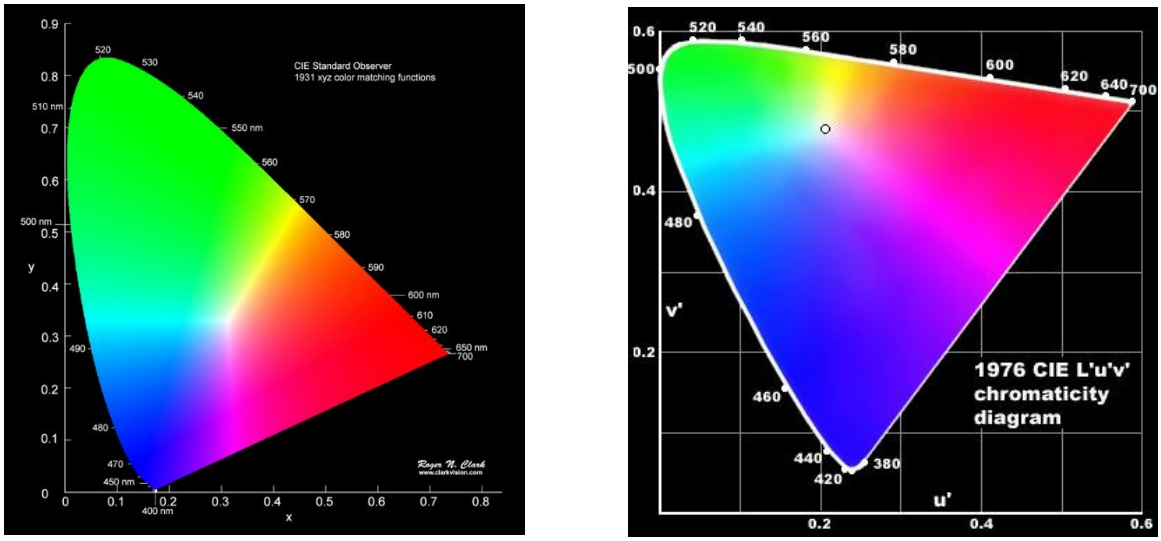

Figure 3.10. CIE Chromaticity (Stiles (1959)). Left graph: xy chrmaticity diagram. Right graph: u'v' chromaticity diagram.

However, the distribution of the colours on xy chromaticity coordinate is not uniform. Then CIE recommended a new colour chromaticity which is u'v' in 1976. The example of u'v'

colour space is shown above in Figure 3.10 (right graph) and values are obtained by the Eqs. (3.8) and (3.9).

$$u' = \frac{4X}{X+15Y+3Z} \tag{3.8}$$

$$v' = \frac{9Y}{X+15Y+3Z} \tag{3.9}$$

- CIELUV colour space

Chromaticity diagrams show only proportions of tristimulus values, and not their actual magnitudes and they are only strictly applicable to colours all having same luminance. Colours however, differ in both chromaticity and luminance, and some methods of combining these variables are required. In 1976, the CIE used the CIELUV colour space as the perceptually uniform colours spaces whose expressions are defined as Eqs. (3.10) to (3.15).

$$L^* = 116f\left(\frac{Y}{Y0}\right) - 16, \text{ if } Y/Y0 > 0.008856, \tag{3.10}$$

else

$$L^* = 903.3\left(\frac{Y}{Y0}\right) \tag{3.11}$$

$$u^* = 13\ L^*\ (u' - u'_0) \tag{3.12}$$

$$v^* = 13\ L^*\ (v' - v'_0) \tag{3.13}$$

$$H = \text{arctan gent}\ (V^* / u^*) \tag{3.14}$$

$$C = \sqrt{(u^*)2 + (v^*)2} \tag{3.15}$$

Where u'_0, v'_0 are the values of u', v' for the appropriately chosen reference white. The L component has the range [0,100], the U component has the range [-134, 220], and the V component has the range [-140, 122]. H is the angle of Hue which express by angle ranging between 0 and 360, C is the value of Chroma which ranging from 0 to 260. So, CIELUV can be visualised in Figure 3.11.

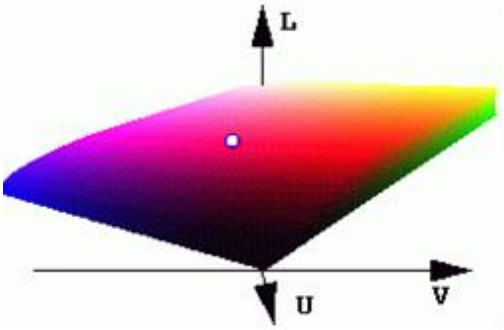

Figure 3.11. CIELUV colour space (CIE (2016)).

In summary, colourimetry is the branch of colour science dealing with specifying the colour of a physically defined visual stimulus by the observer and has the following characters.

a) When viewed by an observer with normal colour vision, under the same observing conditions, reading and measuring the same objects appear similar.
b) Stimuli that appear similar have the same specification.
c) The numbers comprising the specification are functions of the physical parameters defining the spectral radiant power distribution of R, G, and B.

3.5 Introduction on mobile phones

Mobile devices fundamentally changed view of personal computing with people forgoing the smaller, lighter versions of desktop. Doctors and patients are beginning to expect medical images to be available on mobile devices for consultative viewing. This section describes how the trend for mobile devices increased gradually.

3.5.1 Global trend of Smart Phone

Thanks to advances of Computer Technology, our world at present is becoming increasingly more mobile. The number of mobile subscribers continues to grow significantly. Global sales of mobile devices have been rising year by year, driven in particular by purchases in developing economies. It has been estimated that by the end of 2027 the global smartphone users will reach 7.8 billion (Taylor (2023), Laricchia (2022)).

The total amount of mobile devices is already larger than PC desktop computers. Global mobile device sales are not only focused on smartphones alone, but also on feature phones which are classified as non-operating system devices. Since these types are more affordable that current smartphones, these are still a popular choice in countries such an India and China. According to the research by ‘We are Social’, mobile overload has exceeded 100% in many regions of the world, including North America, Western Europe, Central and South America, Central and Eastern Europe, and the Middle East as illustrated in Figure 3.12. This means there are at least as many mobile subscriptions as citizens in those regions, including users of all smartphones (Taylor (2023)).

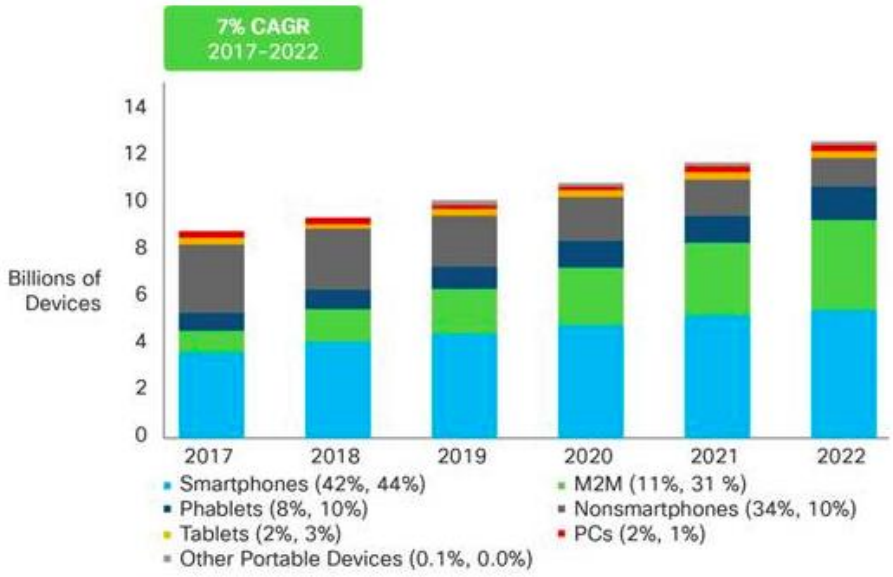

Figure 3.12. Global Mobile Devices and connection growth (2017-2022).

3.5.2 Medical (Digital) Imaging and Smartphones in Health Care Industry

Recently, progress on application of mobile devices to assist medical diagnosis has been made significantly (Rat (2018), Do (2014), Bourne (2010)).

A smartphone is a mobile phone with more advanced computing ability and connectivity than basic feature phones. Smartphones typically include the features of a telephone, as well as the features from other popular user devices, such as a personal assistant, a media player, a digital camera and GPS navigation etc. Mobile telecommunication have been available in UK since the mid-1980s. Since 2015, the mobile usage percentage remained same from 95%, whereas this usage amount was at least half in 2000 (Taylor (2023)).

Due to adaptability and convenience of current mobile phones, people are constantly using a phone to perform various tasks more than just making a call, taking pictures and shopping online. While a smartphone can act as a mini-computer and can be utilized to search the internet in the same way

as a computer due to its inherent limitations. For example, the colour of a desktop computer can be adjusted to its desired colour temperature, i.e., D65, whereas the RGB values on a smartphone normally cannot be modified nor can the white balance be checked. As a result, performing online shopping using a mobile phone can be tricky, as well as seeing digital health images, due to colour sensitivity.

Mobile imaging is one of the main thrusts of smartphone apps for assisted living (Do (2014)). Medical Imaging is visual representation of the interior of a body for clinical analysis and medical intervention, as well as visual representation of the physiology such as organ functions and tissues. Medical Imaging not only seeks to reveal internal structures but also diagnose and treat disease. In widest sense, biological imaging incorporates radiology which uses the technologies of X-ray, MRI (Magnetic Resonance Imaging), ultrasonography, endoscopy, elastography, tactile imaging, thermography and medical imaging.

Today's smartphones are equipped with high resolution image sensors. Typical smartphones can capture photos with a resolution of more than ten megapixels and significant image details. In medical imaging, it mainly deals with the grey scale images to show patient reports. In digital imaging, pixels gather and define as picture element to display on projector or any of the digital screens which is more essential to have in handheld computer morphed into a ubiquitous Internet access device for most physicians.

Benefits of Digital Imaging:

- Allows instant access to the patient care team regardless of location.
- Make images centrally available with access on multiple hard drive or computers.
- It always keeps the backup prevented in any case of damages.

- It always keeps the workflow, productivity throughout imaging process.
- Improves efficiency means it allows radiologists to review and report patient studies in digital format as quickly as possible.
- Eliminates the need to shuffle through files that can be lost or missing.
- Images can be easily viewed, email so that communication, cure can be faster than expected. (Bourne (2010)).

Tablet and smartphones' viability for use in medical imaging has become expectation due to easy use. Nearly 80 percent of physicians are using smartphones and devices in their medical practice with interest in viewing patient information including images. As mentioned above, pixels on smartphones are numerous and small enough to feed human eyes as much possible and are sufficiently bright to be seen in most lighting conditions.

Today's mobile devices are not specifically designed for diagnostic imaging because they are not specifically designed for medical imaging. Smart phones are unable to maintain continuous digital imaging and communication in medicine (DICOM) calibration due to a lack of internal or external sensors necessary to achieve. In order to utilize a mobile device for diagnostic image review, it must be DICOM calibrated image provides accurate image representation and confidence for medical professionals. Once a screen is calibrated properly, radiologist can diagnose images from most modalities like magnetic resonance (MR), ultrasound, digital radiography (DR) for diagnostic reading on a mobile.

Digital technology helps to improve patient care and provides efficient cost and workflow benefits to hospital and radiology department. Digital imaging to be used by smart phones can be helpful in health care for effective and efficient cure results.

Therefore, this research takes an initiative to investigate the variations of grey level colours for several smartphones while making an effort to model their colour appearing using CIECAM02 (Moroney (2002)) and current updated version CIECAM16 (Li (2017)).

Chapter 4. Study on Medical Images

Medical practitioners are increasingly like to make clinical decisions based on images as an important determinant. Medical images provide visualisation tools for diagnosis, treatment and education of pathologies to create opportunities to benefit healthcare (Bankman (2009), Fryback (1991)). Medical images include both grey images and colour ones. Radiological images tend to be grey, including x-ray, computerised tomography (CT), magnetic resonance (MR) and Positron Emission Tomography (PET). Images that are captured using optical cameras are in colour, including retinal images, taken from the eye, and oesophageal videos for inspecting food pipes. The application these images can help clinicians find biomarkers for Alzheimer's disease (Gao (2017a)), detect heart diseases (Gao (2017b)), prediction of multi-drug resistance Tuberculosis (TB) (Gao (2018)), TB severity level (Gao (2020)), and prediction of oesophageal squamous cell cancer from the video captured in the food pipe (Gao (2023)). These applications demonstrate the contribution of medical images in modern medicine.

Medical imaging used to be primarily within the domain of radiology, but with the advent of virtual pathology slides and telemedicine, imaging technology is expanding in the most of healthcare enterprise. As new imaging technologies are developed, they are in need to be evaluated to assess the impact and benefit on patient care.

The work done by Fryback and Thornbury reviews and proposes a hierarchical model of the efficacy of diagnostic imaging systems (Fryback (1991)) as a guiding principle for system evaluation. Evaluation of medical imaging systems encompasses everything from the hardware and software used to acquire, store, and transmit images to the presentation of images to the

interpreting clinicians. Evaluation of medical imaging systems can take many forms, from purely technical (e.g., patient dose measurement) to the increasingly complex (e.g., determining whether a new imaging method saves lives and benefits society). Evaluation methodologies cover a broad range, from receiver operating characteristic (ROC) techniques that measure diagnostic accuracy to timing studies that measure image-interpretation workflow efficiency. The authors review briefly the history of the development of evaluation methodologies and review ROC methodology as well as other types of evaluation methods. They discuss unique challenges in system evaluation that face the imaging community today and opportunities for future advances (Krupinski (2008)).

Since 2013, the international colour consortium (ICC) is engaged with medical imaging community to help finding encountered problems and finding solutions. The ICC Medical Imaging Working Group is also working on key topics like digital microscopy, medical displays, medical photography, dermatology, 3-D imaging for surgery. In the literature review in (DICOM (2001)), problems related to medical imaging are discussed.

Medical image colour modes are greyscale, false-colour and true-colour. Greyscale images arise from mapping of intensities that is X-ray, CT, nMRI Scanner (Nuclear Magnetic Resonance Imaging) to toning in an image. Greyscale mages are the images acquired by systems that record radiometric quantities and map them linearly. Since at present nearly all newly acquired images are digital, there is a potential to view them on any number of computer systems. Computers can be a standard personal computer (PC) or a sophisticated picture archival and communications system (PACS) work station may. Hence there is a need for consistent medical image presentation (Flynn (1999)) on this wide selection of work stations, which was recognized in the early 90s (Blume (1990), Blume (1996), Blume (1999), Fetterly (2008)), leading to a broader description of a high-quality display. For grayscale medical images, the Barten model of the human visual

system's response to contrast stimuli (Barten (1999)) has been used to develop the digital imaging and communication in medicine (DICOM) grayscale standard display function (GSDF) (DICOM 2001)). This GSDF standard provides a mathematical definition of the luminance output versus digital input which ensures perceptually equivalent contrast throughout the grayscale range of the display.

4.1 Digital Imaging and Communications in Medicine (DICOM)

DICOM is the standard for the communication and management of medical imaging information and related data (Kahn (2007)), which is developed by the American College of Radiology (ACR) and National Electrical Manufactures Association (NEMA). DICOM is most commonly used for storing and transmitting medical images enabling the integration of medical imaging devices such as scanners, servers, workstations, printers, network hardware, and picture archiving and communication systems (PACS) from multiple manufacturers. It has been widely adopted by hospitals, health care sectors and medical industry. DICOM files can be exchanged between two entities that are capable of receiving image and patient data in DICOM format. The different devices come with DICOM Conformance Statements which state which DICOM classes they support. The standard includes a file format definition and a network communications protocol that uses TCP/IP to communicate between computer systems.

To ensure image key features are displayed corrected cross varying colour monitors, grey scale calibration of electronic displays is in need to ensure images presented to an observer have equal perceived contrast appearance on all displays, independent of the luminance range of the display. To achieve this goal requires that, given a specific luminance scene, the contrast perceived by the human visual system (HVS) is well known (Roehrig (2003)). Therefore several experimental models have been established based on perceived contrast of the human visual system. In addition,

a number of grayscale display function models are employed to calibrate displays, including CIELAB display function, the log-luminance linear function (Ogawa (1999)), and the DICOM GSDF (DICOM (2001), Roegrig (2003)). DICOM GSDF is built on the work conducted by Barten et al (Barten (1992), Barten (1993)).

As the international standard for medical images and related information, DICOM is used for medical image that are implemented for various formats such as radiology, cardiology images, X-ray, MRI, Ultrasound etc. The usage of DICOM is also extended to dentistry and ophthalmology. DICOM is the standard widely used in healthcare. Since 1993, DICOM has revolutionized the practice of radiology, x-ray film and digital heath workflow. DICOM is the standard makes medical imaging work for doctor as well as patients. It has enabled many medical imaging applications that changes face of medicine field. It also is recognized by the International Organization for Standardization as the ISO 12052 standard (Badano (2015)).

DICOM is one of communication protocol subsets the property that impact interoperability. The protocol is compatible with Transmission and Internet Control Protocol. This enables DICOM application entities to communicate over internet. DICOM services fall into two group: composite and normalized. Composite services are useful for information as reports. Whereas the normalized services were designed to provide broader information management functionality. Normalized is not related to normalization of databases. Normalized services support basic information management operation like create, delete or get information. Composite services normally are used for documents in form of images. Real-World entities are represented in the DICOM semantic data model by templates of attributes.

DICOM is a medium to extend human vision in medical to enable diagnosis of particular diseases. Not only vision but DICOM transforms diagnose possible to save lives and helped patients to survive while ensuring display media to present images correctly. Medical images not only serve to diagnose but also helps to find out disease of patient so that clinical progress can be provided in correct direction. For example, *Picture Archiving and Communications Systems* (PACS) arrange and manage the medical images, as a result modern clinical and imaging facilities are being reliable. PACS is technically added in medical environment for several reasons: it consists of many components such as image acquisition communication, display, archiving, and human-machine interfaces. PACS implementation is expensive and in addition, maintenance is difficult. Administratively PACS is an image management system and its , requires a reorganization of operational procedures in a radiology department (Fetterly (2008), David (2006), Carrino (2002), Wang (2003 Liu (2007), Mcllgorm (2015)).

Particularly, the health care system has been successful to ensure the effective, efficient treatment flow for patient to be cured and DICOM is the important feature that has technical standard for social additions.

4.2 Barten's model based on Luminance Just Noticeable difference (JND) experiment

To ensure images presented on all display devices or monitors have equal perceived contrast to an observer, the Barten model of human visual system(HVS) (Barten (1999)) is adopted by DICOM to define a standardised method of display calibration, which is named as Greyscale Standard Display Function (GSDF) (DICOM PS3.14 (2023)).

GSDF has been developed to map digital images by quantitative mechanism to luminance so that it produces better visual consistency to display on devices. Risk of errors due to visual conflicts

can cause interpretation increment in medical images. GSDF links the digital image and display luminance values measuring them. It is not dependent on characteristic of user preferences but based on the greyscale that come from images of MRI, CT Scan, Ultrasound, X-ray etc.

The visibility by human visions increases when the object is in contrast background. Scientist have performed experiments with different sized objects and different luminance of background. The Barten model did experimental literature on visual contrast threshold and introduced an analytical model, to describe performance of human vision observing sinusoidal pattern of different size and frequency of image luminance.

In. Figures 4.1 & 4.2 the contrast threshold is between 0.010 and 0.007 with luminance between 20 to 500 cd/m^2. This type of images represents medical platform (Kimpe (2006)).

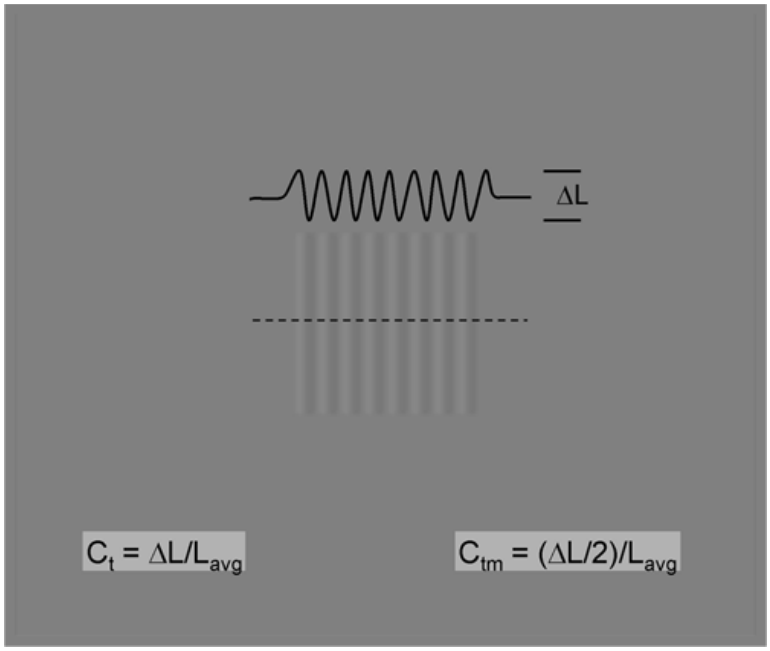

Figure 4.1. Image scene with a sinusoidal pattern used to measure contrast threshold (Kimpe 2(006)).

The contrast threshold, C_t, and the Michelson contrast threshold, C_{tm}, are illustrated in Figure 4.2 (Kimpe (2006)).

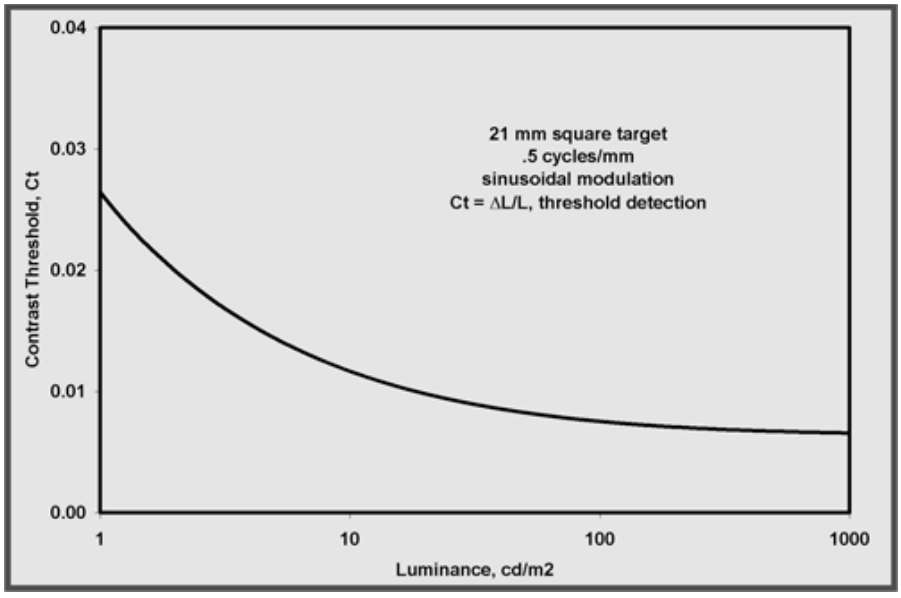

Figure 4.2. Contrast threshold versus luminance for a 21 mm square object pattern

with sinusoidal modulation of 0.5 cycles per mm that is viewed from a distance of 60 cm.

It was developed by measuring the sensitivity of the HVS to a low contrast, sinusoidal luminance signal (four cycles per degree subtending over 2°) presented on uniform luminance backgrounds. These experiments were conducted over a large luminance range (10^5). The luminance difference of the sinusoidal visual target from the background was varied to identify the luminance change, which rendered the target just barely visible. In this manner, a just noticeable difference (JND) was defined as the luminance change in the target that was required for the target to be perceived.

DICOM GSDF is often plotted graphically as luminance versus JND index (j), where j ranges from 0 to 1023 (2^{10}-1) ($j = 1,2, \dots, 1023$) as illustrated on Figure 4.3. A JND is the luminance difference of a given target under given viewing conditions that the average observer can just perceive. As illustrated in Figure 4.3, the relationship between luminance and JND index can be

expressed in a curve, indicating that a human observer is able to perceive around 1000 different shades of grey over this entire luminance range and in optimal conditions. This Barten JND model is based on experimental data in which the eye is adapted to the luminance value of a uniform background.

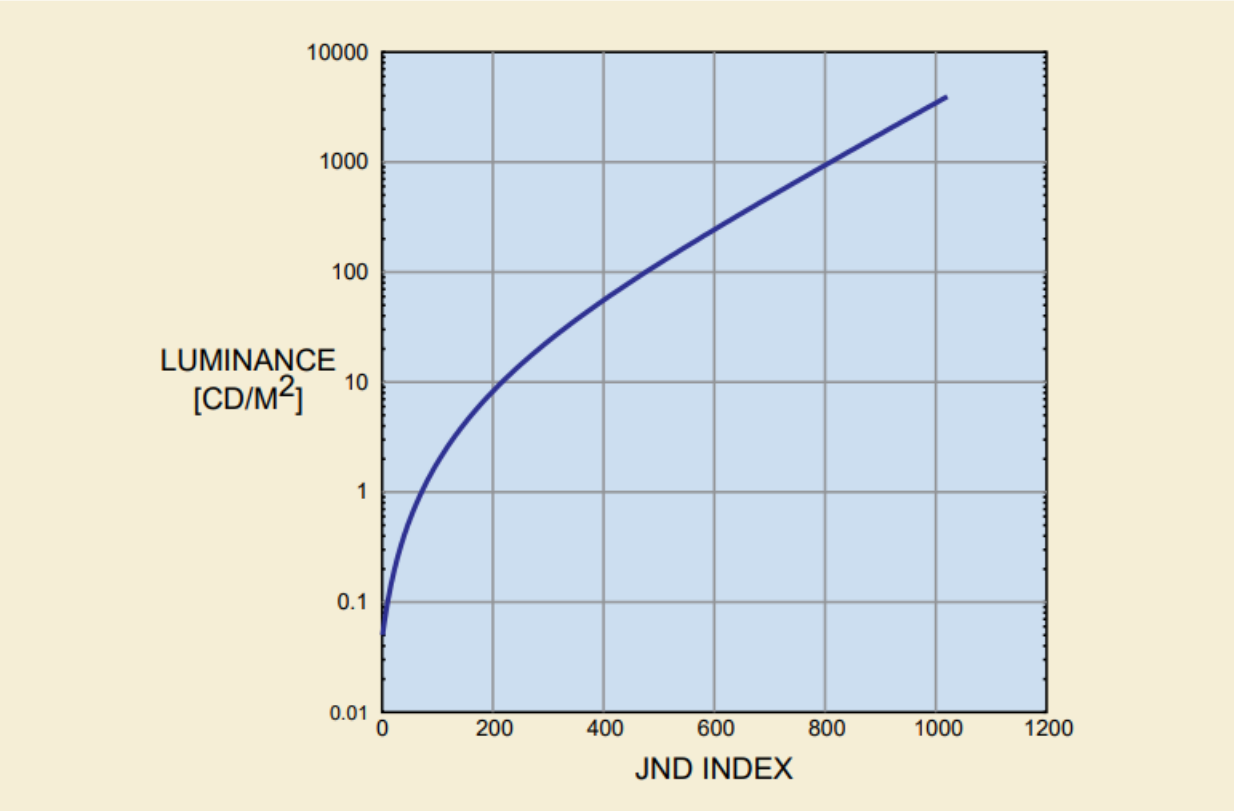

Figure 4.3. The Grayscale Standard Display Function (GSDF) presented as logarithm-of-luminance versus JND-index (Barten (1992), Barten (1993)).

The conversion between JND_j and luminance (cd/m^2) can be expressed in Eqs. (4.1) and (4.2) since the Barten model data can be fitted to a polynomial function. Eq. (4.1) transforms from luminance (L) to JND (j) whereas Eq. (4,2) converts j back to L.

$$j = A + B\log_{10}(L) + C(\log_{10}(L))^2 + D(\log_{10}(L))^3 + E(\log_{10}(L))^4 + F(\log_{10}(L))^5 + G(\log_{10}(L))^6 + H(\log_{10}(L))^7 + I(\log_{10}(L))^8 \quad (4.1)$$

Where the values of A, B, C, D, E, F, G, H and I are provided in Table 4.1.

Table 4.1. Constant values for Eq. (4.1)

Variable	Value
A	71.498068
B	94.593053
C	41.912053
D	9.8247004
E	0.28175407
F	−1.1878455
G	−0.18014349
H	0.14710899
I	−0.017046845

Eq. (4.2) provides formula for $\log_{10}(L)$ to transform $JND\ (j)$ to luminance (L).

$$\log_{10}(L) = \frac{a+c\ln(j)+e(\ln(j))^2+g(\ln(j))^3+m(\ln(j))^4}{1+b\ln(j)+d(\ln(j))^2+f(\ln(j))^3+h(\ln(j))^4+k(\ln(j))^5} \tag{4.2}$$

The constant values (a, b, c, d, e, f, g, h, m, k) are provided in Table 4.2.

Table 4.2. Constant values for Eq. (4.2)

Variable	Value
a	−1.3011877
b	−0.02584019
c	0.080242636
d	−0.10320229
e	0.13646699
f	0.02874562
g	−0.025468404
h	−0.003197898
m	0.001363533
k	0.000129926

4.3 DICOM Calibration of a display

Figure 4.4 illustrates a calibration flow defined by DICOM (DICOM PS3.14).

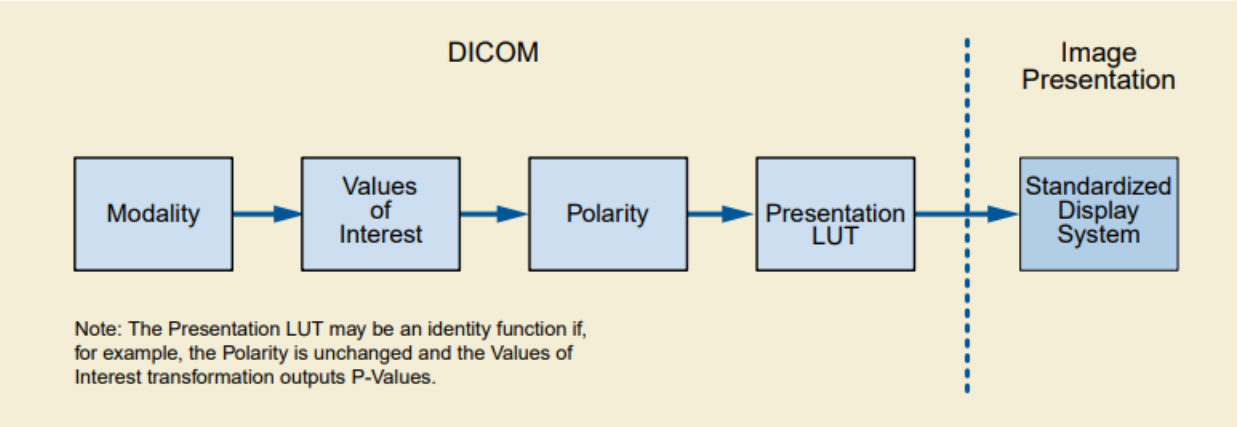

Figure 4.4. The workflow of calibration based on DICOM GSDF (DICOM PS3.14).

The boundary between the DICOM model of the image acquisition and presentation chain, and the Standardized Display System, expressed in P-Values, is intended to be both device independent and conceptually (if not actually) perceptually linear. In other words, regardless of the capabilities of the Standardized Display System, the same range of P-Values will be presented 'similarly'. Hence, P-value is a device independent value defined in a perceptually linear grayscale space. The output of the DICOM Presentation LUT is P-Values, i.e., the pixel value after all DICOM defined grayscale transformations have been applied. P-Values are the input to a Standardized Display System. Figure 4.5 illustrates the conceptual model of a standardized Display System maps P-values to Luminance via an intermediate transformation to Digital Driving Levels (DDL) of an unstandardized display system.

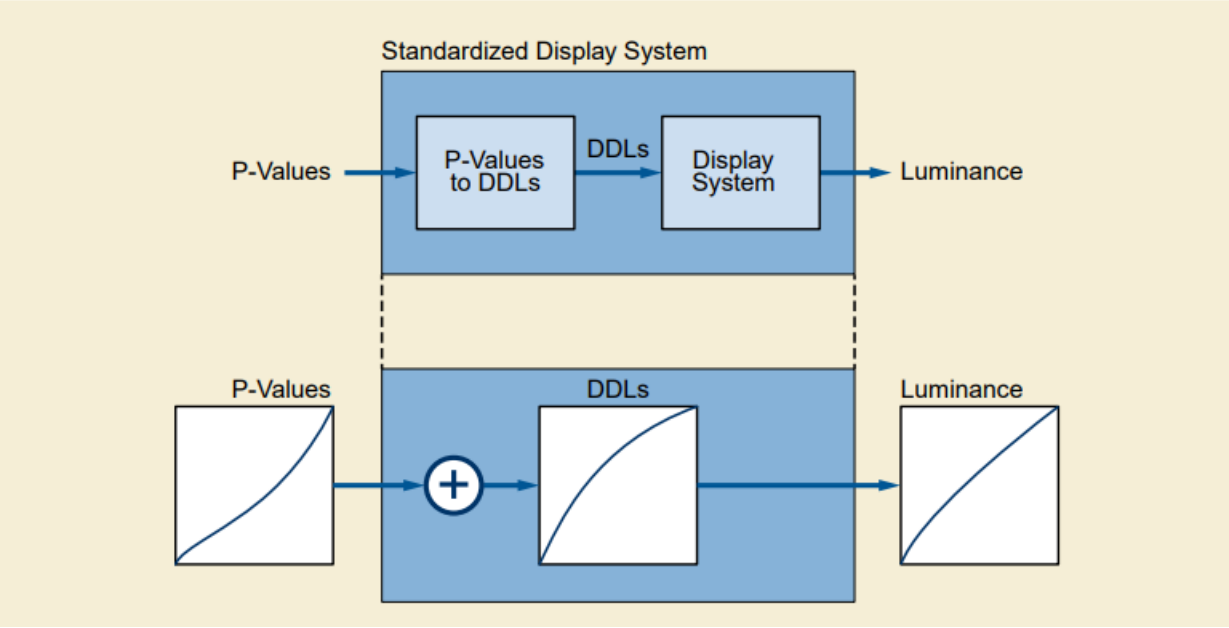

Figure 4.5. The mapping between P-Values, DDLs and standardised system (DICOM PS3.14).

For viewing medical images, display devices are in need of calibration. This requires that the desired post-calibration minimum ($L_{\min}$) and maximum ($L_{\max}$) luminance values should be the same as initially identified.

Since the luminance output of the backlights decreases over time, which might lead to the shorter life expectancy of the concerned display that is calibrated to the maximum luminance intensity. In practice [Fetterly (2008)], diagnostic monochrome monitors are now commonly calibrated to an L_{max} being 400 to 600 cd/cm^2, whereas colour monitors used for clinical review will have an L_{max} ranging from 250 to 450 cd/cm^2. Similarly, L_{min}, corelating to ambient light effects, is often set to be larger than the black level of the display, L^d_{min} that is determined by the ability of a display to block the backlight.

Hence the contrast ratio of a display is defined as Eq. (4.3).

$$C = \frac{L^d_{max}}{L^d_{min}} \quad (4.3)$$

A typical contrast ratios are in the range of 250 to 400 for colour displays and up to 600 for inherently grayscale displays.

For medical image users and handlers, the solution to calibrate monitors depend on types of monitors.

High resolution medical monitors are mostly applied with the calibration. Monochrome devices commonly used to see calibrated greyscale display. The pictures send RGB values to digital driven levels (DDL). The calibration tables can be provided by software manufacturer. They count luminance by their minimum - maximum values and the values can be adjusted by ambient lights. Many providers use monitor performance by luminance or attaching the light meter.

Professional graphics are the monitors used for cross sectional imaging. They have excellent colour rendering facilities by higher pixel visibility. Luminance values are also used in this graphics monitors with setting response of Luminance.

The monitors that physicians or radiologists use are normal consumer systems. The performance of this systems are highly varied to the usage monitors. These monitors are not responsible enough to view high brightness devices. For detailed visibility, an internal look up table (LUT) get luminance response by additional graphic designer.

Medical imaging has the potential to enable earlier and more precise diagnosis of disease and its use during therapy can improve patient outcomes. Imaging can also be used in planning and during

surgery to increase its effectiveness. Many imaging technologies that are suited to clinical environments across the world are needed to improve the patient experience and reduce costs.

Greyscale images are modified by colour aid additionally such as false-colour images that is pseudo-colour. In pseudo-colours intensity levels are mapped continuously to different colours. The images features are categorized to smaller set or discrete colours and colours are mapped in a way that they are statically proportioned. These categorized colours are known as pseudo-colour implies to be known as the false colours. DICOM defines colour palettes used as pseudo-colour pallet. Compared to GSDF, CSDF (Colour Scale Display Function) is based on multi-band sensor arrays rather than a single intensity channel. While there are a few devices as Trichromatic imaging devices to record RGB signals for images, there are several advanced applications for multi spectral and hyperspectral devices. RGB images are often referred to as true colour images as their visual appearance is approximately based on subject rather than arbitrary mapping from colour response to sensors.

Principal requirement for true-colour images is colourimetric accuracy. Medical images have requirement for consistency to judge small differences in appearance between image differences whether using one device using at different times or different devices of same object. Colours in medical imaging has many problems mainly classified as calibration problems when images are captured or need to display on systems. Medical Imaging is critical system associated with life of patient and also has some specific requirement. This literature review summaries some of work done in the area to improve medical imaging system.

4.4 DICOM image format

The format of Digital imaging and communication in medicine (DICOM) is commonly employed to represent images after acquired from an imaging scanner.

DICOM images typically contain 12-16 bits/pixel, corresponds to approximately 4096 to 65538 shades of grey. Most displays or computer screens are of 8-bit and hence can display 256 grey shades. However with computer screen displays 256 shades of grey, human eye can detect only about 30 shades of grey. That means human can detect about 256/6 = 42 shades of grey (Salazer (2014)).

DICOM calibration is a medical calibration form to ensure compliance with GSDF standard. The DICOM defines how greyscale images can be shown on medical display so that they can be displayed consistently. DICOM GSDF was developed to provide an objective, quantitative mechanism for mapping digital images values into range of luminance in order to produce better visual consistency in the way images appear on display. The relationship between digital image values and displayed luminance, as explain above and defined by the GSDF, is always based upon measurements and models of the human perceptual system over a wide range of luminance values. The DICOM GSDF, as the name implies, is intended for use with greyscale images (Salazer (2014), Flynn (2020)).

Figure 4.6 demonstrates an example of display inconsistency. In left image lump is visible whereas when the consistency of display changes, the visibility also becomes blurred. In practice, DICOM has recommended several visual patterns to check the grey-level intensity distribution of a monitor.

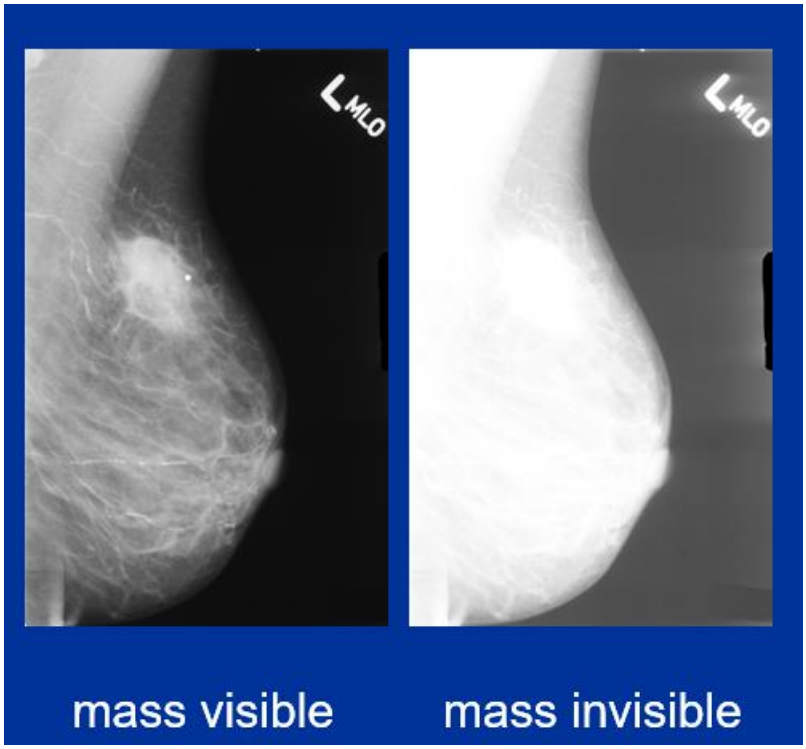

Figure 4.6. Image inconsistency (Kimpe (2016)).

Visualization plays vital role when screen is calibrated. It evaluates the visualisation examining test pattern for contrast in colours for response. Figure 4.7 represents one pattern to develop quality control for better visualisation. This figure helps user to be familiar with colour appearance from calibrated monitors because the test pattern can be done easily and conveniently (Kimpe (2016)).

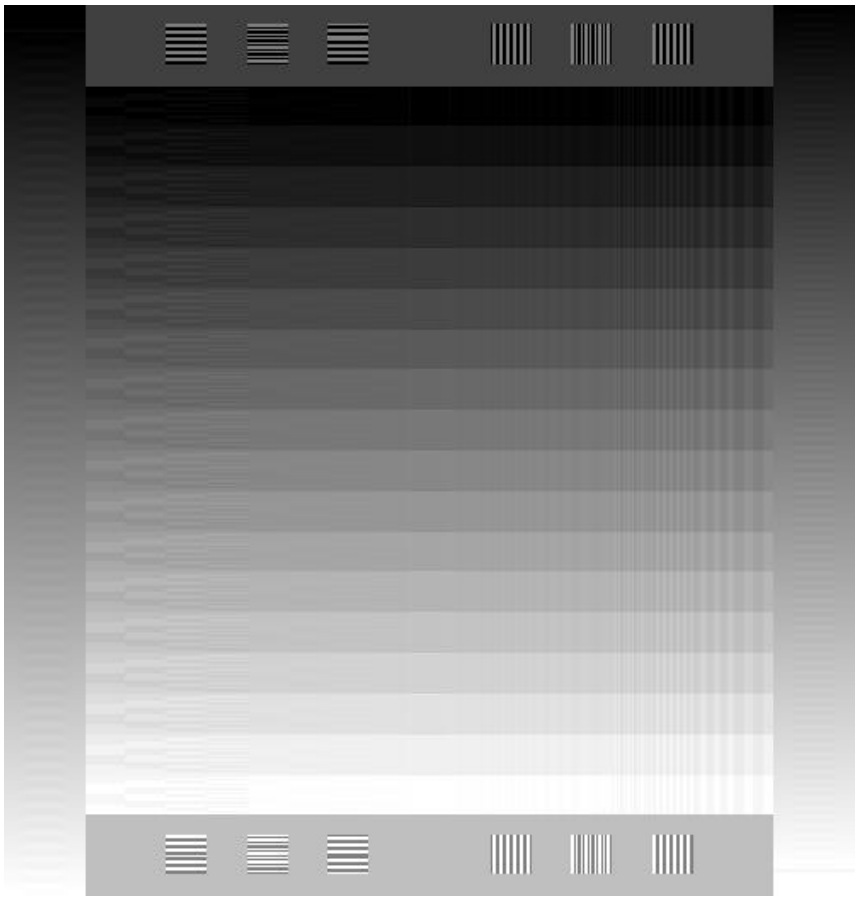

Figure 4.7. A greyscale display pattern demonstrating the contrast characteristics of images presented on a workstation (Flynn (2020))

This evaluation requires quantitative evaluation, typically connected with computer to display via USB cables. It helps to read evaluated data by software application displaying grey colour values. Recommendations done by the American Association of Physicists in Medicine (AAPM) and the International Electrotechnical Commission (IEC) that contrast on colours can be normalized in DICOM standard.

For medical imaging, the Grayscale Standard Display Function (GSDF), has been used extensively for this purpose. The relationship between luminance and display value specified by this function is specifically derived from the Barton model of contrast threshold as detailed in Sections 4.2 and 4.3. Specifically, the contrast, DL/L, as a function of L is proportional to the contrast threshold

where DL/L is associated with the change in luminance between sequential gray levels. The dark portions of an image therefore are thus enhanced in contrast to account for the poor response of the human vision system. Figure 4.8 illustrates a calibration result performed by a medical professional to calibrate a monitor,

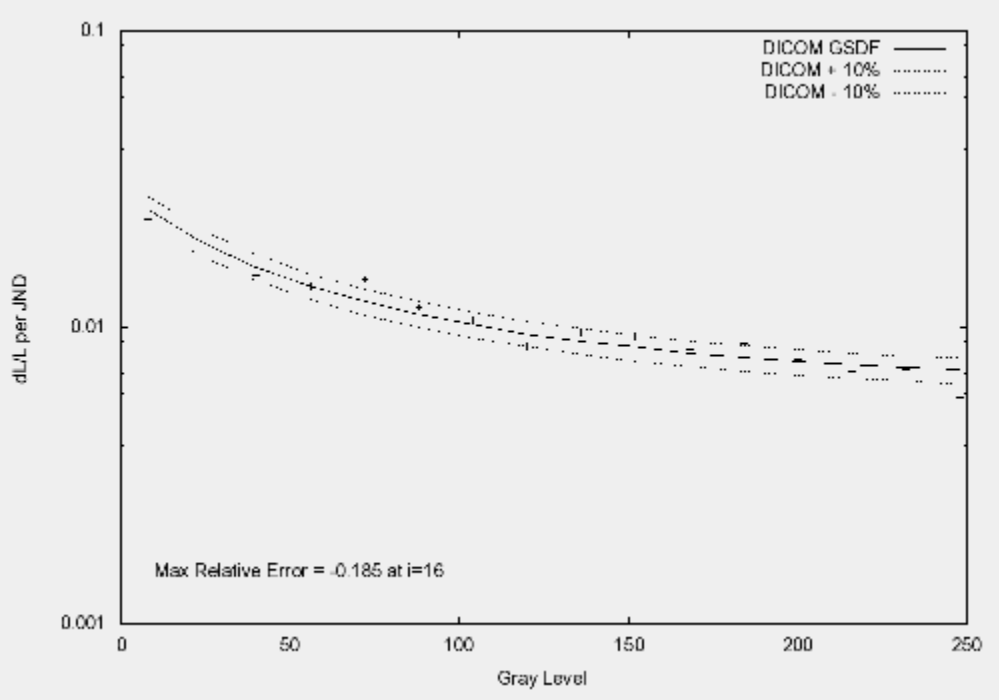

Figure 4.8. The results of a quality control test of the contrast response commercial monitor used by an ultrasound sonographer (Kimpe (2016))

The main aim of this research to achieve the calibration from monitor to mobile phone the same as for monitors shown in Figure 4.9. (Wang (2003)) The performance simplifies calibration by RadiCS software. This software controls quality on DICOM brightness and greyscale tones. It ensures that monitor is capable of displaying breast screening images with high performance with needed brightness. The pixel ratio has to be sharp enough to avoid discrepancies. It allows to display image safely on monitor with true source data per high brightness standards.

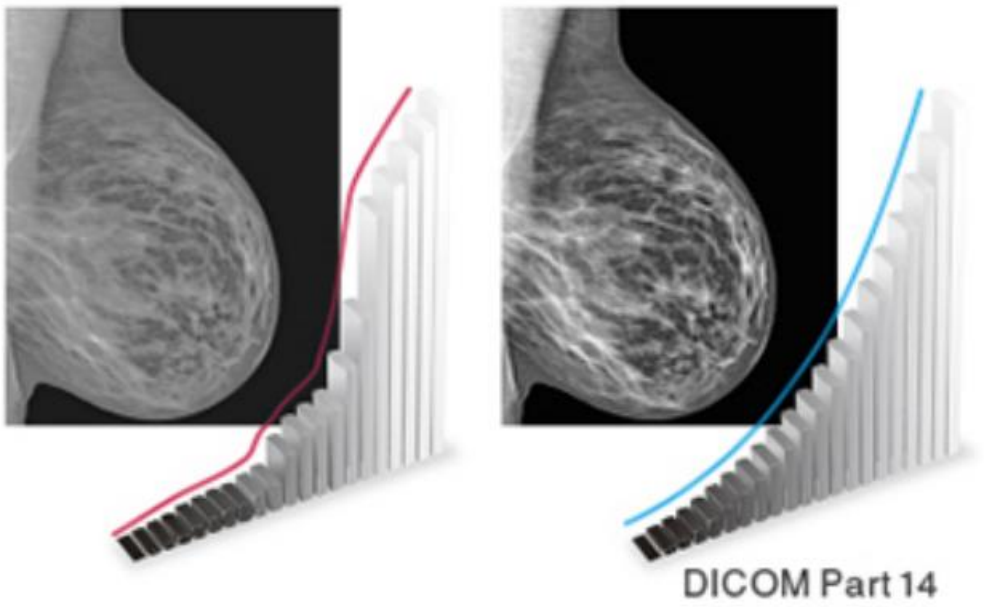

Figure 4.9. Calibration Performance (Wang (2003), showing right graph clearer.

Digital image and display luminance are based upon measurements and models of the human perceptual system over a wide range of luminance. It is not based on device or user preferences. DICOM GSDF is intended for use with greyscale images such as x-ray, MRI, Ultrasound etc. With wide implementation of Picture Archiving and Communication System (PACS), diagnoses are able to be made on medical display system (Carrino (2002)).

Medical softcopy consists of monitor, desktop computer and monitor links between data of image and human observer's brain system (Carrino (2002), Samei (2005)). To make medical softcopy images display systems full of compliance with GSDF, the special characteristics on monitor's responses needs to be maintained performing calibration process routinely (Samei (2005), David (2006)). A calibration method is used for softcopy images to find Just Noticeable Differences (JND) as basis was not achieved by Lookup Table as Computer.

The Liquid Crystal Display (LCD) based monitors have been applied into medical softcopy display to obtain broadly acceptance in years. With the calibration method, the general LCD monitor can be calibrated to be compliance with DICOM GSDF and monitor performance can be improved (Flynn (2020)).

Nowadays the calibration process has been performed on some of the general medical monitors in hospital, and most of clinicians do feedback that the quality of medical softcopy image display was improved on those monitors calibrated. With the calibration method presented in this article, the performance of general medical monitor could be improved, and the calibration is display adapter and computer independent (David (2006)).

4.5 Visualisation

Colours can be more effective on telling a story behind different parts of images, it can be helpful for audience to capture attention quickly. Well-chosen colours can reduce time for viewers and help them to understand message easily. Colours are very effective medium for communication meaning for certain psychological method. Colours can convey different meanings.

Medical visualization applies visualization technique to MRI for diagnosis to one patient that helps for single study participation to explore the cure. Multiple datasets include imaging and non-imaging measurements to extract patterns. Information visualisation approach to visualise the electronic medical records of patients including information, datasets. These datasets acquire their vitals, measurements, diagnoses, medications etc. The radiological data benefits from interactive 2D or 3D visualisation. This radiological data is referred to as medical images (Gao (2017), Gao (2018)).

Medical image data has visualisation methods acquiring scanning devices such as MRI, Computed CT and ultrasound. This image data analysis and visualisation may give view of data depends on original data. Physicians must achieve realistic expectations with medical visualisation. It is essential for images to fulfil requirements of physicians with scanning parameters and image acquisition visualisation (Fetterly (2008)).

4.8 International Color Consortium (ICC)

At present, nearly all computer monitors are in colour. Hence colour management for viewing medical images present a challenge. Green and Luo (Green (2018)) recently propose a pipeline to calibrate colour monitor as illustrated in Figure 4.9, which points a direction. This work follows this framework to enhance lightness scale for mobile phones.

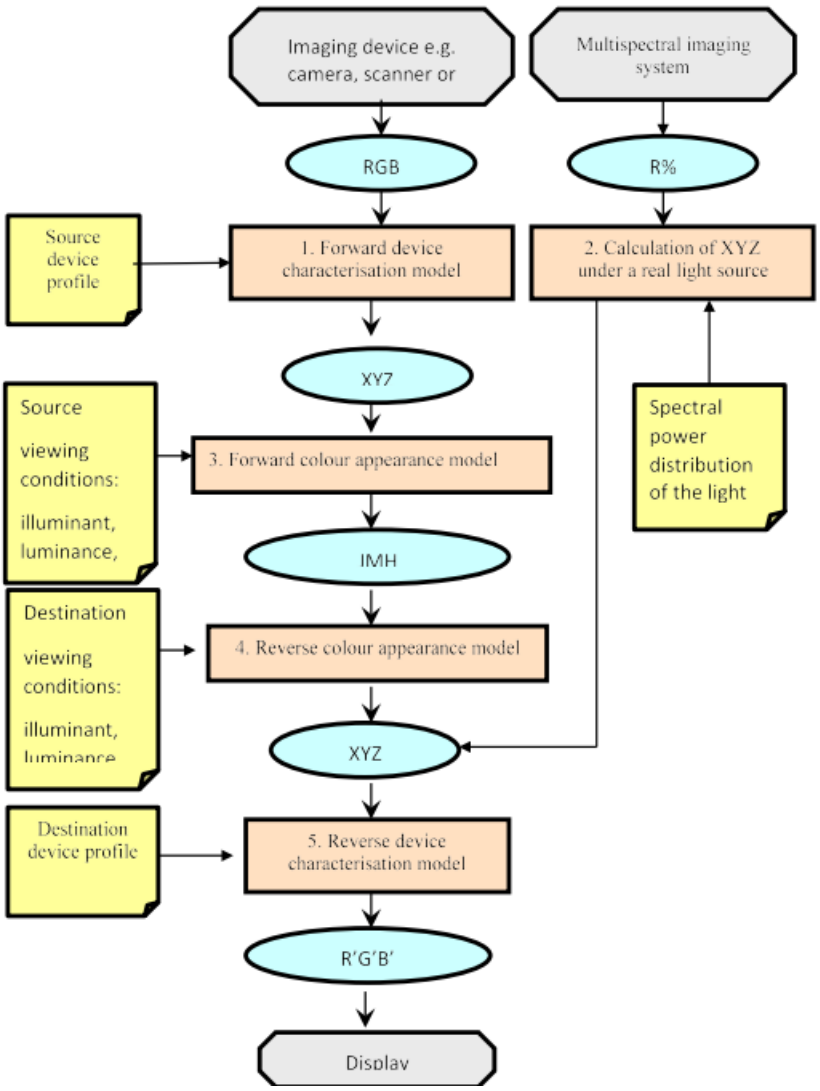

Figure 4.10. A colour management framework proposed by Green and Luo (Green (2018)).

Mobile approach is expected to have identical platform as desktop. It is understood that mobile platforms have restraints of screen size, resolution of screen and lightness. Any text form is easy to read on desktop than mobile screens. Similarly, buttons to click need to large in size that user can make sure they tap on designated link on mobile services. Constraint of content on smaller display is very important (Chao (2017)).

Representation on mobiles is challenging due to smaller screens and less pixels. Typical mobile phones are having screens diagonally 3-6 inches whereas desktop screens are 20-30 inches. For pixels to take example, iPhone 6S having pixel display as 1334 x 750 pixels comparing to MacBook has 2304 x 1440. Presenting important information on screen needs to be usable and look good to user on small browser layout to the regular sized pages.

Even on websites, videos and large graphics rake up large bandwidth and on contrary making same on mobile medium, needs to be fixed with smaller images and lower bit ration of video. Mobile devices also have less processing power than desktop computers. To run the application on mobile the script has to be minimized to make it run smoothly. All the time, the picture images look proper on computer desktop nut changed to mobile devices because mobiles devices are not colour calibrated and need to be balanced on every image. It is not uncommon for images to look slightly different on mobile device than desktop due to colour calibration and resolution. Images display quite consistent result on different platforms. Some platforms are suited for true colour representation and reproduction then others. When mobile device is set on high resolution, noticeable difference can be identified. Result may vary from one mobile device to other.

Best way to visualise colour display on screen is to calibrate the monitor. Calibration is the process of matching colour output from monitor to specific RGB colour space. Calibration tools mainly known as colourimeter can be used for this process. Calibrating process simply adjust the colours that fit with the general standards. It’s not enough to calibrate monitor just once as the displayed colours may change slightly by changing brightness decreasing the lightness. This slight change

in colours and brightness can be seen as drastic change for not only medical images but other normal photographs as well (Badano (2015)).

Monitor calibration is important part of digital workflow as it greatly affects image quality. Working on uncalibrated images have minimal control on finished results. That is how the different visualisation effects on medical images when user uses on mobile devices.

4.9 Medical Imaging Working Group (MIWG)

Experts from colour and medical imaging communities in May 2013 in two-day summit, started working together on medical imaging (Penczek (2014). The meeting was organized by the International Color Consortium (ICC) and US Food and Drug Administration (FDA) with 27 speakers, 250 delegates from 30 countries. Digital microscopy, endoscopy, laparoscopy, displays, telemedicine, ophthalmology, multispectral imaging, mobile devices, medical photography and standards of colour were covered and discussed topics. In this meeting, one new team was formed as a 'Task Force' associated with ICC Medical Imaging Working Group where experts were to work in their lead area. They published a paper summarizing problem in desired topics as discussed in the meeting.

The ICC profile format provides solution frame for few current problems in medical imaging. The primary aim of the Medical Imaging Working Group is to enable the correct use of ICC colour management for medical imaging. The group will identify issues with the implementation and use of colour management for medical imaging. They will establish liaison relationships with medical imaging standard e.g. DICOM, American Carbon Registry (ACR), International Organization for

Standardization (ISO), etc. They also decided to propose new ICC specifications or revised ICC to address medical imaging community needs

MIWG has participation from ICC members and also non-members, each work area is led by an expert in particular field. As with all these ICC also comply MIWG with ISO regulations. These groups hold tele meetings and three face-to-face meeting every year.

The issues faced by MIWG include:

- Calibration for Histopathology (Histopathology is the study of diseases of the tissues and cells under a microscope)
- Colour Eye Model – Fundus Camera is optical system used for imaging the retina of the eye. There is no method of calibrating such cameras that provides accurate images.
- Digital Colour photography in medical – Digital photography rely on digital cameras and lighting condition. This process also depends on camera setup and post colour correction process. Medical photography is used to record patient's appearance mainly in dermatology, wounds etc. Colour accuracy is important and priory considered in medical photography (Nayatani (1972), Xiao (2016), Xiao (2016a)).

This activity helps to minimise colour errors on different cameras. The goal is to implement suitable method that is having colour space independent from any device. Figure 4.11 demonstrates an issue with varying lighting condition. The same colour checker against the same skin background when the picture is taken by the same camera. The only difference is the viewing illuminant. Monitor calibration can recover this partly.

Figure 4.11. An image taken by camera with different illuminating condition.

- Colour support for mobile devices – Medical practitioners need to view images using mobile devices as smartphones, tablets. The colour system on these systems is often weak and methods to support calibration on devices are indeed.
- Petri Plate Imaging – It is automatic process of assessing plates by scanning and implementing image processes (Xiao (2016)). This process increases productivity but reduce resources. Challenge to this process is to provide separate information to each plate. Imaging systems need different light conditions to maximize the information provided by scan.
- Imaging of skin – This activity challenges measurements and reproduction of normal or diseased skin for diagnose (Kalwa (2019)).

Accuracy and consistency of calibration for medical imaging is receiving the attention as working on different fields, the ICC provides basic addresses to problems. As mentioned, ICC has worked on colour management and standardization. As ICC profiles used for visualization of colour medical displays, it also can be for greyscale (GSDF). The standardization content can be presented effectively on pseudo colours images, colour accurate images. Those results are represented and discussed in MIWG.

4.8 Introduction to the work in this study

This study investigates the feasibility of using mobile devices to view grey level medical images. Towards this end, a number of psychophysical experiments are conducted to study human perception perceiving grey patterns on both LCD monitor and mobile phones. The design of these experiments follow the guidelines from DICOM PS3.14, which is depicted in Figure 4.12.

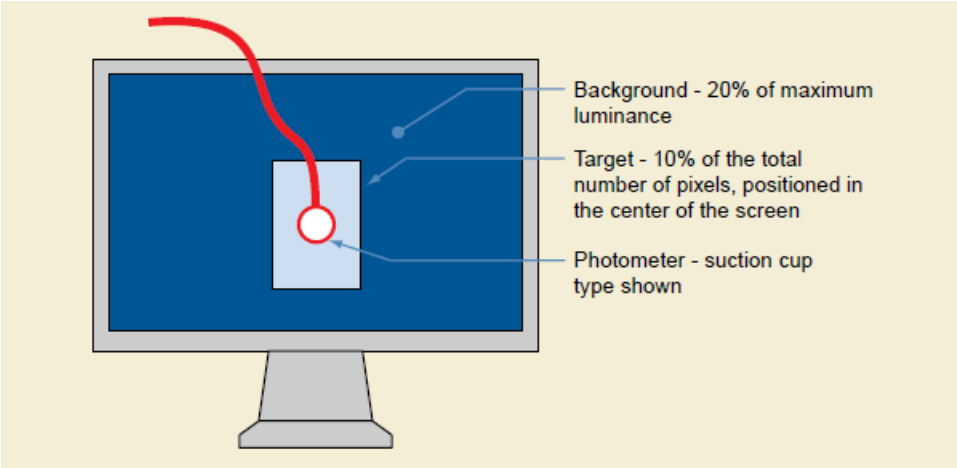

Figure 4.12. The standard layout of test pattern in relationship with surroundings (DICOM PS3.14).

In addition, Table 4.3 provides contrast ratios (Eq.(4.3)) (for all the displays studied in this work, which are all within the DICOM range of 250-500 for colour displays.

Table 4.3. Colour contrast ratio (C) for the colour devices studied in this thesis.

Display	LCD	iPhone6S	Motorola	Samsung S6	iPhone10
Contrast Ratio (C)	400	300	395	200	300

Chapter 5 Methodology

This section details the method of psychophysical experiments (Section 5.3) implemented. It contains how and why these experiments were conducted, what were their impact and outcome. In addition, a number of apparatuses are employed, which are elaborated below.

5.1 ColorMunki (Xtite, Konica-Minolta) and Colour meter CA-100

ColorMunki is applied to calibrate colour monitors into a fixed setting, in our case, D65. Images on different screens usually appear differently to our eyes. This is because the initial colour settings of those monitors are not the same. Most screens are having monitors' colours with different brightness levels. Colour brightness depends on the setting of a monitor, too. This process is called screen or monitor calibration.

To calibrate the screen, a sensor device is needed which fits on screen and measures the colour being displayed. The device is called spectrophotometer and measures the range of colours with a built-insoftware to adjust to an intended leveli Here, ColorMunki Smile is used to perform that, i.e. calibrate a computer screen.

As depicted in Figure 5.1, ColorMunki sensor retuens the measured colour patterns displayed on a screen and to modify these colours according to the pre-set conditions, e.g. D65, ensuring that what we see on display will be the same on all colour monitors..

Figure 5.1. Device ColorMunki (Xrite, Konica-Minolta)

The illuminant in these experiments is set to D65, i.e. average daylight, to be consistent with the other existing studies.

In addition, a colour meter is applied to measure a colour in the unit of tristimulus values of X, Y, Y and x, y, Y values. As such, the colour meter, Konica Minolta CA-100, which is illustrated in Figure 5.2, is a compact meter for taking colour measurement of reflective surfaces and light sources. This device has lens with a viewing window which accurately indicates area of colour to measure. It uses three high sensitivity silicon photocells to closely match with CIE standard observer response to measure light through lenses. Luminance data is displayed in viewfinder. Luminance and chromaticity values are shown in external display mounted on the side of the unit.

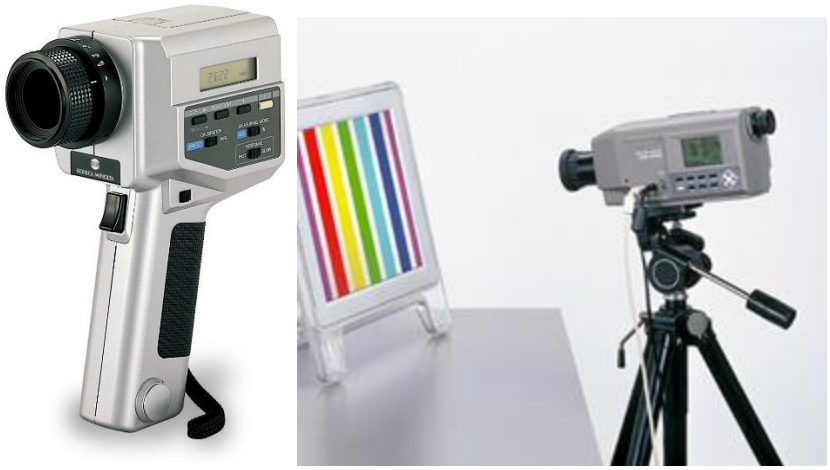

Figure 5.2. Colour meter, Konica Minolta CA-100

5.2 Direct Scaling and Magnitude Estimation

Each observer is asked to make a subjective estimation of the magnitude of visual attributes. The attributes might be lightness, colourfulness, saturation, chroma, and hue. An observer can simply assign a number that in his or her view corresponds to the magnitude of the chosen attribute in the sample being viewed. Alternatively, the observer might be asked to make a subjective estimate of the attribute on some more clearly defined scale, usually an equal-interval scale, or to compare two samples for an estimating parameter.

The magnitude estimation technique was first tested by Stevens et al. (Stevens (1957), Stevens (1975)). and has recently gained in general acceptance. It is a subjective scaling technique by which the magnitudes of perceived attributes are scaled. Rowe (Rowe (1973)) carried out their work to scale hue and saturation. They concluded that a surprising degree of precision can be achieved using this technique. In Ishak et al's study, two observers made estimations in terms of hue, saturation and lightness for 60 surface colours on seven backgrounds (Black, Grey, White, Red, Yellow, Green, and Blue background). They compared their results to these by Helson et al.

(using the memory method), Wassef, Hunt and Gibson (Gibson (1967)) using the binocular matching method). The results showed that the magnitude estimation method was reliable in producing results similar to those found using other methods. They concluded that the method was suitable for measuring colour appearance under a variety of viewing conditions. Following their study, Nayatani et al. (Nayatani (1972)) examined the precision of this method between and within observers, and reconfirmed its effectiveness. They made assessments for three attributes of 100 object colours by a panel of fifteen observers. A fluorescent lamp with a high colour-rendering index was used. Results showed a good agreement with those obtained by Ishaket al. This method was later employed by Bartleson (Bartleson (1979)) , Pointer (Pointer (1980)), and Luo et al (Luo (1991), Luo (1991a), Luo (1992), Luo (1993)).

In using a magnitude estimation technique, an observer simply views the test sample and assigns numbers or names that correspond to the colour attributes of its subjective appearance. Normally they are lightness, saturation, colourfulness, and hue.

Lightness is a subjective attribute that has been studied thoroughly by Stevens et al. and by many others. As far as the method applied to reflecting surfaces, it was relatively grey content that was examined (Pointer (1980)).

Brightness is defined by the CIE as the attribute of a visual sensation according to which an area appears to exhibit more or less light (Luo (1991)). It is a perceptually absolute quantity and has an absolute zero modulus without upper limit. For many years, attempts have been made to characterise perceived brightness as a function of stimulus luminance. A variety of predictive equations has been proposed. Stevens et al. (Stevens (1957), Sevens (1963)) specified brightness as a power function of luminance. Bartleson's brightness-scaling experiments with a complex

stimulus field showed that the resulting brightness vs luminance functions are not simple power functions but are nonlinear in log-log coordinates (Bartleson (1967), Bartleson (1980), Indow (1966), Hunt (1952)).

For estimating hue, four to six names of basic or unique colours are commonly used among which are Red, Yellow, Green, Blue and the two intermediate hue orange and yellowish-green. For colour appearance between the primary colours, i.e. red, yellow, green and blue, interpolations are used either in numerical form [59] such as "80% green, 20% yellow", or as combination names such as Blue-Green. This method is closely associated with NCS Colour System.

Earlier magnitude estimation experiments were conducted using saturation rather than colourfulness. Saturation assessments were reported by many researchers Pointer (1978)). In these studies, observers were asked to scale the saturation of a test colour on a scale which had fixed points at both ends. One end (zero) represented a colour with no saturation (a neutral colour), and the other end (100) represented the most saturated colour that the observer could imagine having the same hue as the test colour. The test colour was then scaled as a number between these two end points. This led to difficulties in analysing the data because the most saturated colour varied in absolute saturation for different hues, for example, a most saturated blue could be more saturated than a most saturated yellow.

The concept of colourfulness was introduced by Hunt (Hunt (1957), Hunt (1987), Hunt (2006)) to denote the attribute of a visual sensation according to which an area appears to exhibit more or less chromatic colour. Pointer's (Pointer (1978)) results showed that this concept is meaningful to the observers who were asked to rank colour chips in order of colourfulness and also able to scale the colourfulness of each individual chip. In this experiment, colourfulness was scaled under various luminance levels and backgrounds. A correlation coefficient of 0.97 was obtained between

mean of saturation and colourfulness. This suggested that there was a high degree of correlation between these two attributes. He concluded that colourfulness was a useful concept which observers were well able to scale and may be more easily scaled than saturation or chroma. If a full measure of the appearance of a colour is required, colourfulness can provide changes in chromatic response caused by the luminance levels.

5.3 Detection of colour vision deficiency with Ishihara test method

Around observers were invited to conduct psychophysical experiments in this study. To start with, each observer was checked whether they have normal colour vision by applying Ishihara colour charts. Ishihara experiment was introduced by Dr Shinobu Ishihara (Ishihara (2017)) in 1917 known as colour blindness test. Each of these tests consists of a set of coloured dotted plates, each of them showing either number or letter. This is most widely used colour vision deficiency test and used by most optometrists and ophthalmologists all around the world. It is also known that even people with normal colour vision sometimes struggle with this test.

The same test was taken for all observers before conducting physiological experiments. Ishihara experiment is based on psychology. This Colour vision test was performed on observers as it measures the ability to tell difference among colours. If an obserber failed to detect the intended patten as illustrated in Figure 5.3, there is high chance that this observer have a poor colour vision and were not included in our study.

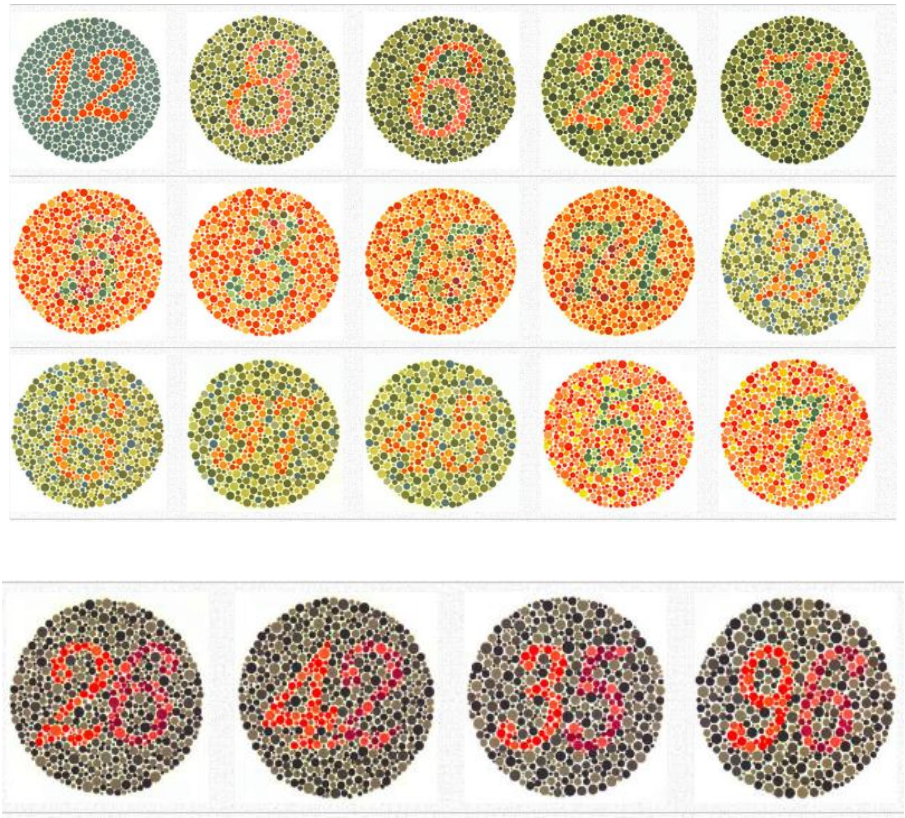

Figure 5.3. Example of number plate in the Ishihara colour vision test (Ishihara (2017)).

Another common colour-blind test is called '100-Hue Test'. That test contains four distinct rows of similar colour hues, containing 25 variations of each hue. Each colour of hue at the polar end of a row is fixed in position. Each hue tile between the anchors can be adjusted as the observers fits into the final arrangement representing the visual system. The difference of vision is calculated per position of tile that where it has placed and where exactly it should be placed.

For this examination, Ishihara test method was chosen as it is an accurate, easy to operate and most common method used to check colour blindness. This test is quick to provide result and easily accessible in the form of either online or on paper. Observers' vision was tested showing the images (Figure 5.3) to check whether a person is colour blind. In this study, psychophysical experiments were performed by those observers who has passed Ishihara test.

5.4 Psychophysical Experiment

This section introduces the methodologies to estimate colours using a magnitude estimation method. With these data, a colour appearance model for modelling colour was enhanced to display images using a smart phone with a small screen with similar features as displayed in a colour monitor (e.g. big screen).

Twenty test colours were selected to cover a wider range of grey colours, which is depicted in Figure 5.4. They were chosen according to the lightness value on a colour monitor calibrated with D65 with an interval of 5, which was completed using Matlab program. That is along the scale of lightness (the sum of Red, Green, and Blue values of an image pixel) in a computer between 0 (minimum) and 100 (maximum), the samples with values of 1, 5, 10, 15, 20, 25, 30, 35, 40, 45, 50, 55, 60, 65, 70, 75, 80, 85, 90 and 95 were selected. The samples in Figure 5.4 was sequenced in the same order as they were appearing in one of psychophysical experiments carried out in this study. This is to avoid memory glitching. Each observer would not use the same order of samples twice.Most observers with normal colour vision that were check using Ishihara colour vision test are recruited in this preliminary experiment. All subjects are aged between 20 and 33 with varying professional background (research students, IT professionals, and staff). All of them perform one or more experiments after initial training.

A series of psychophysical experiments are conducted to estimate the viewing differences when a grey sample presented on both a monitor and an iPhone. In these experiments, a 15” LCD monitor (Dell Latitude E5450Laptop running windows 10 OS) with resolution of 1366x768 is utilized as well as mobile phones with brands of Motorola, Samsung, iPhone 6S, and iPhone 10. The colour

monitor is calibrated to D65 every day before an experiment starts. Twenty test samples are selected to cover wider range of lightness as illustrated in Figure 5.4. The blue background is only for highlighting the grey samples. In the real psychophysical experiments, the viewing pattern shown in Figure 5.5 is applied, where the middle sample is to be estimated by the observers and is changed from sample 1 to sample 20. The rest surrounding samples are fixed and remain the same for the whole experiment. Reference white (RW) has lightness of 100 for all experiments so that observers are asked to estimate the lightness with reference of RW in a linear scale.

All the experiments are conducted in a dark room where the mobile phones have their brightness settings to the maximum.

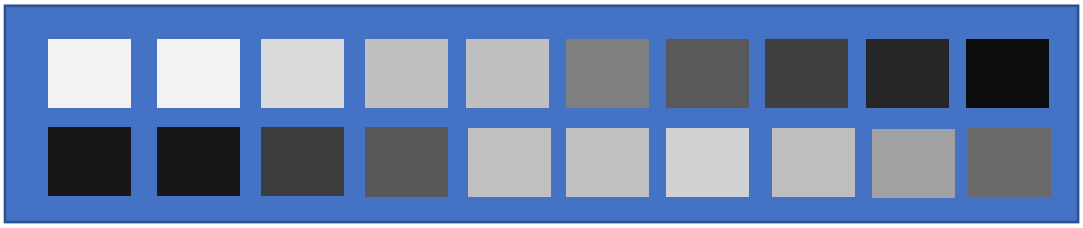

Fig 5.4. The twenty test samples that are applied in the estimation experiments

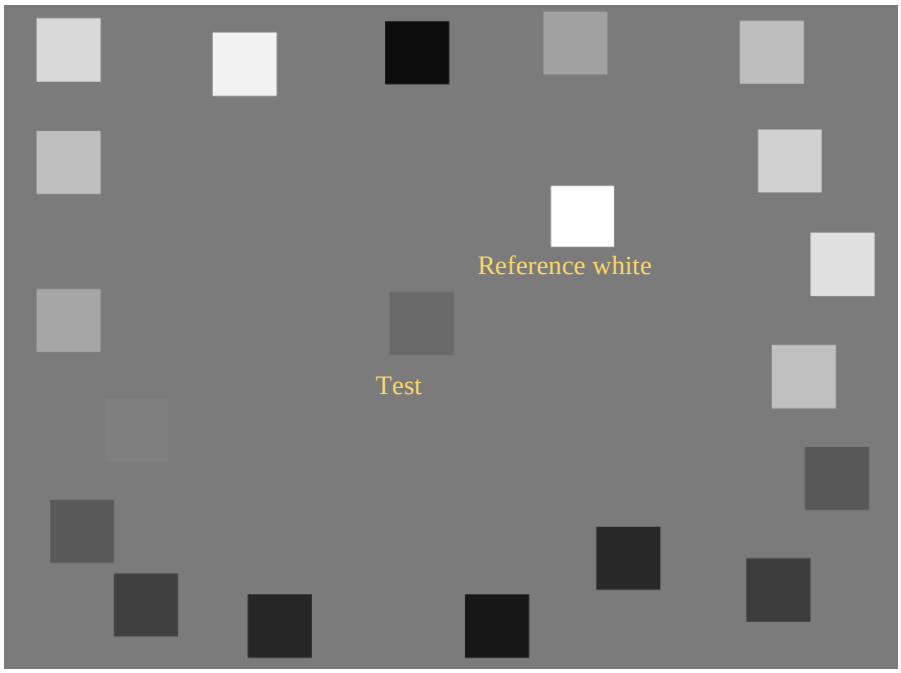

Figure 5.5. The viewing pattern applied in the experiment, where reference white is assigned as 100.

In the experiment, the observers are asked to estimate the lightness of the test sample positioned in the middle of Figure 5.5 with reference to reference white (RW), either on a monitor or an iPhone. As illustrated in Figure 5.5, each test sample is placed at the centre against a grey background (with 20% of luminance of reference white) and surrounded by the reference white and surrounding grey samples. In other words, lightness represents the degree of brightness colour shows. With reference white being 100 and an imaginary black being zero, observers are asked to give an estimation between 0 and 100 that is proportion to the reference white. For example, if a test sample appears half as bright as the reference white to a subject, 50% of lightness should be assigned to the colour. Neutral colours including white, black and grey have zero colourfulness.

The test field in the centre subtends a visual angle of 2^{o} at a viewing distance of approximately 60cm. The subjects are instructed that the lightness of RW is 100 whereas their imaginary black is

0. Then the lightness of the test sample should be a value between 0 and 100, in proportion to RW. For example, if a test sample is given a value of 60, then its lightness is 60% as bright as the lightness of RW.

10 observers with mixed gender participated in each experiment. Observers' age, occupation and the number of experiment repetition is represented in Table 5.1.

Table 5.1 Observers' information

Age	Gender	Occupation	no of experiments
28	Female	Student	8
31	Male	IT Professional	2
33	Female	IT Professional	1
19	Female	Student	1
22	Male	Student	1
21	Male	Student	1
21	Female	Student	1
22	Male	Student	1
38	Female	House Maker	1
29	Male	Business Manager	1

5.5 Sample measurements using Minolta CA-100 colour meter

Psychophysical experiments are conducted to estimate colours subjective. To obtain colour physical data of each sample, measurements take place by using colour apparatuses.

At the start of each experiment, the LCD laptop monitor is calibrated to D65 (average daylight) using ColorMunki Smile software. During the experiment, only the middle test sample in Figure 5.5 changed between different grey levels as illustrated in Figure 5.4. The surround samples and RW remain the same. This design of the viewing pattern is to reflect the real-world viewing conditions. For the iPhone 6S, the brightness is set to the maximum.

To calibrate the screen, device is needed which fits on screen and measures the colour being displayed. The device is called spectrophotometer and it measures the range of colours and match software ranges to it. Here, ColorMunki Smile is used to calibrate screen as demonstrated in Figure 5.6 (a), whereby the colour patches in the middle changes (Figure 5.6(b)) Then the colour measurements in tristimulus values of X, Y, Z will be sent back the system to compare with the pre-settings, e.g. D65. Adjustments will be made if needed to ensure the final monitor setting will be D65.

(a)

(

(b)

Figure 5.5. The process to calibrate a colour monitor using ColorMunki package. a) colour patch starts with white; b) colour patch changes with varying colours.

In addition, a Minolta Chroma Meter CS-100A, was used to measure each colour in terms of CIE tri-stimulus values x, y, Y. While using CS-100A, the view finder is adjusted to be 2^{o} at a distance

of 45 cm. While focus is correct, the readings of Y, x, y will be displayed on the Chroma Meter small screen as well as showing on the view finder.

Figure 5.7 displays the measurements of 20 test samples given in Figure 5.3 in a chromaticity diagram.

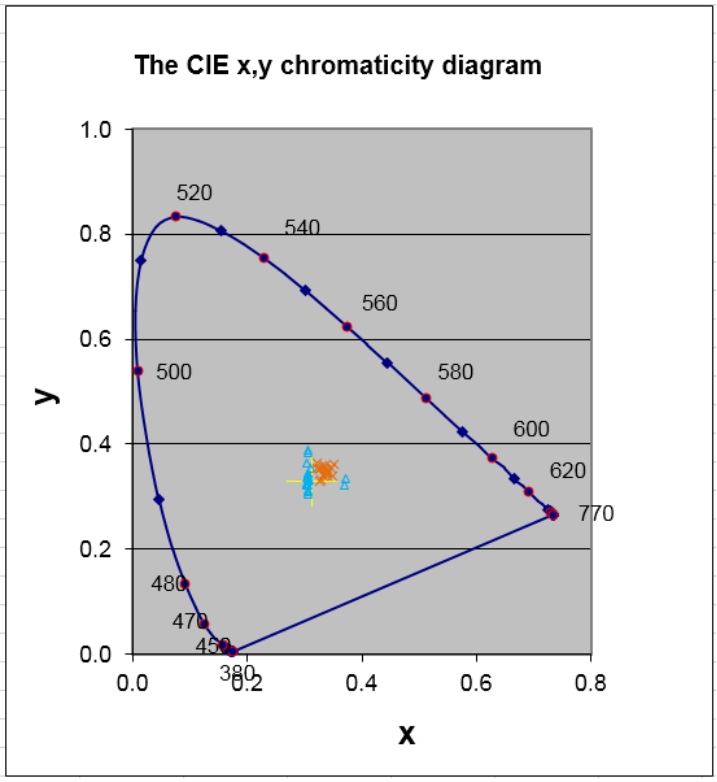

Figure 5.7 The xy measurements for both LCD monitor (x) and iPhone 6s (blue triangle) presented on a xy-chromaticity diagram. The big yellow sign + refers to D65 white point (x=0.3128, y= 0.329).

Chromaticity values of x and y are the relative values of tristimulus values of X, Y, and Z, where Y represents luminance. The conversion between x, y, Y and X, Y, Z are expressed in Eqs (5.1) to (5.3).

$$X = \frac{x}{y} Y \qquad 5.1)$$

$$Y = Y \tag{5.2}$$

$$Z = \frac{1-x-y}{y} \mathrm{Y} \tag{5.3}$$

Sample measurements using Colour meter CS-100A takes before and after each psychophysical experiment on the samples display in Figure 5.5 in order to reflect the real experimental environment. In particular, the background and reference white are measured 3 times, at the beginning, middle and end of measuring 20 test samples to evaluate the consistency of colour monitors, mobile phones as well as colour meter itself. These measurements are provided in Appendixes A1.1 to A1.3 for Y, x, y values with a standard deviation of 7.9%, 6.5% and 5.5% respectively, which appears to be consistent with regarding to both LCD monitor, mobile phone and colour meter. Figure 5.8 depicts these twenty colour samples in a xy-chromaticity diagram.

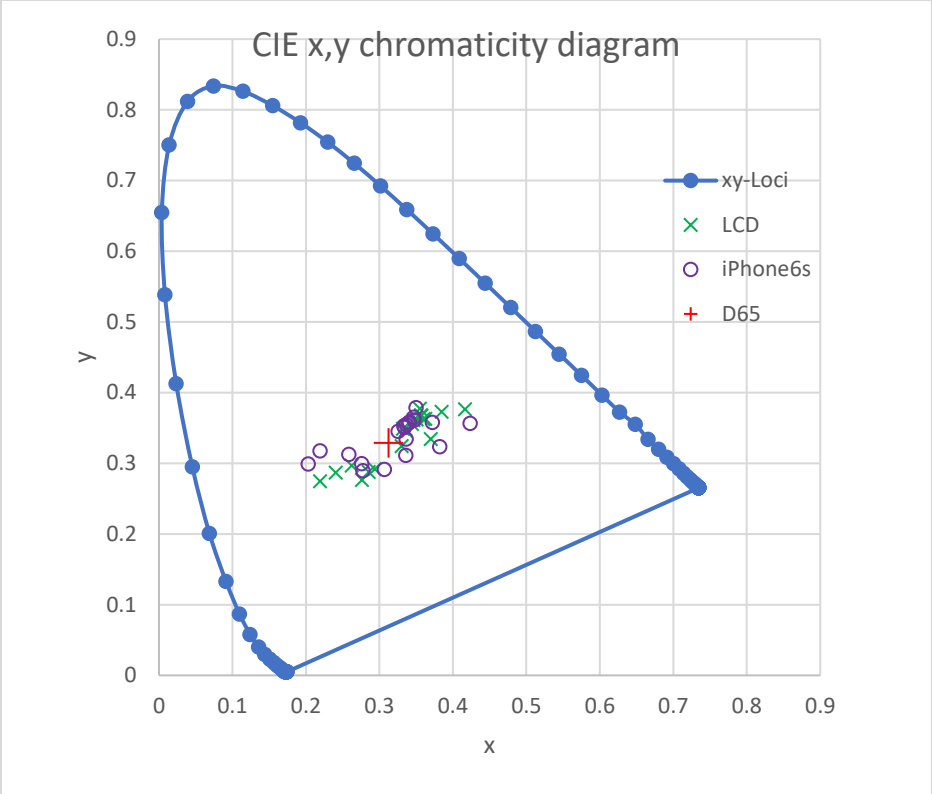

Figure 5.8. Presentation of twenty colour samples for studying the consistency of LCD monitor (x), mobile phones (o) and CS-100A colour meter. D65 is represented using big cross (+).

Chapter 6. Experimental results for LCD colour monitor

This chapter discusses the experimental results, including both subject estimations and physical colour measurements from both monitors and mobile phones. Statistical measure of correlation of variation (CV) is applied to study observers' performance. Correlation of variation (CV) value is calculated using Eq. (6.1).

$$CV = \frac{Standard\ Deviation}{Mean} \tag{6.1}$$

Whereas standard deviation (SD) is formulated in Eq. (6.2).

$$\mathrm{SD} = \sqrt{\frac{\sum(\mathrm{xi}-\bar{\mathrm{x}})^2}{(n-1)}} \tag{6.2}$$

6.1 Observer study

Before commence of psychophysical experiments, observer training takes place to ensure that each observer understand the technique of subject estimation. This training is conducted on an LCD monitor. Around 20 observers were invited for the training, which are divided into 2 groups with observer numbers being 15 and 5 respectively. For the first group, their estimations on lightness are provided in Appendix A0, whereas the CV values in comparison with mean is given in Table 6.1. In Table 6.1, sample #17 has lightness close to 0. Hence the corresponding CV values appear quite large. When consider observer's performance, this sample estimation is ignored. The last row of Table 6.1 is the mean CV values for each observer. Observers 1, 4, 5, 7, and 13 have considerable larger CVs (in red), i.e., 25.9%, 30.2%, 24.8%, 22.8% and 23% respectively. Hence these observers are not invited for the following psychophysical experiments.

Table 6.1 CV values for the fifteen observers for training.

	Ob1	Ob2	Ob3	Ob4	Ob5	Ob6	Ob7	Ob8	Ob9	Ob10	Ob11	Ob12	Ob13	Ob14	Ob15
1	5.3	3.1	5.3	0.1	5.2	3.1	4.1	3.1	5.3	5.3	0.1	5.2	3.1	0.1	5.3
2	0.2	5.6	6.1	5.6	10.3	0.2	6.1	0.2	5.6	4.5	0.2	6.1	12.0	6.1	5.6
3	7.2	14.9	7.2	7.2	16.0	0.5	8.2	0.5	8.2	8.2	8.2	0.5	22.7	0.5	8.2
4	10.3	10.3	37.9	10.3	44.9	17.3	10.3	6.3	17.3	37.9	37.9	17.3	44.9	17.3	10.3
5	4.6	1.1	1.2	2.2	10.4	4.6	1.2	4.6	4.7	7.0	8.2	1.2	4.6	1.2	7.0
6	22.3	16.6	16.6	16.6	41.7	22.3	2.8	22.3	16.6	28.2	8.8	2.8	2.8	2.8	16.6
7	2.3	3.1	3.1	2.3	7.7	3.1	2.3	0.1	8.5	3.1	3.1	2.3	7.7	3.1	2.3
8	4.5	22.7	4.5	9.1	18.2	4.5	9.1	9.1	9.1	18.2	4.5	22.7	31.8	18.2	22.7
9	12.4	3.6	12.4	3.6	4.4	3.6	4.4	11.7	3.6	0.4	8.5	11.7	12.4	4.4	3.6
10	2.7	23.3	2.7	2.7	48.6	28.1	2.7	23.3	17.8	2.7	2.7	54.1	48.6	23.3	2.7
11	5.5	40.9	29.1	41.7	29.9	17.3	5.5	6.3	6.3	5.5	18.1	6.3	29.1	6.3	18.1
12	21.9	4.2	4.2	21.9	56.3	21.9	21.9	30.2	4.2	4.2	6.3	21.9	30.2	4.2	21.9
13	4.5	4.5	4.5	4.5	9.1	2.3	4.5	9.1	2.3	4.5	2.3	9.1	2.3	4.5	4.5
14	25.9	1.9	20.4	7.4	11.1	16.7	7.4	20.4	11.1	1.9	16.7	1.9	11.1	1.9	7.4
15	33.8	44.9	37.9	37.9	17.3	44.9	33.8	10.3	26.8	10.3	17.3	37.9	17.3	10.3	37.9
16	2.8	2.6	3.9	2.6	2.8	2.6	2.6	2.6	2.6	2.8	2.6	2.6	2.8	2.8	2.8
17	**294.7**	**100.0**	**57.9**	**294.7**	**100.0**	**57.9**	**294.7**	**100.0**	**100.0**	**100.0**	**100.0**	**100.0**	**100.0**	**100.0**	**100.0**
18	10.1	23.9	10.1	23.9	31.2	17.4	3.7	10.1	3.7	10.1	23.9	3.7	31.2	17.4	3.7
19	36.5	20.6	58.7	98.4	20.6	19.0	20.6	28.6	36.5	20.6	4.8	19.0	34.9	20.6	20.6
10	10.3	6.3	10.3	10.3	9.8	0.3	9.8	10.3	9.8	10.3	0.3	0.3	9.8	0.3	19.8
Mean	**25.9**	**17.7**	**16.7**	**30.2**	**24.8**	**14.4**	**22.8**	**15.4**	**15.0**	**14.3**	**13.7**	**16.3**	**23.0**	**12.3**	**16.1**

After training, fourteen observers (7 males and 7 females) with normal colour vision are recruited in this study. Each experiment is usually conducted by 10 of 14 observers depending on their availability.

Tables 6.2 and 6.3 illustrates observers' estimation for 20 samples on both LCD and iPhone-6S together with mean and CV values.

Table 6.2 Subjects' estimations for 20 samples on LCD monitor

Observers **Sample no**	**1**	**2**	**3**	**4**	**5**	**6**	**7**	**8**	**9**	**10**	**Mean**	**CV**
1	90	96	98	95	98	90	95	95	96	95	94.8	2.78
2	85	85	90	80	90	80	86	80	85	90	85.1	4.56
3	60	60	55	60	55	60	62	55	65	60	59.2	5.28
4	20	24	20	25	20	25	27	25	20	20	22.6	11.91
5	90	88	87	85	75	85	92	82	95	88	86.7	6.06
6	20	30	30	30	25	30	35	20	25	30	27.5	16.76
7	95	85	90	90	95	90	90	80	85	95	89.5	5.27
8	35	40	45	30	40	35	45	38	30	40	37.8	13.37
9	70	60	60	75	65	70	75	60	60	60	65.5	9.32

10	10	15	12	8	10	10	10	10	10	10	10.5	16.63
11	40	35	25	25	40	30	45	50	55	60	40.5	28.40
12	15	23	20	20	10	20	15	18	15	15	17.1	21.00
13	70	78	70	75	75	70	80	70	75	70	73.3	4.92
14	40	45	55	40	45	65	55	50	60	50	50.5	15.62
15	12	20	10	15	20	25	15	18	10	25	17	31.02
16	95	95	90	90	95	96	85	90	95	90	92.1	3.71
17	5	5	0	3	0	2	5	5	5	5	3.5	57.50
18	40	40	45	40	35	40	30	45	35	45	39.5	11.94
19	8	10	10	20	15	20	20	10	25	25	16.3	37.92
20	55	52	53	50	50	55	45	55	50	55	52	6.02
Average												15.50

represent the estimated white colour percentage in the grey shades of chosen colour based on Monitor visibility. Observers are trained and explained on how to do the estimation and give the proper percentage amount. Same experiment was done on iPhone 6S by same observers for the same colour shades. The left numbers 1 to 20 show the number of shade and right are the noted readings. This experiment was carried out in the dark room where no light rays are entered to get actual idea of the colour shade.

Table 6.3. Observers' estimation of lightness form 20 samples on an iPhone6S mobile

Observer **Sample no**	**1**	**2**	**3**	**4**	**5**	**6**	**7**	**8**	**9**	**10**	**Mean**	**CV**
1	92	95	99	98	98	92	95	90	99	95	95.3	3.18
2	85	80	95	80	95	85	80	85	85	90	86	6.26
3	65	60	65	55	60	60	68	55	68	65	62.1	7.36
4	25	20	15	20	25	28	20	22	15	20	21	18.93
5	95	80	85	85	80	87	90	85	90	88	86.5	5.05
6	25	20	25	29	28	30	30	25	20	35	26.7	16.59

7	90	75	85	80	90	95	95	85	80	90	86.5	7.33
8	35	40	40	35	45	30	50	30	35	50	39	17.95
9	65	60	65	70	70	70	75	79	65	60	67.9	8.55
10	8	10	10	8	12	10	8	10	10	10	9.6	12.50
11	35	30	35	20	45	35	40	55	50	50	39.5	25.60
12	10	25	15	20	15	20	10	18	20	12	16.5	28.46
13	75	88	75	70	70	75	85	75	78	70	76.1	7.67
14	45	40	50	45	45	55	60	54	65	55	51.4	14.38
15	10	25	15	10	15	20	10	15	18	20	15.8	30.19
16	95	90	96	92	90	90	85	95	98	90	92.1	3.99
17	0	5	0	5	5	1	3	0	5	5	2.9	77.80
18	50	20	40	43	35	45	26	42	30	45	37.6	24.18
19	10	10	10	12	15	15	20	10	20	25	14.7	34.56
20	50	46	55	50	50	50	45	55	45	50	49.6	6.82
Average												**17.87**

Every observer provided an estimated percentage of lightness with reference to reference white (100) for each of 20 grey samples subjectively. Figure 6.1 presents an example of comparison of estimation given by observer 1 for the LCD monitor and iPhone 6S. Figure 6.2 plots the comparison results for average observer between LCD and iPhone6S. Appendices A0.1 to A0.11 detail observers' estimations on mobiles of iPhone6S, Motorola, Samsung and iPhone10 together with their CV values. The average CV values are 23.96, 14.72, 14.03, 11.67 respectively for iPhone6S, Motorola, Samsung, and iPhone10. Since observers start with iPhone6S and are less experienced, the CV is the largest for iPhone6S. Their performance is getting better when they are more experienced with estimating on phones of Motorola (14.72), Samsung (14.30) and iPhone10 (11.67). For modelling of iPhones, the estimation on iPhone6S is repeated several times with 3

iPhon6S after they are getting more experienced. In average, the CV values for estimating lightness in this study is around 14%.

In Figure 6.1, blue dots are for monitor readings and orange dots for iPhone 6S readings.

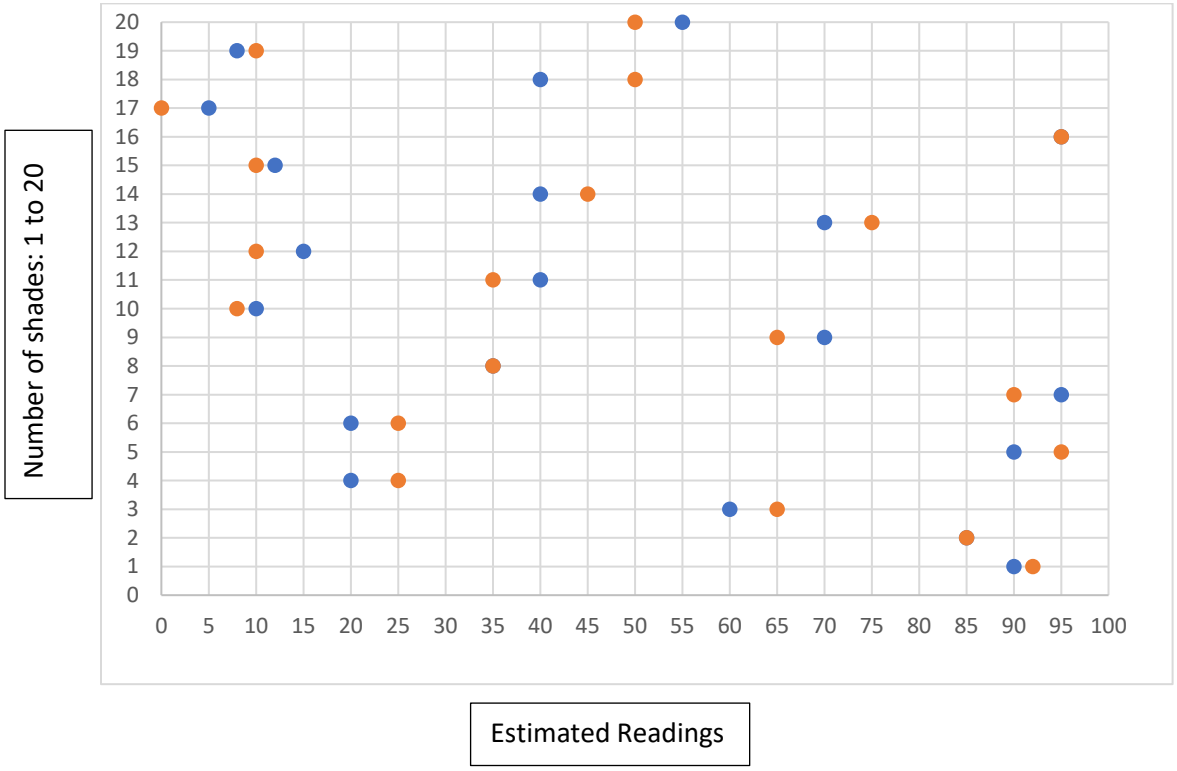

Figure 6.1. Comparison between monitor (blue dot) and iPhone6S (orange dot) by observer 1 for 20 test samples.

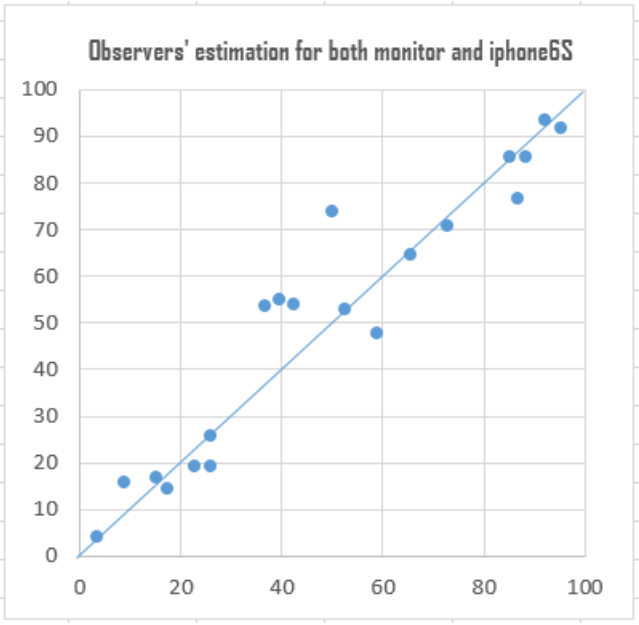

Figure 6.2. Comparison of estimations between monitor (x) and iphone-6S.

The average CV values for estimating 20 samples on LCD and iPhone are 15.50% and 17.87% respectively. It indicates that more errors occur for observers when they estimate on iPhone screen, which is expected given the fact that a phone has a small screen.

In the existing publications [Gao (2015), Luo (1993], Green (2018)] , the CV values for estimating lightness is around 10%. Our study appears to have 5.5% more errors while on LCD. This is partially due to the face that the 4 (20%) selected samples are very darker and close to black with lightness smaller than 20, which are quite challenging to estimate. In the future, more samples will be included to verify this.

These conducted physiological experiments provide an insight on human's perception on estimating lightness when they view grey level samples on either LCD monitor or mobile phones. Lightness attribute is a relative term and has a value between 0 (totally dark, not light going through) and 100 (the brightest patch with all lights coming through.

6.2 Grey colours measurement on an LCD monitor

LCD laptop monitor is calibrated to D65 (average daylight) using Colormunki Smile software. While conducting the experiment, only the middle test sample in Figure 5.5 is changing between different grey levels as illustrated in Figure 5.3. The surround samples and RW remain the same. This design of the viewing pattern is to reflect the real-world viewing conditions. For the mobile phones of Motorola, Samsung, iPhone 6S and iPhone 10, the brightness is set to the maximum.

The measurements of x, y and Y values for these 20 samples are performed using Minolta CS-100A colour meter and are given in **Appendices A1.1 to A1.3**. The conversions between tristimulus values of X, Y, Z and CIEL*a*b* are provided in **Appendices A2.1 to 2.3** according to Eqs. (6.3) to (6.7). Equation Eq. (6.8) provide information for calculation of colour difference (ΔE^*_{ab}) in form of CIELAB.

$$L^* = 116f\left(\frac{Y}{Y_n}\right) - 16 \tag{6.3}$$

$$a^* = 500(f\left(\frac{X}{X_n}\right) - f\left(\frac{Y}{Y_n}\right)) \tag{6.4}$$

$$b^* = 200(f\left(\frac{Y}{Y_n}\right) - f\left(\frac{Z}{Z_n}\right)) \tag{6.5}$$

Where

$$F(t) = \begin{cases} \sqrt[3]{t} & if\ t > 0.008856 \\ \frac{t}{0.1284} + \frac{4}{29} & otherwise \end{cases} \tag{6.6}$$

For standard illuminant D65:

$$X_n = 96.4212$$
$$Y_n = 100 \quad (6.7)$$
$$Z_n = 82.5188$$

Given two colors in CIELAB color space, (L_1^*, a_1^*, b_2^*) and (L_2^*, a_2^*, b_2^*), the CIE76 color difference formula is defined as

$$\Delta E_{ab}^* = \sqrt{({L_1}^* - {L_2}^*)^2 + ({a_1}^* - {a_2}^*)^2 + ({b_1}^* - {b_2}^*)^2} \quad (6.8)$$

In particular, the value of $\Delta E_{ab}^* \approx 2.3$ corresponds to s Just noticeable difference (JND) (Sharma (2003)).

In this study, the average measurements for 20 samples on an LCD monitor is 3.93 as given in Table 6.4. The corresponding values of L*,a*,b* are provided in Appendices A2.1 to A2.3. The calculation of ΔE_{ab}^* is carried out using Eq. (6.9) based on mean values of $((L_m^*, a_m^*, b_m^*)$, which might be one of the reasons of ΔE_{ab}^* being slightly higher than 2.3.

$$\Delta E_{ab}^* = \sqrt{({L_1}^* - {L_m}^*)^2 + ({a_1}^* - {a_m}^*)^2 + ({b_1}^* - {b_m}^*)^2} \quad (6.9)$$

Table 6.4. The values of ΔE_{ab}^* for each sample that is calculated using Eq. (6.9).

ΔE_{ab}^*										Mean |mb*|
3.44	4.28	2.82	12.69	2.68	4.84	2.82	2.39	4.26	2.79	4.30
6.32	3.42	7.62	3.05	10.85	3.77	7.62	3.06	3.42	3.06	5.22
4.37	7.20	4.30	3.82	10.30	7.28	4.30	3.79	7.15	3.83	5.63
1.26	1.33	1.30	1.60	3.82	1.37	0.26	1.31	1.33	1.53	1.51
2.93	6.63	5.99	1.49	2.84	9.20	5.26	4.92	6.58	4.92	5.08

1.33	1.25	0.65	1.24	1.25	0.97	0.65	2.36	1.70	2.16	1.36
2.32	7.23	4.02	3.70	1.01	12.63	4.02	3.07	7.35	2.98	4.83
1.56	2.56	0.54	3.17	0.65	3.17	0.54	2.81	2.49	3.51	2.10
4.05	6.02	3.52	3.53	3.31	6.79	3.52	4.61	6.02	4.61	4.60
1.82	1.48	1.22	0.47	2.60	2.52	1.22	3.37	2.98	1.44	1.91
1.01	4.00	1.29	0.89	4.12	1.76	1.29	3.39	4.00	3.39	2.51
2.45	4.23	1.46	11.03	2.97	3.88	2.35	1.36	4.53	2.17	3.64
1.98	8.34	4.51	5.51	4.77	6.26	4.51	4.04	8.38	4.45	5.28
2.12	4.19	1.06	4.49	3.13	5.77	1.06	1.41	4.18	1.41	2.88
0.93	1.00	0.88	0.96	0.56	0.60	0.88	0.25	0.84	1.20	0.81
4.35	11.72	6.61	5.45	4.02	16.23	6.61	5.24	11.98	5.34	7.76
1.56	4.66	6.55	6.57	1.17	13.09	6.55	5.58	4.69	5.85	5.63
3.37	3.26	6.46	2.11	3.42	6.80	6.46	1.08	3.77	1.21	3.79
2.58	4.52	3.97	3.40	2.69	5.07	3.97	3.37	5.99	3.62	3.92
3.97	7.78	3.88	3.58	5.41	16.45	3.88	3.08	7.89	3.02	5.89
									Average	**3.93**

In additional of grey samples, 14 observers (Table 6.5) are recruited to estimate 25 colour samples including lightness, colourfulness, and hue. These colour samples are presented in Figure 6.3 on a xy-Chromaticity diagram.

Table 6.5. The information about the observers with normal vision who are trained in this study.

Age	Gender	Occupation	No of experiments
28	Female	Student	3
31	Male	IT Professional	2
33	Female	IT Professional	2
19	Female	Student	3
22	Male	Student	1
21	Male	Student	2
21	Female	Student	1
22	Male	Student	2

33	Female	House Maker	1
29	Male	Business Manager	2
23	Female	Student	2
19	Male	Student	1
18	Female	Student	2
26	Male	Student	1

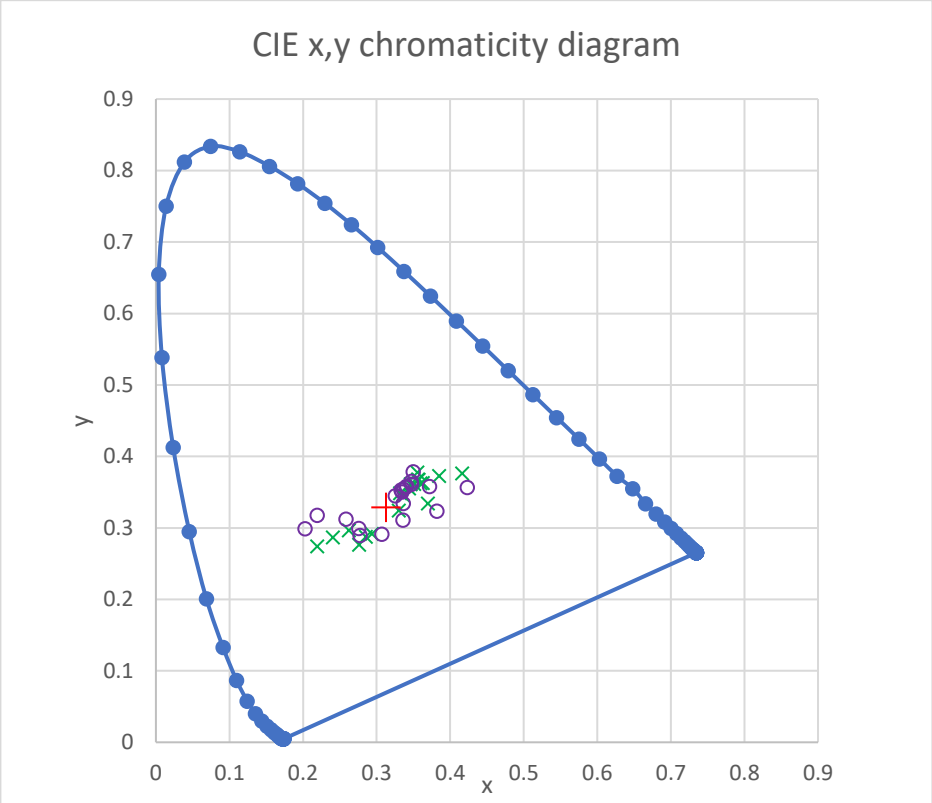

Figure 6.3. The xy measurements for both LCD monitor (x) and iphone 6s (triangle) presented on a xy-chromaticity diagram. The big yellow sign + refers to D65 white point (x=0.3128, y= 0.329).

Chapter 7. Experimental Results for mobile phones

7.1 Grey sample measurements on Mobile Phones

Task of measuring grey colours was performed on mobile devices as well to find difference between measurements. The experiments were conducted on 4 different models of mobile phones as listed in Table 7.1.

Table 7.1. Information on smart phones that are studied in this project.

	iPhone 6S	iPhoneX	Motorola	Samsung S8	iPhone 13 pro max
Screen	4.7 inches	5.8 inches	5.70 inches	5.8 inches	6.7 inches
Resolution	1334x750	2436x1125	720x1440	2960x1440	2778x1284

Figures 7.1 illustrates the experiment measurements for the 4 phones, which are iPhone 6S, Motorola, Samsung and iPhoneX.

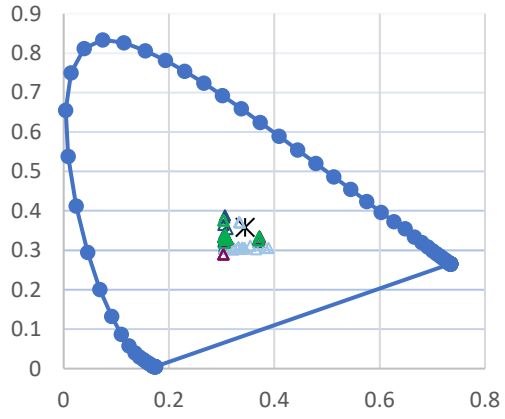

iPhone6S

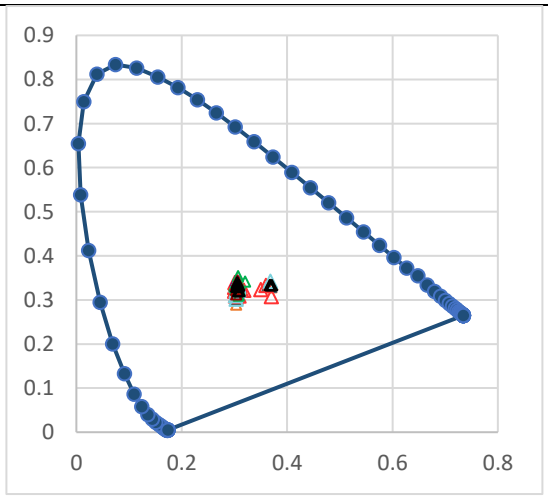

Motorola

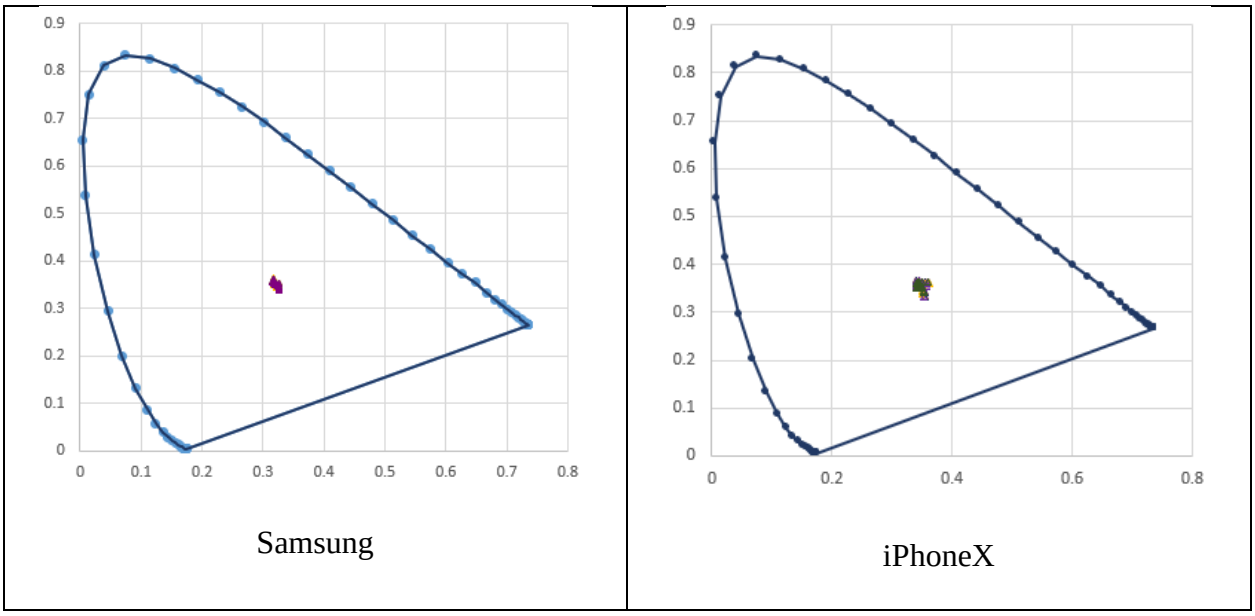

Figure 7.1. The x, y data plotted in CIE diagram for twenty sample on iPhone 6S, Motorala, Sumasung, and iPhoneX.

It appears the measurements for iPhone6S and Motorola spread slightly wider than those on Samsung and iPhoneX. **Appendix A3** details x , y, Y measurements for those mobiles phones.

7.1 Observer's Study

As discussed in Section 5.3, all observers who cleared Ishihara Test were trained for psychophysical experiments. In this section the differences between observers' perception on colour monitor and mobile phones are investigated. Tables 7.2 to 7.5 provides the observers' information for conducting psychophysical experiments.

Table 7.2. Observers information for iPhone6S experiment.

Age	Gender	Occupation	No of experiments
28	Female	Student	2
31	Male	IT Professional	2
22	Male	Student	1
19	Female	Student	2

23	Male	Student	1
32	Female	House Maker	1
19	Male	Student	1

Table 7.3. Observers information for Motorola experiment.

Age	Gender	Occupation	no of experiments
28	Female	Student	1
31	Male	IT Professional	1
18	Male	Student	1
22	Female	Student	1
22	Male	Student	1
19	Female	Student	2
23	Male	Student	1
32	Female	House Maker	1
19	Male	Student	1

Table 7.4. Observers information for Samsung experiment.

Age	Gender	Occupation	no of experiments
28	Female	Student	1
31	Male	IT Professional	1
18	Male	Student	1
22	Female	Student	1
28	Female	Student	1

Table 7.5. Observers information for iPhoneX experiment.

Age	Gender	Occupation	no of experiments
28	Female	Student	1
31	Male	IT Professional	1
18	Male	Student	1
22	Female	Student	1
28	Female	Student	1

Observer number vary between 5 to 9 based on the availability of participants.

7.2 Statistical method of mean for evaluation

In statistical terms continuous variables are described by a mean and measures of variation. Standard deviation and coefficient of variation are the forms to describe the variations for the data.

The mean is calculated as the sum of values divided by the number of readings taken per observer as given in Eq. (7.1)

$$\bar{x} = \frac{x_1 + x_2 + \cdots + x_n}{n} \tag{7.1}$$

Figure 7.2 exemplifies the observer's performance for Observer 1 on both LCD monitor and iPhone6S. Each observer was asked to perform 4 experiments (Exp) to estimate 20 grey samples on both LCD monitor and Mobile phones.

	Exp 1	Exp 2	Exp 3	Exp 4	Mean
1	90	98	90	95	93.25
2	85	90	80	90	86.25
3	60	55	60	60	58.75
4	20	20	25	20	21.25
5	90	87	85	88	87.5
6	20	30	30	30	27.5
7	95	90	90	95	92.5
8	35	45	35	40	38.75
9	70	60	70	60	65
10	10	12	10	10	10.5
11	40	25	30	60	38.75
12	15	20	20	15	17.5
13	70	70	70	70	70
14	40	55	65	50	52.5
15	12	10	25	25	18
16	95	90	96	90	92.75
17	5	0	2	5	3
18	40	45	40	45	42.5
19	8	10	20	25	15.75
20	55	53	55	55	54.5

	Exp 1	Exp 2	Exp 3	Exp 4	Mean
1	92	95	99	98	96
2	85	80	95	80	85
3	65	60	65	55	61.25
4	25	20	15	20	20
5	95	80	85	85	86.25
6	25	20	25	29	24.75
7	90	75	85	80	82.5
8	35	40	40	35	37.5
9	65	60	65	70	65
10	8	10	10	8	9
11	35	30	35	20	30
12	10	25	15	20	17.5
13	75	88	75	70	77
14	45	40	50	45	45
15	10	25	15	10	15
16	95	90	96	92	93.25
17	0	5	0	5	2.5
18	50	20	40	43	38.25
19	10	10	10	12	10.5
20	50	46	55	50	50.25

(a) Monitor	(b) iPhone6S

Figure 7.2. Mean values for Observer 1 evaluating 20 samples in four experiments (Exp) on both LCD monitor (a) and iPhone6S (b).

Figure 7.3 compares the mean values for Observer 1 between LCD monitor (x) and iPhone6S (y). It appears that for darker samples (<60%), perceived lightness on monitor appeared to be slightly brighter than that on iPhone6S.

Other statistical measures are standard deviation (SD) (Eq. (6.2) and correlation variation (CV) (Eq. (6.1)), which are employed in this study.

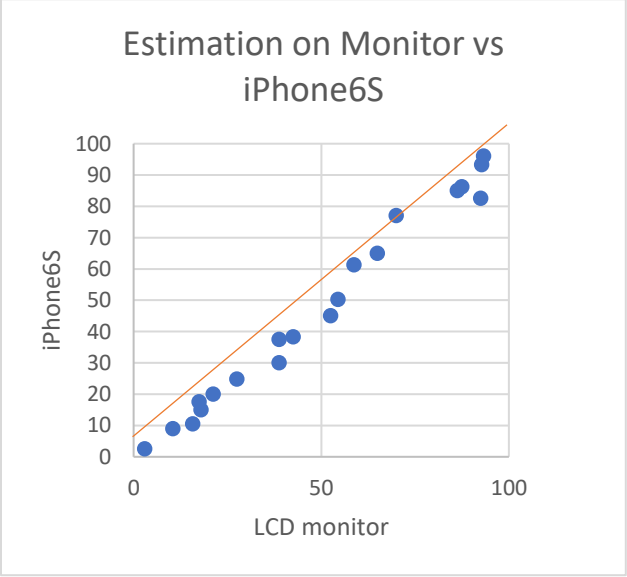

Figure 7.3. Comparison between estimation on Monitor (x) and iPhone6S (y) for Observer 1.

The differences for the estimation for each colour sample for the same observer is depicted in Figure 7.4, which shows the same trend that darker samples appear to be different when they are presented on a LCD monitor and a mobile phone and lighter samples appear much lighter on a phone.

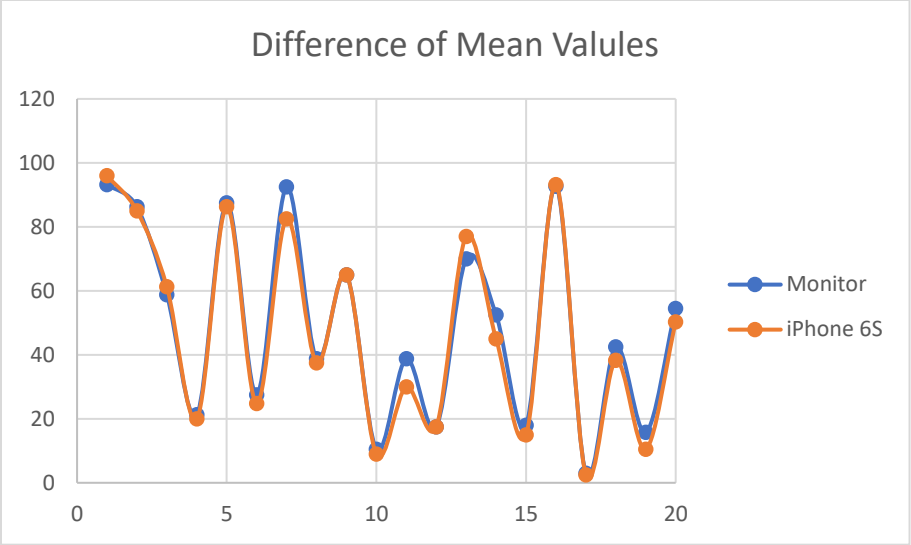

Figure 7.4. Difference of Mean values for monitor and iPhone 6S by Observer 1 .

Chapter 8. Modelling of lightness for mobile phones

8.1 Summary of psychophysical experiments on both LCD monitors and mobile phones

As explained in Chapter 5, a series of psychophysical experiments are conducted to estimate the viewing differences when a grey sample presented on both a monitor and an iPhone. In these experiments, a 15" LCD monitor (Dell Latitude E5450 Laptop running windows 10 OS) with resolution of 1366x768 is utilised as well as an iPhone 6S. Twenty test samples are selected aiming to cover a wider range of lightness distribution as illustrated in Figure 5.4. The blue background is only for highlighting the grey samples. In the real psychophysical experiments, the viewing pattern shown in Figure 5.5 is applied.

In an experiment to be conducted either on LCD monitor or on a phone, the observers are asked to estimate the lightness of a test sample positioned in the middle of Figure 5.5 with reference to reference white (RW), either on a monitor or an iPhone. As illustrated in Figure 5.5, each test colour is placed at the centre against a grey background (with 20% of luminance of reference white) and surrounded by the reference white and surrounding grey samples. The test field in the centre subtends a visual angle of 2^{o} at a viewing distance of ~60cm. The subjects are instructed that the lightness of RW is 100 whereas their imaginary black is 0. Then the lightness of the test sample should be a value between 0 and 100, in proportion to RW. For example, if a test sample is given a value off 60, then its lightness is perceived 60% as bright as the lightness of RW.

Fourteen observers (7 males and 7 females) with normal colour vision are recruited in this preliminary experiment, who are aged between 19 and 33 with varying professional background (research students, IT professionals, staff). All of them perform one or more experiments after initial training.

Before each experiment, the LCD laptop monitor is calibrated to D65 (average daylight) using ColorMunki Smile software. During the experiment, only the middle test sample in Figure 5.5 is changing between different grey levels as illustrated in Figure 5.4. The surround samples and RW remain the same. This design of the viewing pattern is to reflect the real-world viewing conditions. For the iPhone 6S, the brightness is set to the maximum.

Figure 8.1 presents the 20 test samples shown in Figure 5.4 on an xy-chromaticity diagram measured using Minolta CS-100A colour meter from both colour monitor (cross) and mobile phone (triangle). As it can be seen, the samples distributed much wider on the monitor than on the phone.

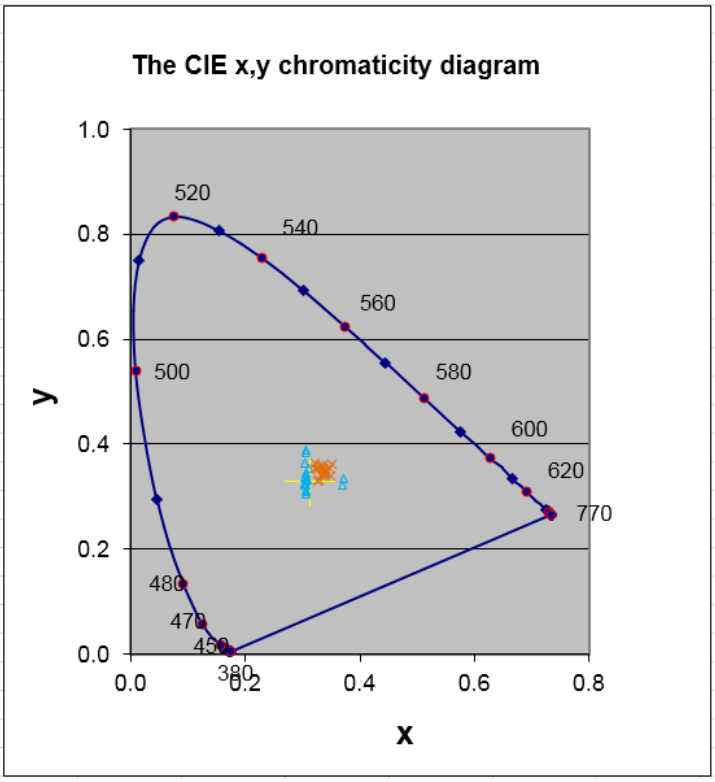

Figure 8.1. The xy measurements for both LCD monitor (x) and iPhone 6s (triangle) presented on a xy-chromaticity diagram. The big yellow cross sign (+) refers to D65 white point (x=0.3128, y= 0.329).

Figure 8.2 compares observers' estimations (average) for the test samples from both monitor (x) and iphone-6S (y). The result shows large discrepancy (>20%) occurs on the samples in the middle lightness range, e.g. a lightness of 50% is perceived as 73% on the iPhone. This phenomenon will be further investigated in the future by including more test samples in this range. In general, for medium grey samples, they appear brighter on iphone-6S than on LCD monitor.

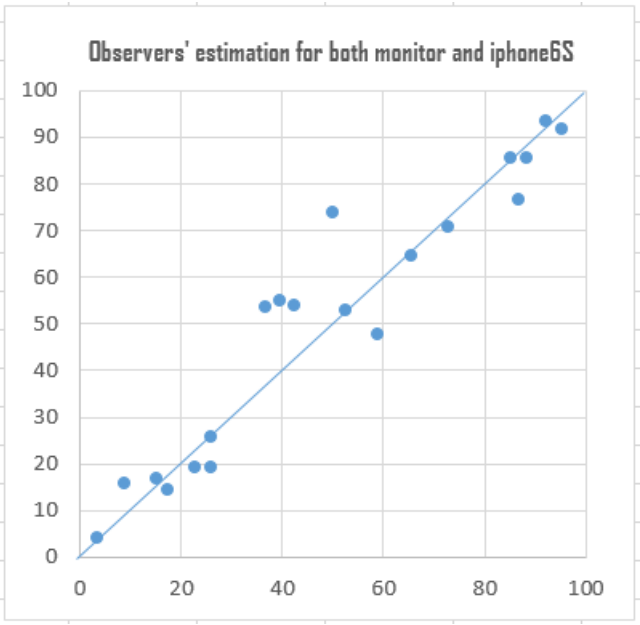

Figure 8.2. Comparison of estimations between monitor (x) and iphone-6S(y).

8.2 Modelling Lightness using CIECAM02 Model

To predict users' perception on a colour, CIE has recommended a colour appearance model CIECAM02 (Moroney (2002) and latest CIECAM16 (Li (2017), CIE (2016)) to predict colours appear on any media under a number of viewing conditions. Stemmed from Hunt's early colour vision model (Hunt (2014), Luo (1993), Luo (1992)), by employing a simplified theory of colour vision for chromatic adaptation together with a uniformed colour space, CIECAM02 and currently CIECAM16 can predict the change of colour appearance as accurately as an average observer under a number of given viewing conditions. In particular, the way that the model describes a colour is reminiscent of subjective psychophysical terms, i.e., hue, colourfulness, chroma, brightness and lightness. **Appendix A4** provides detailed calculation of model of CIECAM02.

With regard to the representation of the colour appearance of an image, in this investigation, the perceptual colour attributes of lightness (*J*), chroma (*C*), is calculated in Eqs. (8.1) to (8.5) (Li (2016)) .

$$J = 100^{1}(\frac{A}{A_w})^{cz} \tag{8.1}$$

Where A_w is A for reference write and

$$A = \left[2R'_a + G'_a + \frac{1}{20}B'_a - 0.305\right]N_{bb} \tag{8.2}$$

$$a = R'_a - \frac{12G'_a}{11} + \frac{B'_a}{11} \tag{8.3}$$

$$b = \frac{1}{9}(R'_a + G'_a - 2B'_a) \tag{8.4}$$

and R'_a, G'_a, B'_a indicate the post-adaptation cone responses with detailed calculations specified in (Li (2016)) whereas A_W refers to the A value for reference white. Constants N_{bb}, N_{cb} are calculated as

$$N_{bb} = N_{cb} = 0.725(\frac{1}{n})^{0.2} \tag{8.5}$$

where $n = Y_b/Y_w$, with Y_b *and* Y_W representing the Y value for both background and reference white respectively. The input and output parameters of CIECAM model are listed in Table 8.1.

Input	Output
X,Y, Z: Relative tristimulus values of colour stimulus	Lightness (J)
X_W, Y_W, Z_W: Relative tristimulus values of white	Colourfulness (M)
L_A: Luminance of the adapting field (cd/m*m) = 1/5 of adapted D65;	Chroma (C)
Y_b: Relative luminance of the background;	Hue angle (h)
Surround parameters: c, Nc, F = 0.41, 0.8, 0.2 respectively for luminous colours (i.e., monitor).	Brightness (Q)
	Saturation (S)

Figure 8.3 schematically illustrates the procedures to model lightness for mobile phones. (Elham 2015)

To begin with, the model CIECAM takes into account of measured physical parameters of viewing conditions, including tristimulus values (X, Y, and Z) of a stimulus, its background, its surround, the adapting stimulus, the luminance level, and other factors such as cognitive discounting of the illuminant. The output of the colour appearance model predicts mathematical correlates of perceptual attributes.

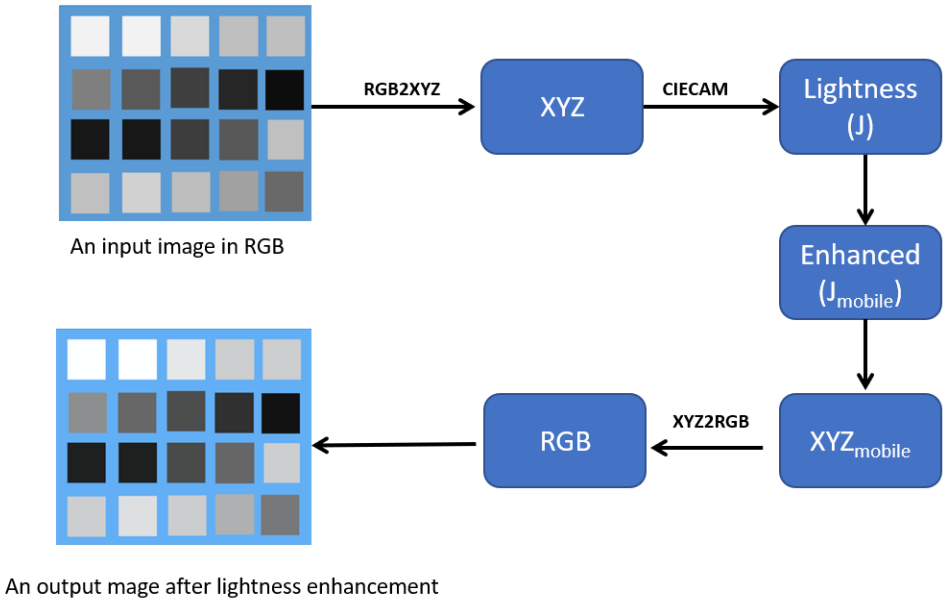

Figure 8.3. Steps for modelling lightness for mobile phone applying CIECAM J.

The conversion between RGB and XYZ is calculated as shown in Figure 8.4 where 24 standard colour checker is displayed on a monitor that has been calibrated into D65. Then the measurement of 24-colour-checker is conducted under a D65 viewing cabinet using a tele-spectroradiometer (TSR) to obtain tristimulus values of XYZ. The RGB values of 24-colour-checker will be obtained when the checker is on display on a calibrated (D65) monitor.

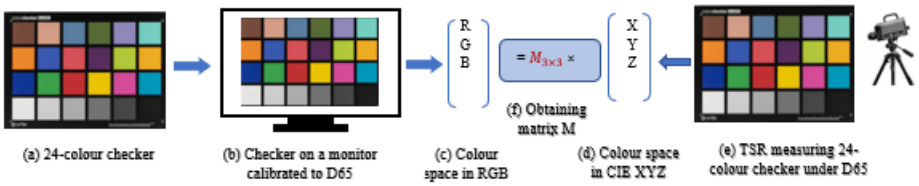

Figure 8.4. Steps to obtain conversion between an image RGB and CIE tristimulus values of XYZ.

Eqs. (8.1) and (8.2) present the conversion matrix between RGB to XYZ and XYZ to RGB respectively. (Elham 2015)

$$M = \begin{matrix} 0.0213 & 0.0069 & -0.0095 \\ 0.0185 & 0.0449 & 0.0058 \\ 0.0040 & -0.0070 & 0.0632 \end{matrix} \quad (8.1)$$

$$M^{-1} = \begin{matrix} 51.09 & -6.56 & 8.281 \\ -20.34 & 24.56 & -5.312 \\ -5.486 & 3.136 & 14.71 \end{matrix} \quad (8.2)$$

With regard to the prediction of the colour appearance of a grey-level image, in this investigation, only the perceptual colour attribute of lightness (*J*) is employed.

For the original model of CIECAM, after the setting of environmental parameters as listed in Table 8.1 to 'dim' condition to compensate lightness differences between LCD and iPhone, the comparison results are given in Figure 8.5 for the iPhone-6S and for the LCD monitor in Figure 8.6. For LCD monitor, parameters are set as c=0.33, Nc=0.8, F=0.2; whereas for iphone6S, c=0.59, Nc=0.9, F=0.9.

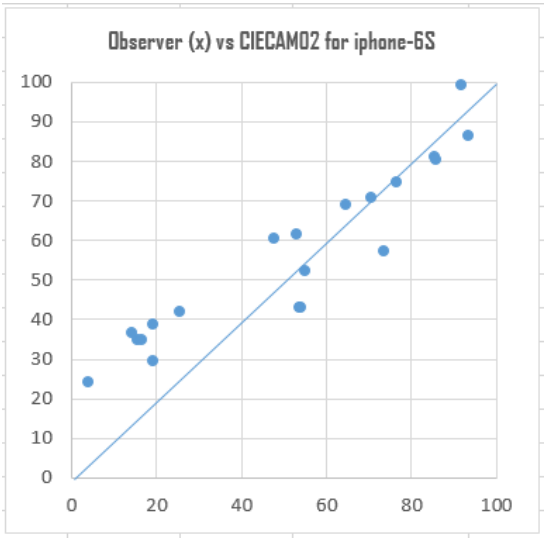

Figure 8.5 Comparison between estimation by observers (x) and the prediction by CIECAM for iphone-6S.

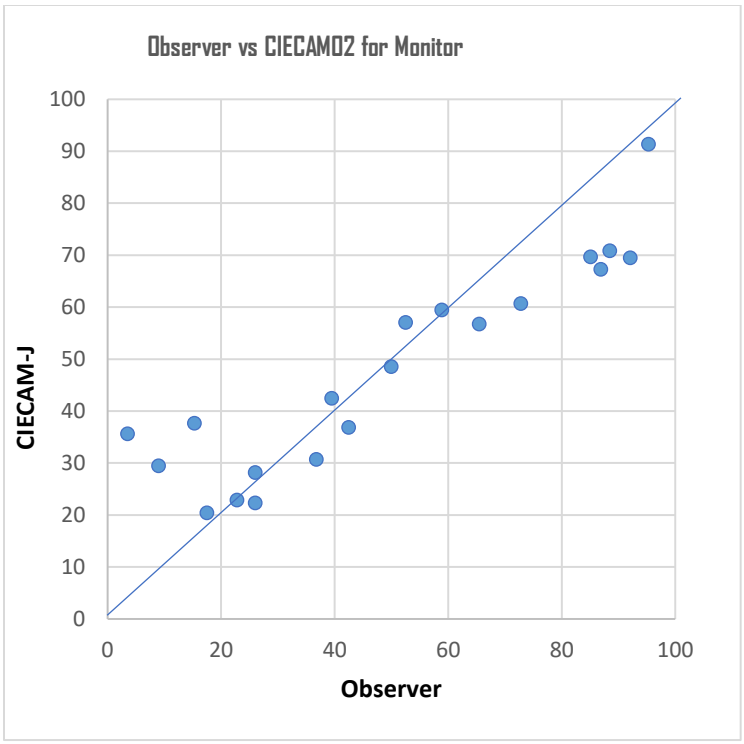

Figure 8.6. Comparison between average observer (x) and CIECAM02 model (y).

It appears that by modifying the *c* value, the factor for colour compensation for an environment, the prediction of lightness for mobile phones can be made. Figure 8.7 compares different setting of c parameter for predicting mobile lightness (J).

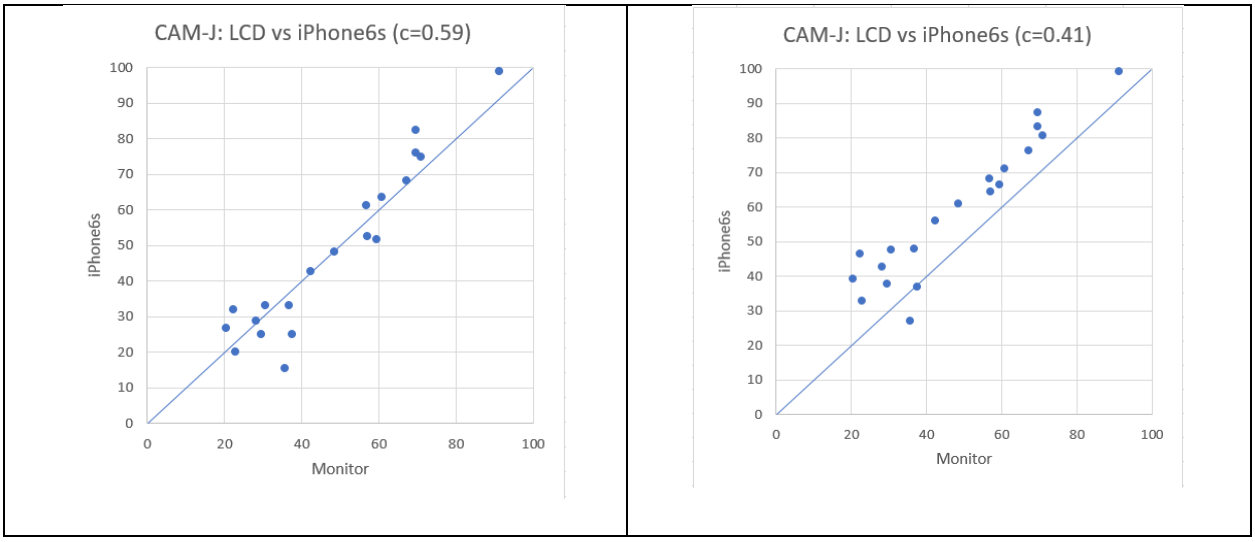

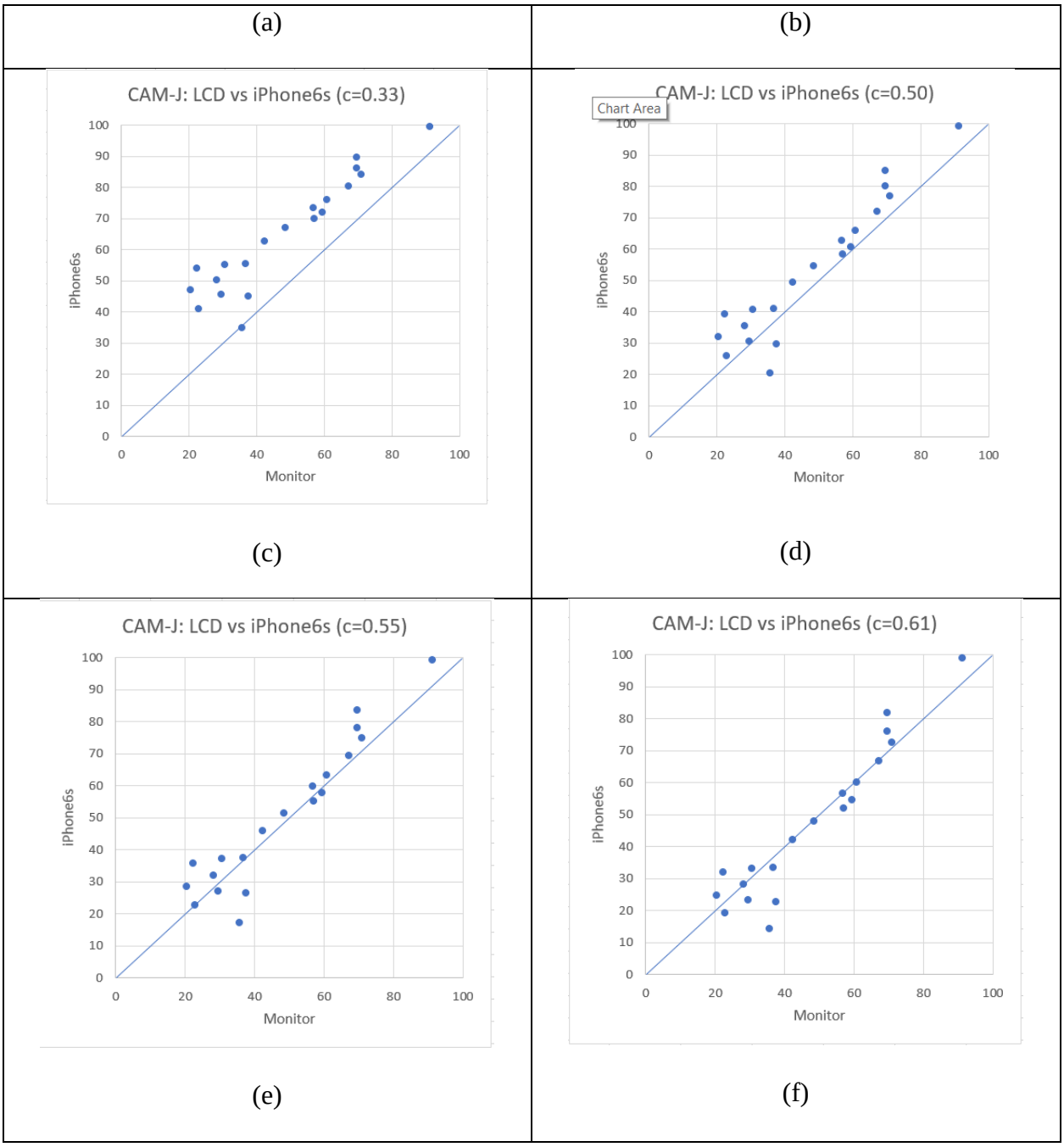

Figure 8.7. Comparison of parameter c for enhancing lightness (J) of iPhone3S in comparison with predictions for the LCD monitor. (a) $c = 0.59$; (b) $c = 0.41$; (c) $c = 0.33$; (d) $c = 0.55$; (e) $c = 0.55$; (f) $c = 0.61$.

Table 8.2 provides CV values for calculation between predicted J and observers' estimation with the change of parameter c.

The selection of *c* value with the corresponding CV value between Predicted CIECAM-J and observers' estimation for iPhone6s.

Table 8.2 CV values between predicted J and estimated lightness with varying *c* parameter.

c	0.33	0.41	0.50	0.55	0.59	0.61
CV(%)	28.75	22.45	20.45	**19.16**	**19.56**	20.24

Figure 8.7 presents comparisons between predicted J and observers' estimation for iPhone6S.

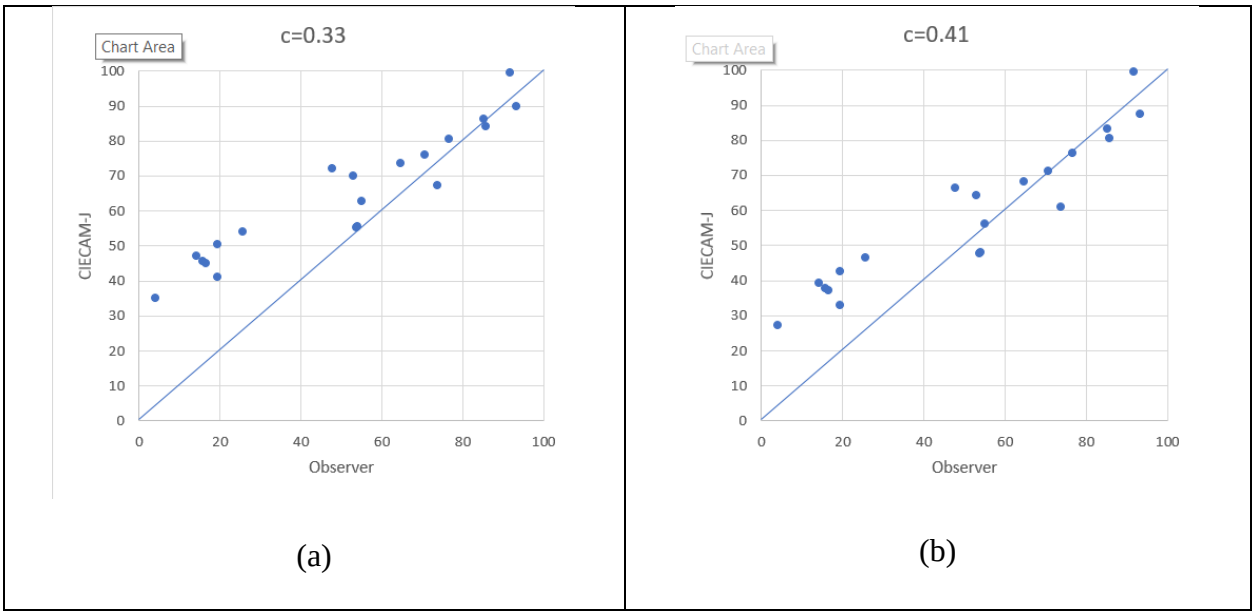

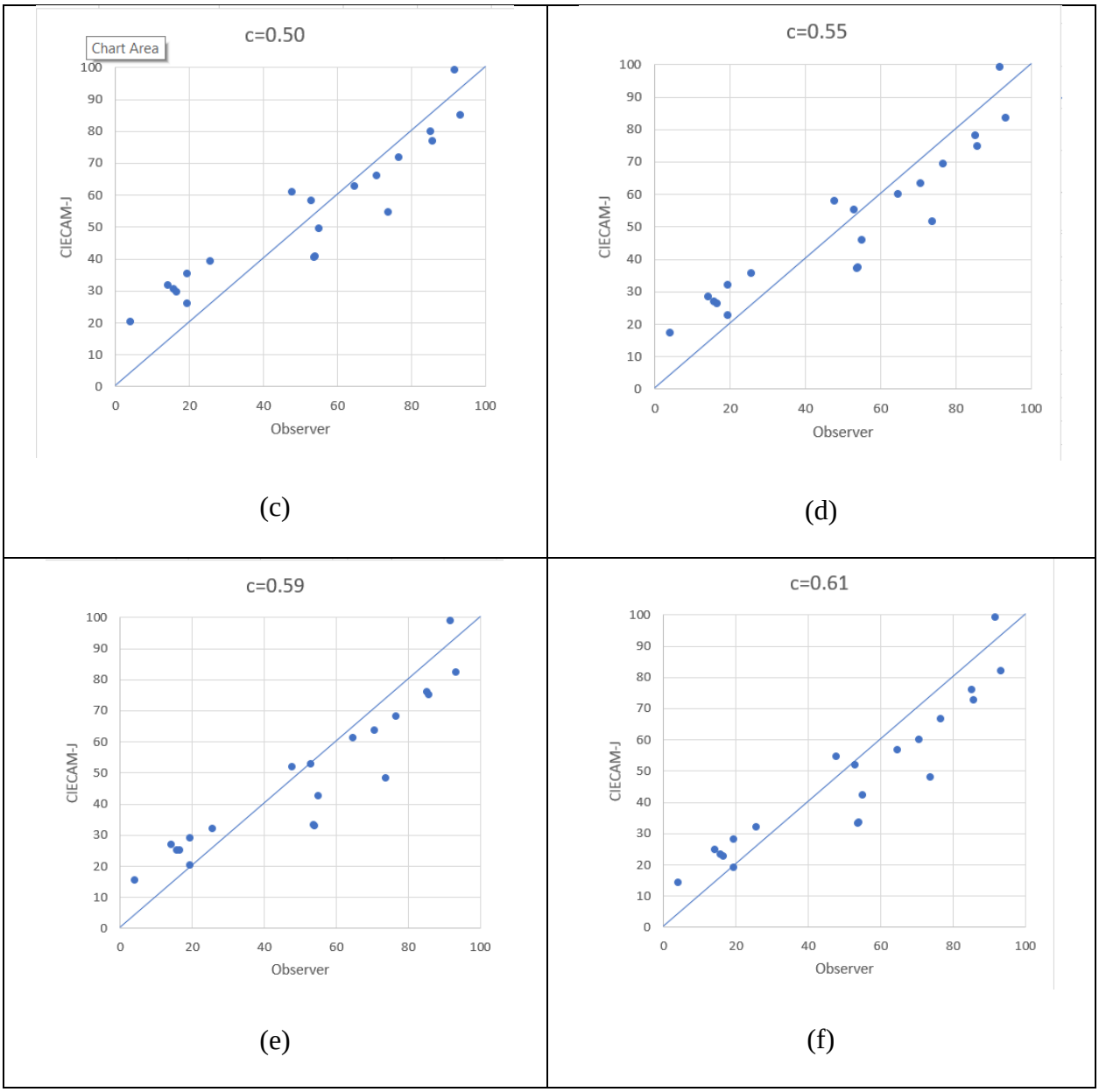

Figure 8.8. Comparison results between predicted lightness using CIECAM J and estimated lightness by observers for different c values.

As shown in Table 8.2 and Figure 8.8(e), $c = 0.55$ gives the most accurate prediction with the least CV value (19.16) when in comparison with observers' estimations. Hence in this study, c is setting to 0.55 as a way of lightness enhancement for iPhone6S.

8.3. Evaluation of lightness enhancement on images

8.3.1 Image enhancement for iPhone6S

Evaluations are also conducted on images. Figure 8.9 displays the image of colour checker displayed on LCD monitor and iPhone6S.

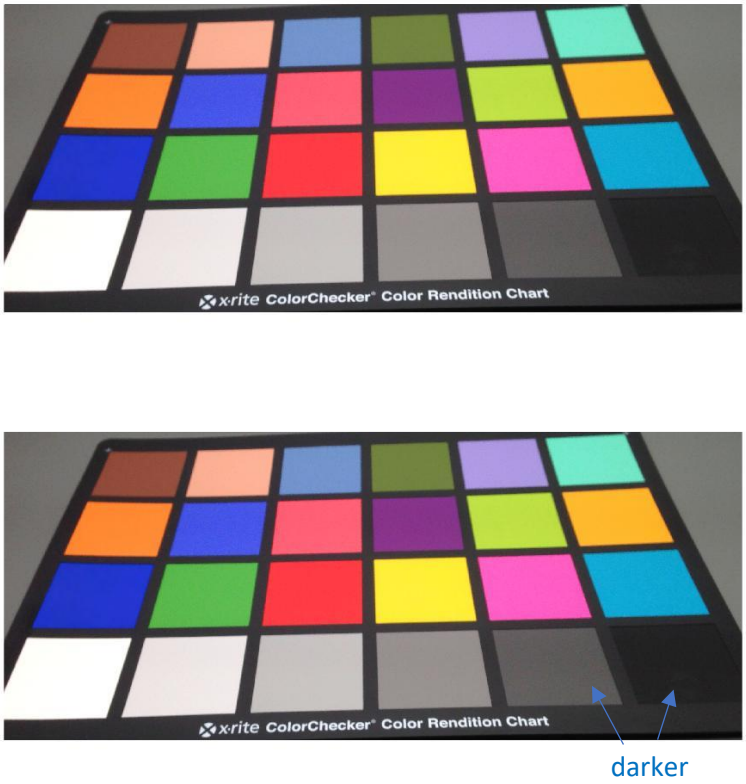

Figure 8.8. The colour checker that should appear the same on both monitor (top) and iphone-6S (bottom) after enhanced by applying CIECAM.

Figure 8.9 shows the difference between original image on monitor (a) (b) and mobile (c)(d). IN theory, in the figures showing below, (a) should match (d), representing the same image displayed on a LCD monitor and iPhone6S (after lightness enhancement).

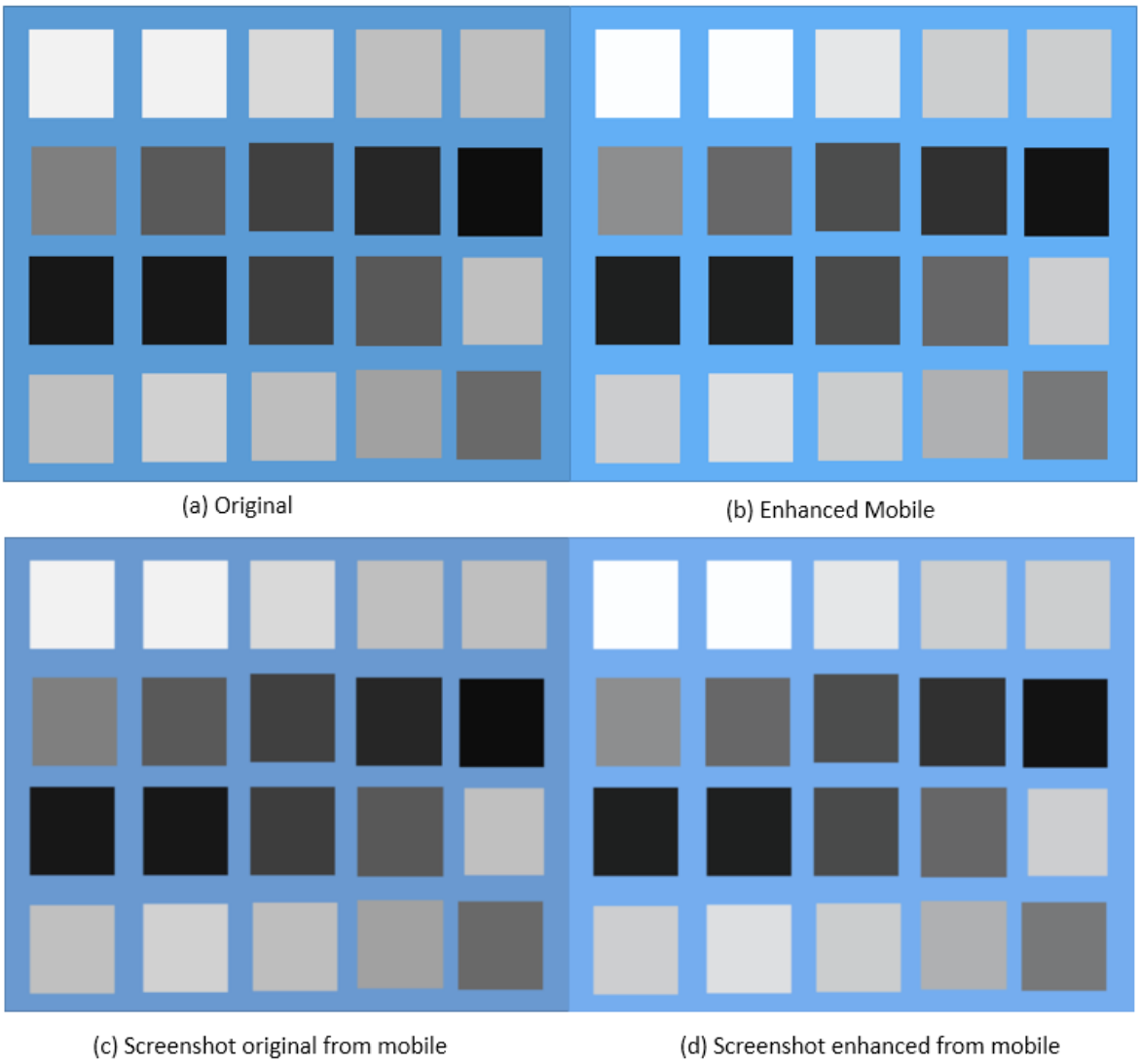

Figure 8.9. Enhanced grayscale images on mobile. (a)(b) Screenshots from monitor. (c)(d) Screenshots from mobile phone.

Figures 9.10 and 8.11 further demonstrate the effectiveness of enhanced lightness on viewing COVID19 features from x-Ray images. The images (with green circles) demonstrates the COVID19 specific features that are more apparent after lightness enhancement than without.

For example, in Figure 9.10(d), the COVID19 feature should be cloudy patches as pointed in arrow in Figure 9.10(a) (green circle). In Figure 9.10(c), this cloudy patch is less apparent.

After lightness enhancement, this patch comes back in (d). Figure 9.10 is for iPhone7. In Figure 9.11, example for iPhone10 is demonstrated. Similar to Figure 9.10, the COVID19 feature becomes clearer after enhancement (d) than without (c), in comparison with the orginal displayed on a LCD monitor (a).

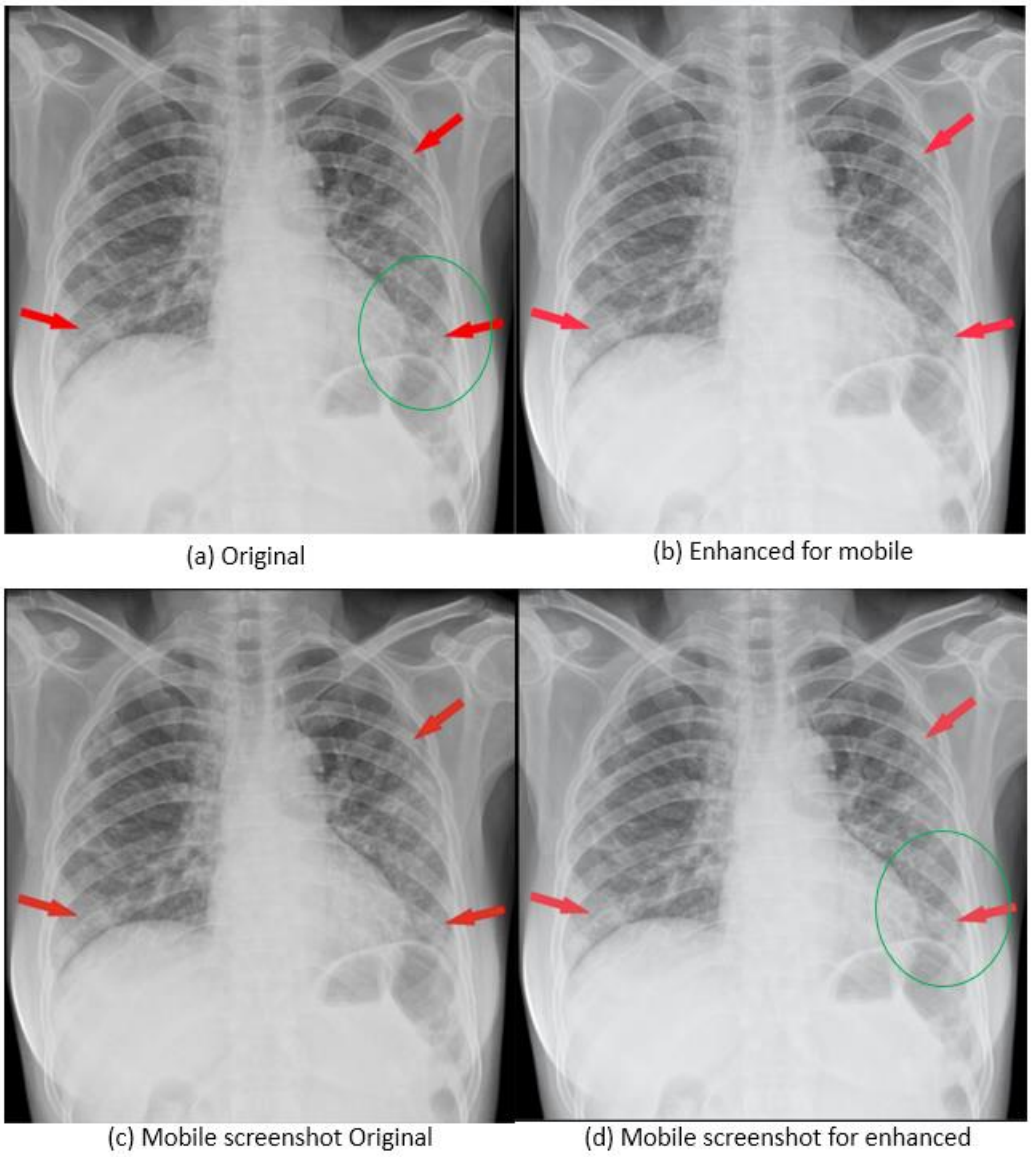

Figure 8.10. Demonstration of enhanced mobile phone images for detection of COVID19. Red Arrows: COVID19 specific features. Green circle, the cloud patch became more apparent after lightness enhancement for mobile phone (iPhone 7).

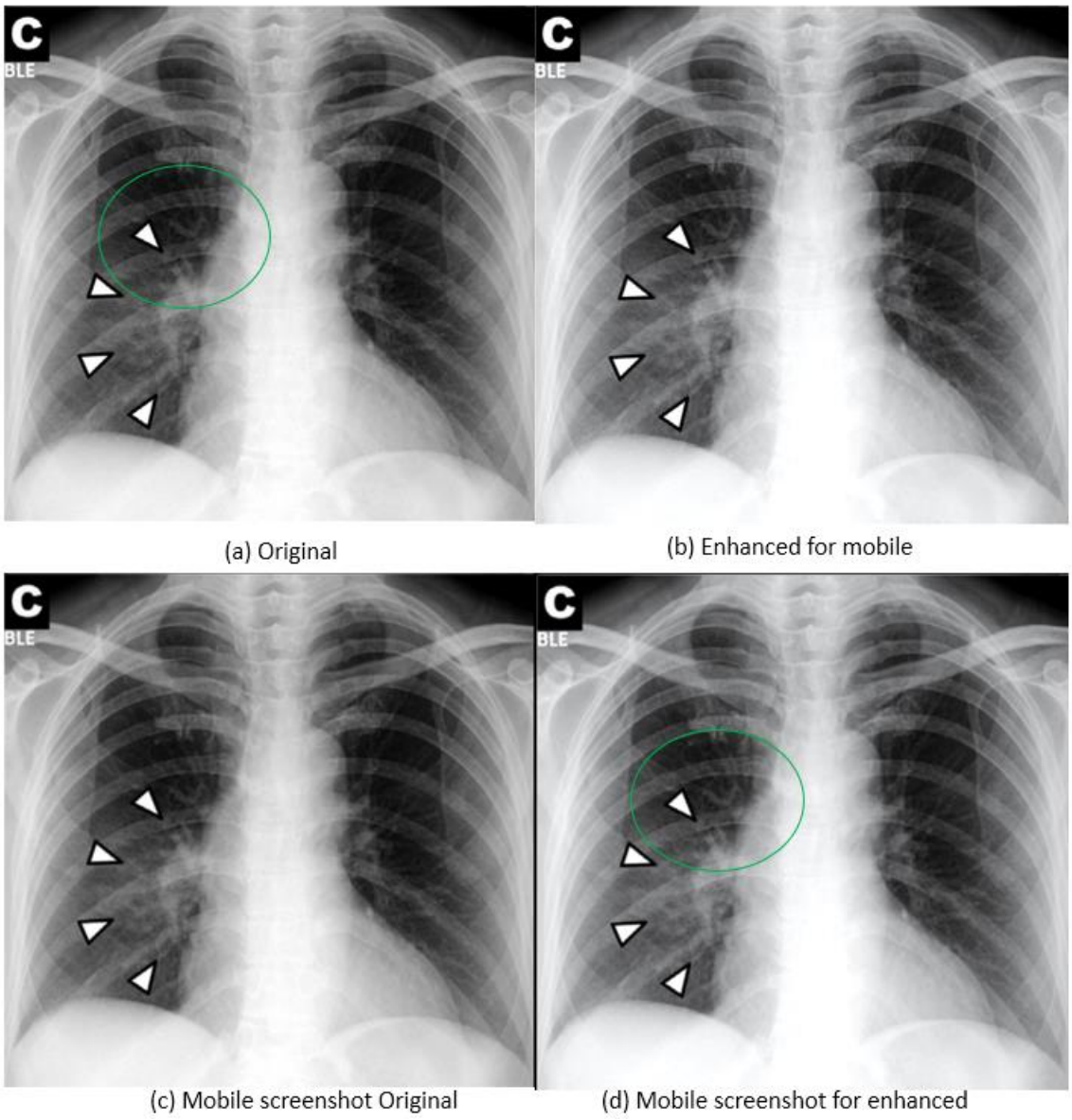

Figure 8.11. An example showing enhanced mobile phone images for detection of COVID19. White arrows: COVID19 specific features. Green circle, the white cloud patch became more apparent after lightness enhancement for iPhone10.

8.3.2 Visual evaluation of key features from enhanced medical images

To further evaluate the importance of image enhancement for mobile phones, visual subject evaluation takes place. Two observers are invited to detect key features pointed on Figures A5.1 to A5.4 in Appendix A5, which demonstrate x-ray COVID specific features and colour

checker, in comparison with the original image (a) displayed on a computer screen as demonstrated in Figure 8.12. Firstly, image (a) is displayed on the LCD monitor (calibrated into D65) in a darker room. Then original image (b) and its enhancement (c) is displayed on a phone side by side. Observers are then asked to compare with (a) to see which one is closer with reference to the region pointed by arrow. Both observers have chosen enhanced image for Figures A5.1 to A5.4. The appearance of enhanced image and original one is ordered at random order, i.e. original-enhanced or enhanced-original. Some images appear twice to ensure robustness of the visual experiments.

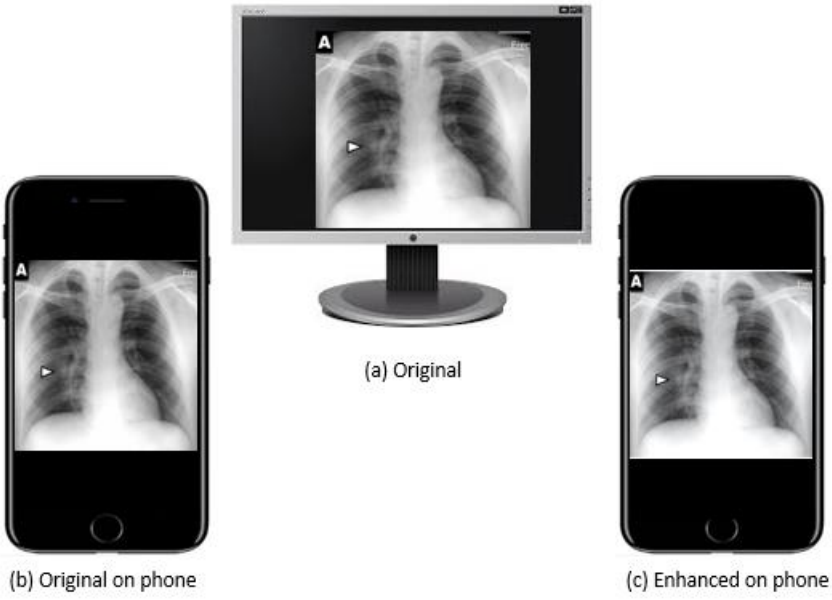

Figure 8.12. Visual experiment setting for medical images. (a) original image. (b) original image displayed on a phone. (c) Enhanced image displayed on the same phone.

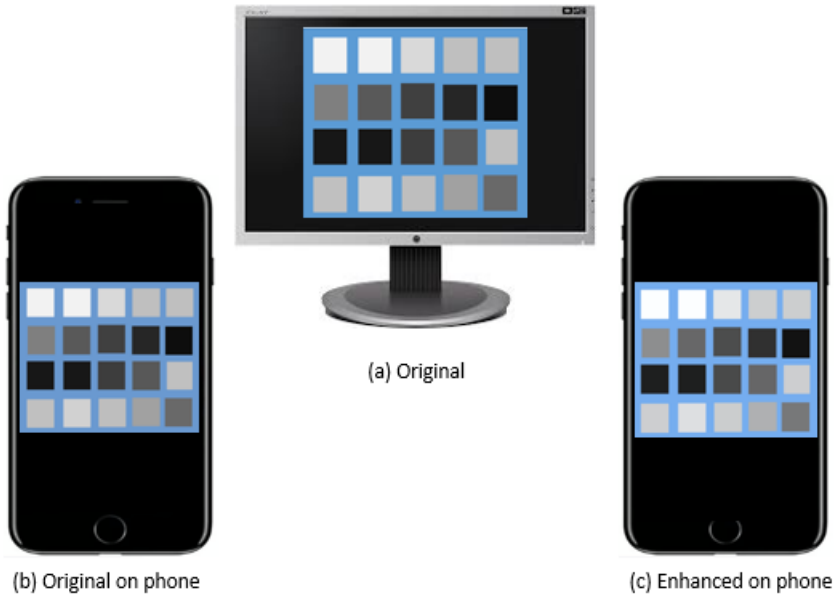

Figure 8.13. Visual experiment setting for grey patches (a) original image. (b) original image displayed on a phone. (c) Enhanced image displayed on the same phone.

These figures and visual experiments confirm that after lightness enhancement, medical images appear to increase the contrast between normal and diseased regions in mobile phones, and therefore to allow phones with smaller screen size to detect some diseased features of COVID19 on x-ray images. Further studies are needed to detect other diseases from varying imaging modalities (CT, MR, etc.).

Chapter 9 Conclusion & Future Work

The aim of this study is to investigate the feasibility of using mobile phones to view medical images, in particular grey-level images. Towards this end, modelling of lightness for mobile phone takes place. A number of psychophysical experiments are conducted to evaluate observers' response to view grey samples on both LCD and mobile phones. The 15" LCD colour monitor is calibrated to CIE standard viewing condition of D65 whereas each mobile phone has its brightness turned in to maximum.

In total, 20 grey samples are selected to conduct psychophysical experiments, which covers a large spectrum of grey scale, ranging from 1% to 95%. Each experiment is conducted by 5 to 10 subjects that are invited from a pool of 14 observers with normal colour vision. These observers are aged between 19 to 33 with background from research students to IT professions and are all from Middlesex University.

When comparing observers' estimations between LCD and iPhone6S, medium range colours on a phone appear much brighter than on an LCD colour monitor. Hence modelling of lightness for a phone takes place through the employment of CIE colour appearance model CIECAM16, (former model CIECAM02). While this colour appearance model has been widely applied to predict colour appearance under varying viewing environments, it has not yet to t cover mobile devices.

It has found that when colour compensation factor, c, is set to **0.59**, the model CIECAM performs the best, with similar results to that on a computer monitor, with CV value of 19% between observers' estimation and model prediction.

The performance of lightness enhancement with $c = 0.59$ has been further evaluated when the model is applied to x-ray images to inspect COVID19 features on iPhones. Three iPhones are evaluated, which are iPhone6S, iPhone7 and iPhone10. Based on two observers' visual evaluation, the COVID features are well preserved on those phones when the concerned images are enhanced.

There are a number of limitations in this study.

One limitation is the variety of phones applied in this work. Apart from iPhones (6S, 7, 10, 13Pro), 2 other phones are measured physically using the CS-100A colour meter, ie. Samsung, Motorola. However, because of those phones belong to individuals, psychophysical experiments could not be conducted using these private personal phones by other observers apart from owns.

Second is the limitation of sample numbers. Only 20 samples are selected. In the future, more samples will be included. Furthermore, colour samples will be included as well.

Further study will also include, the precise result based on colourfulness, hue and lightness for more mobile phone samples. The analysis done on this experiment is based on measured colours and CIE co-ordinate grey colour definitions of grey scale image phenomena. The study designed to establish as separate variables of grey shade appearance, a model of the grey scale appearance of formulation through model was validated using grey scale appearance on a computer screen that has been calibrated so that each colour phenomena could be controlled and reproduced to within an average D65.

Doctors and patients are beginning to expect medical images to be available on mobile devices for consultative viewing. However, this expectation raises concerns to ability of existing mobile

devices to quickly and securely send and receive images. This study looks to establish computational relationship between grey colours and mobile phones as distinct contributing variables in medical stream. The result from proposed methods show that it can be a contribution to bridging semantic gap in the area of medical colour appearance in smartphones as these devices are in daily use. An application can also be built in future which helps to keep the image visibility in mobile phones same as monitor to get precise result. In future, it would be ideal to plan and aim that the analysis will take into account of grey scale more accurately in smart phones.

In conclusion, this study has identified the setting of c value (=0.59) for the application of CIECAM model in iPhones (6S, 7, 10, 13Pro), which can produce an image with near the same appearance as appearing in an LCD colour monitor that is calibrated to D65. Evaluation on medical images has shown that the key features remain on a phone when compared with those images displayed on the LCD monitor.

Future work includes,

- Putting in more grey samples, colour samples and other smartphones.
- More experience on different phone models considering value c.
- Each grey sample's a*, b* including mobile phones model display factors can be calculated.
- Luminous computer display factors c, Nc and F value can be worked on for different phone models.

References:

Agoston, MK. (2005). Computer Graphics and Geometric Modeling: Implementation and Algorithms. London: Springer. pp. 300–306, 2005.

Badano A (2015), C Revie, W Cheng, P Green, et. Al., Consistency and standardization of colour in medical imaging, a consensus report, Journal of Digital Imaging, pp: 45-53, 2015.

Bankman IN (2009), Medical Imaging Processing and Analysis, 2009, Pages 19-22, Elsevier, Academic Press, 2009.

Barten PGJ (1992), "Physical model for the contrast sensitivity of the human eye", SPIC 1666, pp: 55-75, 1992.

Barten PGJ(1993), "Spatial-temporal model for the contrast sensitivity of the human eye and temporal aspects", Proc. SPIE 1913, pp: 4-15, 1993

Barten PGJ (1999), Contrast sensitivity of the human eye and its effects on image quality. Bellingham, WA: SPIE Press; 1999.

Bartleson, CL. (1967), Breneman, E.l., Brightness Perception in Complex Fields, 1. Opt. Soc. Am., 57, 1967, 953-975, 1967

Bartleson, CL (1979), Changes in Colour Appearance with Changes in Adaptation, Colour Res. Appl., 4, 119-138, 1979.

Bartleson, C.L. (1980), Measures of Brightness and Lightness, Die Farbe, 28, 132-148, 1980

Blume H (1990), Roehrig H, Browne M, Lan Ji T. Comparison of the physical performance of high resolution CRT displays and films recorded by laser image printers and displayed on light-boxes and the need for a display standard. Medical Imaging IV: Image Capture and Display. SPIE. 1232:97–114, 1990.

Blume H., (1996), The ACR/NEMA proposal for a grey-scale display function standard. Image Display. SPIE. 1996;2707:344–360, 1996.

Billmeyer F.W.Jr. (1981), Saltzman, M., Principles of Color Technology, 2nd ed, John Wiley & Sons, New York, 1981.

Bourne, R. (2010), Fundamentals of digital imaging in medicine, Springer, London. 2010.

Burnham, R.W., Hanes, R.M., Bartleson, C.J., Color: A Guide to Basic Facts and Concepts, John Wiley & Sons, New York, 1963.

Chao E (2017), Meenan CK, Ferris LK. Smartphone-Based Applications for Skin Monitoring and Melanoma Detection, *Dermatol Clin*, 2017 , 35(4):551-557.

Carrino J. (2002), "Image Quality: a clinical perspective", In: Siegel E, Reiner B. and Carrino J., SCAR University Primer 3: Quality Assurance in the Digital Medical Enterprise, Society for Computer Applications in Radiology, 2002.

Cheng, HD (2001), Jiang, X; Sun, A; Wang J, Color image segmentation: Advances and prospects, Pattern Recognition. 34 (12): 2259, 2001.

CIE (1971), International Commission on Illumination, , Publication CIE no. Colorimetry: Official Recommendations of the International Commission on Illumination 15, Bureau Central de la CIE, Paris, 1971.

CIE (2016), The CIE 2016 Colour Appearance Model for Colour Management Systems: CIECAM16, *https://cie.co.at/publications/cie-2016-colour-appearance-model-colour-management-systems-ciecam16* . Retrieved 2022-09-16.

David MJ (2006), "Utilization of DICOM GSDF to Modify Lookup Tables for Images Acquired on Film Digitizers", J. of Digital Imaging, pp. 167-171, 2006.

DICOM (2001), Digital Imaging and Communications in Medicine, Part 14: Grayscale Standard Display Function, published by National Electrical Manufacturer's Association, 2001.

DICOM PS3.14, 2023b: Grayscale Standard Display Function. https://dicom.nema.org/medical/dicom/current/output/pdf/part14.pdf. Access in May 2023.

Davis A. (1998), Fennessy P., Digital Imaging for Photographers, 3rd ed.. 1998: Focal Press.

Do TT (2014), Zhou Y, Zheng H, Cheung NM, Koh D., Early melanoma diagnosis with mobile imaging. Annu Int Conf IEEE Eng Med Biol Soc. 2014; 2014:6752-7.

Elham K (2015), Modelling of colour appearance of textured colours and smartphone using CIECAM02 (Private Communication)

Fairchild, MD. (2005). Color Appearance Models (2nd ed.). Addison-Wesley. *2005.*

Falk D. (1986), Brill D., Stork D., Seeing the Light: Optics in Nature, Photography, Color, Vision and Holography, John Wiley, 1986.

Fetterly KA (2008), Blume HR, Fkkynn MJ, Samei E., Introduction to grayscale calibraton and related aspects of medical imaging grade liquid crystal displays, Journal of Digital Imaging, 21(2):193-207, 2008.

FDA (2011), FDA clears first diagnostic radiology application for mobile devices. U.S. Food and Drug Administration; 2011. https://wayback.archive-it.org/7993/20170114063521/http://www.fda.gov/NewsEvents/Newsroom/PressAnnouncements/ucm242295.htm. Retrieved in November 2022.

FDA (2022), Policy for Device Software Functions and Mobile Medical Applications, Guidance for Industry and Food and Drug Administration Staff, September 2022. *https://www.fda.gov/regulatory-information/search-fda-guidance-documents/policy-device-software-functions-and-mobile-medical-applications. Accessed in May 2023.*

Fetterly K (2008), H Blume, M Flynn, E Samej, Intrduction to Greyscale Calibration and Related Aspects of Medical Imaging Grade Liquid Crystal Displays, J Digital Imaging, 21(2): 193–207, 2008.

Flynn MJ (1999), Kanicki J, Badano A, Meyer WR. High-fidelity electronic display of digital radiographs. RadioGraphics, 19:1653–1669, 1999.

Flynn M. (2020), Clinical Physics in Informatics Display

Current and Emerging Practice, in Samei & Pfeiffer eds., Clinical Imaging Physics: Current and Emerging Practice, Wiley, 2020.

Foley JD.; et al. (1995). Computer Graphics: Principles and Practice (2nd ed.). Redwood City, CA: Addison-Wesley, 1995.

Fryback D. (1991), Thornbury J., , The Efficacy of Diagnostic Imaging, Medical Decision Making, 11(2): 88-94,1991,

Gao XW (2015), Y. Wang, Y. Qian, A. Gao**,** Modelling of chromatic contrast for retrieval of wallpaper images**,** *Color Research and Application, 40(4):361-373, 2015.*

Gao, XW. (2017a), Hui R., Tian Z., Classification of CT images based on deep learning networks, *Computer Methods and Programs in Biomedicine*, 138:49-56, 2017.

Gao XW. (2017b), Li W., M. Loomes, Wang Li., A fused deep learning architecture for viewpoint classification of echocardiography, *Information Fusion, 36:103-113, 2017.*

Gao, XW (2018), Quan, Y., Prediction of multi-drug resistant TB from CT pulmonary Images based on deep learning techniques, *Molecular Pharmaceutics*, 2018, 15(10) : 4326-4335.

Gao, XW (2020)., , Carl James-Reynolds, Edward Currie, Analysis of Tuberculosis Severity Levels From CT Pulmonary Images Based on Enhanced Residual Deep Learning Architecture, *NeuroComputing, 392:233-244,2020.*

Gao XW (2023), Taylor S, Pang W., Hui R., Lu X., Braden B., Fusion of colour contrasted images for early detection of oesophageal squamous cell dysplasia from endoscopic videos in real time , Information Fusion 92(2023):64-79, 2023.

Gottsegen G, (2017), More people are using the iPhone than any other brand of camera combined, Flickr, 2017, https://www.cnet.com/news/iphone-top-camera-flickr-2017-report/, accessed in May 2023.

Green P. (2018), M. R. Luo, ICC colour management specification for medical image applications, Nuclear medicine and biomedical imaging, 3(2), pp1-3, 2018.

Guild, J., The Colorimetric Properties of the Spectrum, *Phil. Trans. Royal Society,* A, 230, 149, 1931.

Helmhotz, H.V. (1924), Handbook of Physiological Optics, Vol.II, Ed., Southall, Optical Society of American, New York, 1924.

Hardin CL (1988), Color for Philosophers: Unweaving the Rainbow, Hackett, 1988.

Hering E. (1964), Outline of a Theory of The Light Source, Translated by Hurvich, L. & Janeson, D., Harvard University Press, Massachusetts, 1964.

Henderson, S.T. (1970), Daylight and Its Spectrum, Adam Hilger Ltd., London, 1970.

Stiles, W.S. (1959), Burch, J.M., NPL Colour-matching Investigation: Final Report (1958), *Opt. Acta*, 6, 1, 1959.

Hiley, C. (2023), UK mobile phone statistic, 2023. Uswitch. UK Mobile Phone Statistics 2023 - Mobiles Facts and Stats Report (uswitch.com). Accessed in May 2023.

Hunt, R.W.G. (1952), Light and dark adaptation and the perception of colour, J. Opt. Soc. Am., 42, 190-199, 1952.

Hunt, R.W.G. (1987), Measuring Colour, John Wiley & Sons, New York, 1987.

Hunt RWG (2004), The Reproduction of Colour (6th ed), John Wiley, 2004.

Hunter, R.S., & Harold, R.W., The Measurement of Appearance, 2nd ed, John Wiley & Sons, New York, 1987.

Indow, T. (1966), and Stevens, S.S., Scaling of Saturation and Hue, Perception & Psychophysics, 1, 253-271, 1966.

Ishihara S. (2017), Ishihara's test for colour deficiency, 24 Plates Edition, Kanehara Trading Inc, Tokyo, Japan, 2017.

Jacobson, A.E. (1948), Non-Adaptability of the ICI System to Some Near-White which

Show Absorption in the Far Blue Region of the Spectrum, J. Opt. Soc. Am., 38, 442-444,1948.

Judd, D.B. (1964), David, L.M., & Wyszecki, G., Spectral Distribution of Typical Daylight As a Function of Correlated Color Temperature, *J. Opt. Soc. Am.*. 54, 1031-1040 & 1382, 1964.

Kagadis GC (2013), Walz-Flannigan A, Krupinski EA, *et al.*, Medical imaging displays and their use in image interpretation, *Radiographics*, 2013, 33: 275-290.

Kahn CE.(2007), Carrino JA.; Flynn, MJ.; Peck, DJ, Horii SC, DICOM and Radiology: Past, Present, and Future". *Journal of the American College of Radiology*. **4** (9): 652–657, 2007.

Kaiser P. (1994), Boynton R., Human Color Vision (2nd edition), Optical Society of America, 1994.

Kalwa U (2019), Legner C, Kong T, Pandey S , Skin Cancer Diagnostics with an All-Inclusive Smartphone Application, *Symmetry*, 2019, 11,790.

Kimpe T (2006), Marchessoux C, Important Differences Between Medical Displays and Normal Desktop Displays and Underlying Reasons, ADEAC, 2006

Kimpe, T. (2016), Rostang, J., Van Hoey, G. and Xthona, A. (2016), Color standard display function: A proposed extension of DICOM GSDF. Med. Phys., 43: 5009-5019.

Krupinski E. (2008), Jiang Y, Evaluation of Medical Imaging Sytems, 2008, Med. Phys, 35(2):645-59, 2008.

Lamb T. (1995), Bourriau J., Color: Art and Science, Cambridge University Press, 1995.

Laricchia F (2022), Forecast number of mobile devices worldwide from 2020 to 2025 (in billions), Statista, 2022.

Lee HC (2005), Introduction to Color Imaging Science**,** Cambridge University Press, 2005.

Li CJ (2017), Li Z, Wang Z, et al., Comprehensive color solutions, CAM16, CAT16 and CAM16-UCS, *Col., Res. and Appl.*, 2017, 42(6):703-718.

Liu J (2007), Feng J, Tao D, "DICOM GSDF Based Calibration Method of General LCD Monitor for Medical Softcopy Image Display", IEEE CIBBE, 2007.

Luo, M.R. (1991), Clarke, A.A., Rhodes, R.A., Schappo, A., Scrivener, S.A.R., Tait, CJ, Quantifying Colour Appearance, Part I, LUTCHI Colour Appearance Data, Calor Res. Appl., 16, 166-179, 1991.

Luo, M.R. (1991a), Clarke, A.A., Rhodes, R.A., Schappo, A., Scrivener, S.A.R., Tait, CJ., Quantifying Colour Appearance, Part 11, Testing Colours Models Performance Using LUTCHI Colour Appearance Data, Calor Res. Appl., 16, 181-197, 1991.

Luo MR (1992), Gao XW, Phodes PA, Xin HJ, Clark AA, Scrivener SAR, Quantifying colour appearance - Part IV., Transmissive media, *Color Research and Application*, 1992, 18:191-206.

Luo MR (1993), Gao XW, Phodes PA, Xin HJ, Clark AA, Scrivener SAR, Quantifying colour appearance - Part III., Supplementary LUTCHI colour appearance data, *Color Research and Application*, 1993, 18:98-113.

Mcllgorm DJ (2015), J P McNuilty, GSDF-calibrated medical grade monitor *vs* a DICOM part 14: GSDF-calibrated "commercial off-the-shelf" (COTS) monitor for viewing 8-bit dental images, Dentomaxillofac Radiol. 44(3): 20140148, 2015.

Moroney N (2002), Fairchild MD, Hunt RWG, Li C, Luo MR, Newman T, The CIECAM02 Color Appearance Model, In IS@T/SID Tenth Color Imaging Conference, 2002, pp. 23-27.

Nassau K. (1997), Color for Science, Art and Technology , North Holland, 1997.

Nayatani, Y. (1972), Yamanaka, T., and Sobagaki, H., Subjective Estimatation of Colour Attributes for Surface Colours (Part 1: Reproducibility of Estimations), Acta Chromatica, 2, 129-138, 1972.

Nejati N. (2016), V. Pomponiu, T. -T. Do, Y. Zhou, S. Iravani and N. -M. Cheung, Smartphone and Mobile Image Processing for Assisted Living: Health-monitoring apps powered by advanced mobile imaging algorithms, *IEEE Signal Processing Magazine*, 33 (4): 30-48, 2016.

Ogawa E (1999), Shimura K. Appearance matching of radiographic images using lightness index. Image Perception and Performance. SPIE. 3663:324–332. doi: 10.1117/12.349656, 1999.

Penczek J (2014), Boynton PA, Splett, JD, "Colour error in the digital camera image capture process, J Digital Imaging, 2014 Apr;27(2):182-91, 2014.

Pointer, L.M. (1978), Two decades of opponent processes, AIC Colour 77, Bristol, 33-61, 1978.

Pointer, MR (1980), The Concept of Colourfulness and Its Use for Deriving Grids for Assessing Colour Appearance, Calor Res. Appl., 5, 99-107, 1980.

Ramakrishnan S (ed) (2016) , Pattern Recognition - Analysis and Applications, pp81-108, Rijeka, Croatia, 2016.

Rat C (2018), Hild S, Rault Sérandour J, Gaultier A, Quereux G, Dreno B, Nguyen JM. Use of Smartphones for Early Detection of Melanoma: Systematic Review. J Med Internet Res, 13;20(4):e135, 2018.

Rowe, SCH (1973), The Subjective Scaling of Hue and Saturation, in Colour 73, 391-393, Adam Hilger, London, 1973.

Roehrig H (2003), Chawla A, Krupinski E, Fan J, Gandhi K. Why should you calibrate your display? Penetrating Radiation Systems and Applications V. SPIE, 5199:181–192, 2003.

Roy S (2000), Billmeyer and Saltzman's Principles of Color Technology, 3rd Edition, John Wiley & Sons, New York, 2000.

Samei E (2005), A. Badano, D. Chakraborty, et al, AAPM Online Report No. 03, "Assessment of Display Performance for Medical Imaging Systems", 2005, Med Phys, 32(4):1205-25, 2005.

Salazer AJ (2014), Aguirre DA, Ocampo J, Camacho JC, Díaz XA, "DICOM Grey-Scale Standard Display Function: Clinical Diagnostic Accuracy of Chest Radiography in Medical-Grade Grey-Scale and Consumer-Grade Colour Displays", AJR Am J Roentgenol, 2014 Jun;202(6):1272-80, 2014.

Sangwine SJ (1998), Horne REN, The Colour Image Processing Handbook, Chapman & Hall, 1998.

Sharma, G (2003). *Digital Color Imaging Handbook* (1.7.2 ed.). CRC Press. 2003.

Shevell S. (2003), The Science of Color (2nd edition), Optical Society of America, 2003.

Speranskaya, N.I. (1959), Determination of Spectrum Colour Coordinates for Twenty-Seven normal Observers, *Optical Spectroscopy*, **7**, 424-428, 1959.

Stevens, J.C. (1963), & Stevens, S.S., Brightness Function: Effect of Adaptation, 1. Opt. Soc Am., 53, 375-385, 1963.

Stevens, SS(1975), *Psychophysics: Introduction to its Perceptual, Neural, and Social Prospects*. New York: John Wiley, 1975.

Stevens, SS (1957) & Galanter, E. H., Ratio scales and category scales for a dozen perceptual continua. *Journal of Experimental Psychology, 54*(6), 377–411, 1957.

Susstrunk S. (2018), Buckley R., Swen S., Standard RGB Color Spaces, InfoScience, *2018*.

Taylor, F.A. (1962), Colour Technology, Oxford University Press, 1962.

Tayloy P (2023), Smartphone mobile network subscriptions worldwide 2016-2028, Statista, 2028.

Varma DR (2012), Managing DICOM images: Tips and tricks for the radiologist, *Indian J Radiol Imaging*, 2012, 22(1): 4–13, 2012.

Wang J (2003), Q. Peng and K. Compton, "Proposal of A Quality-Index or Metric for Softcopy Display Systems: Contrast Sensitivity Study", J. of Digital Imaging, Vol. 16, No. 2, pp. 185-202, 2003.

Webster MA (2000), Wilson JA. Interactions between chromatic adaptation and contrast adaptation in color appearance. Vision Res. 2000;40(28):3801-16, 2000.

Wright, W.D. (1929), A Re-determination of the Trichromatic Coefficients of the Spectral Colours, *Trans. Optical Society*, **30**, 141, 1928-1929, 19cali29.

Wright, W.D. (1964), The Measurement of Colour, 96-118, 3rd ed, Hilger & Watts Ltd, London, 1964.

Wyszecki G. (1973) , Current Developments in Colorimetry, in Colour 73, 21-50, Adam Hilger, London, 1973.

Wyszecki G. (1982), W.S. Stiles, Science: Concepts and Methods, Quantitative Data and Formula (2nd edition), John Wiley,1982.

Xiao K. (2016), Z. Qin, T. Chauhan, C. Li and S. M. Wuerger, "Principal Component Analysis for Skin Reflectance Reconstruction", Society of for Imaging Science and Technology, 2016, pp. 146-150, 2016.

Xiao K (2016a), Zhu Y, Li C, Connah D, Yates JM, Wuerger S. Improved method for skin reflectance reconstruction from camera images. Opt Express. 2016 Jun 27;24(13):14934-50.

Young T. (1802), On the Theory of Light and Colours, *Phil. Roy. Soc., London*, **92**, 12, 1802.

Appendixes (A)

A0. Observers' estimations.

A0.1. Lightness estimation for observer (Ob) training by 15 subjects.

Ob1	Ob2	Ob3	Ob4	Ob5	Ob6	Ob7	Ob8	Ob9	Ob10	Ob11	Ob12	Ob13	Ob14	Ob15
90	98	90	95	100	98	99	98	90	90	95	100	98	95	90
85	90	80	90	94	85	80	85	90	89	85	80	75	80	90
60	55	60	60	75	65	70	65	70	70	70	65	50	65	70
20	20	25	20	10	15	20	17	15	25	25	15	10	15	20
90	87	85	88	95	90	85	90	82	80	79	85	90	85	80
20	30	30	30	15	20	25	20	30	33	28	25	25	25	30
95	90	90	95	100	90	95	93	85	90	90	95	100	90	95
35	45	35	40	30	35	40	40	40	30	35	45	25	30	45
70	60	70	60	65	60	65	55	60	62	57	55	70	65	60
10	12	10	10	5	7	10	12	8	10	10	15	5	12	10
40	25	30	60	55	35	40	45	45	40	50	45	30	45	50
15	20	20	15	30	15	15	25	20	20	18	15	25	20	15
70	70	70	70	80	75	70	80	75	70	75	80	75	70	70
40	55	65	50	60	45	50	65	60	55	45	55	60	55	50
12	10	25	25	15	10	12	20	23	20	15	25	15	20	25
95	90	96	90	95	90	90	90	90	95	90	90	95	95	95
5	**0**	**2**	**5**	**0**	**2**	**5**	**0**	**0**	**0**	**0**	**0**	**0**	**0**	**0**
40	45	40	45	25	30	35	40	35	40	45	35	25	30	35
8	10	20	25	10	15	10	9	8	10	12	15	17	10	10
55	53	55	55	45	50	45	55	45	55	50	50	45	50	40

A0.2 Observers' estimation for iPhone6S.

Ob 1	Ob2	Ob3	Ob4	Ob5	Ob6	Ob7	Ob8	Ob9	Ob10
100	95	98	100	90	95	100	100	100	100
85	75	70	80	70	80	85	80	75	85
60	65	60	60	50	55	65	60	60	55
5	10	10	10	20	5	5	15	5	15
55	65	60	60	90	65	60	60	60	65
30	25	30	30	20	25	20	25	30	30
60	75	65	65	95	70	75	65	70	85
25	30	35	30	35	25	30	35	25	20
70	75	70	75	70	65	60	70	75	65
15	10	10	5	10	15	5	5	15	10
65	75	55	70	40	65	70	75	60	65
80	85	75	85	15	80	85	80	70	75
25	30	15	10	70	20	25	30	10	15
30	30	35	45	40	35	45	40	50	40
65	80	75	75	12	70	60	75	80	85
70	85	90	98	95	95	85	90	80	95
100	100	100	100	95	90	98	92	95	100
25	35	30	45	40	40	45	30	25	35
12	10	15	15	8	20	10	5	15	15
50	65	60	60	55	60	65	50	55	60

A0.3 CV values for the observers in A0.2 for iPhone6S.

	cv-1	cv-2	cv-3	cv-4	cv-5	cv-6	cv-7	cv-8	cv-9	cv-10
	2.25	2.86	0.20	2.25	7.98	2.86	2.25	2.25	2.25	2.25
	8.28	4.46	10.83	1.91	10.83	1.91	8.28	1.91	4.46	8.28
	1.69	10.17	1.69	1.69	15.25	6.78	10.17	1.69	1.69	6.78
	50.00	0.00	0.00	0.00	10.00	50.00	50.00	50.00	50.00	50.00
	14.06	1.56	6.25	6.25	40.63	1.56	6.25	6.25	6.25	1.56
	13.21	5.66	13.21	13.21	24.53	5.66	24.53	5.66	13.21	13.21
	17.24	3.45	10.34	10.34	31.03	3.45	3.45	10.34	3.45	17.24
	13.79	3.45	20.69	3.45	20.69	13.79	3.45	20.69	13.79	31.03
	0.72	7.91	0.72	7.91	0.72	6.47	13.67	0.72	7.91	6.47
	50.00	0.00	0.00	50.00	0.00	50.00	50.00	50.00	50.00	0.00
	1.56	17.19	14.06	9.38	37.50	1.56	9.38	17.19	6.25	1.56
	9.59	16.44	2.74	16.44	79.45	9.59	16.44	9.59	4.11	2.74
	0.00	20.00	40.00	60.00	180.00	20.00	0.00	20.00	60.00	40.00
	23.08	23.08	10.26	15.38	2.56	10.26	15.38	2.56	28.21	2.56
	3.99	18.17	10.78	10.78	82.27	3.40	11.37	10.78	18.17	25.55
	20.72	3.74	1.93	10.99	7.59	7.59	3.74	1.93	9.40	7.59
	3.09	3.09	3.09	3.09	2.06	7.22	1.03	5.15	2.06	3.09
	28.57	0.00	14.29	28.57	14.29	14.29	28.57	14.29	28.57	0.00
	4.00	20.00	20.00	20.00	36.00	60.00	20.00	60.00	20.00	20.00
	13.79	12.07	3.45	3.45	5.17	3.45	12.07	13.79	5.17	3.45
Mean	24.10	20.25	19.57	20.17	31.01	24.43	24.46	25.80	27.74	22.17

A0.4 Observers' estimation for Motorola.

Ob 1	Ob2	Ob3	Ob4	Ob5	Ob6	Ob7	Ob8	Ob9	Ob10
95	90	98	92	100	90	95	90	100	100
80	85	75	80	75	85	80	85	70	80
50	50	55	65	60	70	65	50	65	60
10	20	15	10	20	15	10	5	5	15
65	70	60	60	65	50	60	65	60	65
30	20	35	30	30	20	25	25	35	30
75	55	65	60	70	50	75	65	70	65
25	20	35	30	35	20	30	35	25	20
75	65	70	70	70	80	60	75	65	70
10	5	15	10	9	14	5	5	10	10
65	55	75	70	60	50	65	75	75	70
85	65	70	85	70	55	90	85	75	70
25	15	30	35	15	10	15	25	10	15
30	20	35	45	40	25	35	45	30	45
65	80	75	75	70	85	70	65	70	80
90	65	90	95	90	100	95	80	90	95
100	90	100	95	100	90	98	100	100	95
45	30	40	45	40	25	30	35	30	25
10	5	12	10	15	8	15	5	15	10
50	60	65	55	50	65	60	60	65	60

A0.5 CV values for the observers for Motorola in Table A0.4.

	cv-1	cv-2	cv-3	cv-4	cv-5	cv-6	cv-7	cv-8	cv-9	cv-10
	0.00	5.26	3.16	3.16	5.26	5.26	0.00	5.26	5.26	5.26
	0.63	6.92	5.66	0.63	5.66	6.92	0.63	6.92	11.95	0.63
	15.25	15.25	6.78	10.17	1.69	18.64	10.17	15.25	10.17	1.69
	20.00	60.00	20.00	20.00	60.00	20.00	20.00	60.00	60.00	20.00
	4.84	12.90	3.23	3.23	4.84	19.35	3.23	4.84	3.23	4.84
	7.14	28.57	25.00	7.14	7.14	28.57	10.71	10.71	25.00	7.14
	15.38	15.38	0.00	7.69	7.69	23.08	15.38	0.00	7.69	0.00
	9.09	27.27	27.27	9.09	27.27	27.27	9.09	27.27	9.09	27.27
	7.14	7.14	0.00	0.00	0.00	14.29	14.29	7.14	7.14	0.00
	7.53	46.24	61.29	7.53	3.23	50.54	46.24	46.24	7.53	7.53
	1.52	16.67	13.64	6.06	9.09	24.24	1.52	13.64	13.64	6.06
	13.33	13.33	6.67	13.33	6.67	26.67	20.00	13.33	0.00	6.67
	28.21	23.08	53.85	79.49	23.08	48.72	23.08	28.21	48.72	23.08
	14.29	42.86	0.00	28.57	14.29	28.57	0.00	28.57	14.29	28.57
	11.56	8.84	2.04	2.04	4.76	15.65	4.76	11.56	4.76	8.84
	1.12	26.97	1.12	6.74	1.12	12.36	6.74	10.11	1.12	6.74
	3.31	7.02	3.31	1.86	3.31	7.02	1.24	3.31	3.31	1.86
	30.43	13.04	15.94	30.43	15.94	27.54	13.04	1.45	13.04	27.54
	4.76	52.38	14.29	4.76	42.86	23.81	42.86	52.38	42.86	4.76
	15.25	1.69	10.17	6.78	15.25	10.17	1.69	1.69	10.17	1.69
Mean	10.54	21.54	13.67	12.44	12.96	21.93	12.23	17.39	14.95	9.51

A0.6 Observers' estimation for Samsung.

Ob 1	Ob2	Ob3	Ob4	Ob5	Ob6	Ob7	Ob8	Ob9	Ob10
100	80	90	100	95	95	100	80	95	100
85	90	80	75	70	70	75	70	80	70
65	50	45	50	60	55	60	65	65	55
10	5	5	10	10	10	10	20	10	10
65	55	50	60	65	60	65	70	65	60
30	20	25	35	31	25	35	25	30	30
60	75	50	65	65	60	65	55	70	65
25	40	35	20	25	25	30	45	20	25
70	60	55	75	70	75	70	60	65	75
15	5	5	10	10	15	10	5	15	10
65	75	55	60	65	65	70	80	60	65
80	60	70	85	80	80	85	65	75	80
25	15	10	25	30	25	35	10	20	25
30	15	20	35	40	35	45	25	45	40
65	80	75	65	70	60	55	75	65	65
70	85	90	75	80	75	70	70	90	85
100	90	95	100	100	100	100	90	95	100
45	35	30	45	40	40	45	25	40	35
15	10	10	15	20	20	10	5	15	15
55	60	60	50	55	65	55	65	50	60

A0.7 CV values for the observers for Samsung in Table A0.6.

	cv-1	cv-2	cv-3	cv-4	cv-5	cv-6	cv-7	cv-8	cv-9	cv-10

	6.95	14.44	3.74	6.95	1.60	1.60	6.95	14.44	1.60	6.95
	11.11	17.65	4.58	1.96	8.50	8.50	1.96	8.50	4.58	8.50
	14.04	12.28	21.05	12.28	5.26	3.51	5.26	14.04	14.04	3.51
	0.00	50.00	50.00	0.00	0.00	0.00	0.00	100.00	0.00	0.00
	5.69	10.57	18.70	2.44	5.69	2.44	5.69	13.82	5.69	2.44
	4.90	30.07	12.59	22.38	8.39	12.59	22.38	12.59	4.90	4.90
	4.76	19.05	20.63	3.17	3.17	4.76	3.17	12.70	11.11	3.17
	13.79	37.93	20.69	31.03	13.79	13.79	3.45	55.17	31.03	13.79
	3.70	11.11	18.52	11.11	3.70	11.11	3.70	11.11	3.70	11.11
	50.00	50.00	50.00	0.00	0.00	50.00	0.00	50.00	50.00	0.00
	1.52	13.64	16.67	9.09	1.52	1.52	6.06	21.21	9.09	1.52
	5.26	21.05	7.89	11.84	5.26	5.26	11.84	14.47	1.32	5.26
	13.64	31.82	54.55	13.64	36.36	13.64	59.09	54.55	9.09	13.64
	9.09	54.55	39.39	6.06	21.21	6.06	36.36	24.24	36.36	21.21
	3.70	18.52	11.11	3.70	3.70	11.11	18.52	11.11	3.70	3.70
	11.39	7.59	13.92	5.06	1.27	5.06	11.39	11.39	13.92	7.59
	3.09	7.22	2.06	3.09	3.09	3.09	3.09	7.22	2.06	3.09
	18.42	7.89	21.05	18.42	5.26	5.26	18.42	34.21	5.26	7.89
	11.11	25.93	25.93	11.11	48.15	48.15	25.93	62.96	11.11	11.11
	4.35	4.35	4.35	13.04	4.35	13.04	4.35	13.04	13.04	4.35
Mean	9.83	22.28	20.87	9.32	9.01	11.02	12.38	27.34	11.58	6.69

A0.8 Observers' estimation for iPhone10.

Ob 1	Ob2	Ob3	Ob4	Ob5	Ob6	Ob7	Ob8	Ob9	Ob10
100	98	100	100	100	99	85	99	100	100
80	75	80	65	80	75	80	80	75	70
60	65	70	75	60	55	60	58	65	50
10	5	8	15	10	15	5	10	10	10
60	65	65	50	60	55	50	60	65	65
30	25	30	15	25	20	35	30	35	25
65	65	50	45	55	60	55	65	55	50
30	35	25	20	30	35	30	25	20	25
75	70	75	75	75	65	60	70	70	75
5	0	2	10	5	5	5	5	5	10
70	60	65	80	75	60	65	70	75	65
85	80	70	75	85	70	75	80	85	85
10	15	10	5	10	10	10	5	15	10
45	50	55	35	40	45	45	35	45	40
75	70	65	70	75	60	60	70	75	65
98	90	85	100	90	95	99	95	90	95
100	98	100	100	100	99	85	99	100	100
45	35	45	30	40	35	30	45	40	35
15	10	15	9	10	15	10	10	10	10
60	70	65	55	60	58	66	60	65	60

A0.11 CV values for the observers for iPhone10 in Table A0.10.

	cv-1	cv-2	cv-3	cv-4	cv-5	cv-6	cv-7	cv-8	cv-9	cv-10
	1.94	0.10	1.94	1.94	1.94	0.92	13.35	0.92	1.94	1.94
	5.26	1.32	5.26	14.47	5.26	1.32	5.26	5.26	1.32	7.89
	2.91	5.18	13.27	21.36	2.91	11.00	2.91	6.15	5.18	19.09

	2.04	48.98	18.37	53.06	2.04	53.06	48.98	2.04	2.04	2.04
	0.84	9.24	9.24	15.97	0.84	7.56	15.97	0.84	9.24	9.24
	11.11	7.41	11.11	44.44	7.41	25.93	29.63	11.11	29.63	7.41
	15.04	15.04	11.50	20.35	2.65	6.19	2.65	15.04	2.65	11.50
	9.09	27.27	9.09	27.27	9.09	27.27	9.09	9.09	27.27	9.09
	5.63	1.41	5.63	5.63	5.63	8.45	15.49	1.41	1.41	5.63
	3.85	100.00	61.54	92.31	3.85	3.85	3.85	3.85	3.85	92.31
	2.19	12.41	5.11	16.79	9.49	12.41	5.11	2.19	9.49	5.11
	7.59	1.27	11.39	5.06	7.59	11.39	5.06	1.27	7.59	7.59
	0.00	50.00	0.00	50.00	0.00	0.00	0.00	50.00	50.00	0.00
	3.45	14.94	26.44	19.54	8.05	3.45	3.45	19.54	3.45	8.05
	9.49	2.19	5.11	2.19	9.49	12.41	12.41	2.19	9.49	5.11
	4.59	3.95	9.28	6.72	3.95	1.39	5.66	1.39	3.95	1.39
	1.94	0.10	1.94	1.94	1.94	0.92	13.35	0.92	1.94	1.94
	18.42	7.89	18.42	21.05	5.26	7.89	21.05	18.42	5.26	7.89
	31.58	12.28	31.58	21.05	12.28	31.58	12.28	12.28	12.28	12.28
	3.07	13.09	5.01	11.15	3.07	6.30	6.62	3.07	5.01	3.07
Mean	7.00	16.70	13.06	22.62	5.14	11.66	11.61	8.35	9.65	10.92

A1. Ten repeated measurements for 20 colour samples on LCD monitors using colour meter CS-100A.

A1.1. Value of Y

Y										Mean	SD/Mean
59.50	55.6	56.4	50.8	59.6	56.5	56.4	54.1	56.5	52.7	55.81	0.047
17.90	17.5	17.6	17.90	16.8	17.5	17.6	17.60	17.5	17.80	17.57	0.017
8.12	10.7	9.80	9.66	9.38	10.9	9.80	8.88	8.95	8.65	9.48	0.088
0.39	0.40	0.40	0.39	0.39	0.36	0.40	0.36	0.41	0.42	0.39	0.047
24.40	23.50	26.4	23.9	24.90	25.80	24.40	23.90	23.80	23.90	24.49	0.037
0.35	0.28	0.28	0.40	0.35	0.28	0.28	0.18	0.34	0.21	0.30	0.216
22.90	21.6	21.0	22.00	22.06	21.0	21.0	24.0	21.0	23.89	22.05	0.051
0.77	0.77	0.68	0.39	0.66	0.91	0.68	0.54	0.67	0.63	0.67	0.197
9.74	9.18	8.25	8.50	9.20	9.18	8.25	8.20	9.18	8.16	8.78	0.062
0.73	0.78	0.76	0.80	0.80	0.78	0.76	0.72	0.87	0.72	0.77	0.056
0.76	0.76	0.78	0.76	0.65	0.75	0.78	0.65	0.76	0.80	0.75	0.066
1.48	1.33	1.50	1.50	1.45	1.51	1.50	1.45	1.52	1.76	1.50	0.067
13.0	13.8	12.8	11.9	13.40	11.9	12.8	11.90	11.54	10.54	12.36	0.075
5.60	5.50	5.74	5.80	5.80	5.20	5.74	5.76	5.54	5.76	5.64	0.032
0.31	0.28	0.40	0.28	0.28	0.30	0.40	0.32	0.33	0.45	0.34	0.171
30.50	28.82	29.85	28.9	28.6	28.90	29.85	27.65	26.78	28.43	28.83	0.036
8.33	8.55	8.89	8.09	8.54	8.67	8.89	8.64	8.32	8.97	8.59	0.031
2.84	2.82	2.80	3.20	2.90	2.89	2.80	2.91	2.43	2.76	2.84	0.063
3.39	3.82	3.40	3.60	3.43	3.33	3.40	3.25	3.25	3.12	3.40	0.055
7.90	8.70	8.80	7.90	6.69	8.86	8.80	8.65	7.68	6.98	8.10	0.093
										Average	0.075

A1.2. Value of x and X

x										Mean	SD/mean
.339	.312	.339	.340	.339	.309	.339	.345	.312	.345	0.33	0.042
.357	.316	.348	.350	.357	.319	.348	.324	.316	.324	0.34	0.049
.376	.319	.375	.375	.376	.329	.375	.377	.319	.377	0.36	0.069
.352	.320	.352	.362	.352	.326	.352	.284	.320	.284	0.33	0.082
.351	.316	.368	.328	.354	.316	.368	.362	.316	.362	0.34	0.062
.296	.318	.285	.285	.296	.318	.285	.269	.318	.269	0.29	0.061
.355	.318	.364	.324	.334	.378	.364	.355	.318	.355	0.35	0.058
.325	.319	.325	.340	.325	.321	.325	.325	.319	.325	0.32	0.017
.365	.317	.360	.359	.365	.317	.360	.375	.317	.375	0.35	0.065
.229	0.22	.230	.220	.267	.223	.230	.260	.223	.240	0.23	0.066
.427	.420	.428	.425	.376	.389	.428	.376	.420	.376	0.41	0.056
.198	.208	.199	.260	.198	.205	.199	.206	.208	.206	0.21	0.084
.360	.320	.375	.385	.360	.319	.375	.380	.320	.380	0.36	0.072
.381	.319	.370	.370	.367	.320	.370	.369	.319	.369	0.36	0.067
.331	.324	.285	.290	.331	.304	.285	.290	.324	.290	0.31	0.062
.351	.318	.375	.380	.352	.398	.375	.380	.318	.380	0.36	0.071
.257	.260	.260	.260	.255	.243	.260	.285	.260	.285	0.26	0.047
.396	.368	.380	.369	.398	.387	.380	.326	.368	.326	0.37	0.065
.259	.220	.280	.275	.259	.241	.280	.246	.260	.246	0.26	0.070
.374	.320	.375	.369	.373	.398	.375	.380	.320	.380	0.37	0.066
										Average	0.062

X										Mean	SD/mean
58.47	50.28	55.42	44.75	59.08	49.18	55.42	55.06	51.10	53.63	53.24	0.083
17.60	16.12	18.90	18.48	15.54	16.28	18.90	16.39	16.12	16.57	17.09	0.070
8.10	9.89	9.75	9.66	10.62	10.39	9.75	8.93	8.28	8.70	9.41	0.087
0.36	0.38	0.37	0.36	0.49	0.34	0.40	0.29	0.39	0.34	0.37	0.132
23.66	21.59	26.84	21.78	24.35	25.32	24.80	23.51	21.86	23.51	23.72	0.068
0.40	0.34	0.30	0.41	0.40	0.33	0.30	0.17	0.41	0.20	0.33	0.251
22.33	19.91	21.53	19.91	20.24	19.94	21.53	23.41	19.36	23.30	21.15	0.067
0.66	0.73	0.59	0.36	0.57	0.89	0.59	0.41	0.63	0.48	0.59	0.247
9.53	8.46	7.92	8.14	9.03	8.56	7.92	8.54	8.46	8.50	8.51	0.055
0.63	0.72	0.67	0.70	0.81	0.74	0.67	0.81	0.83	0.75	0.73	0.088
0.87	0.94	0.89	0.85	0.65	0.84	0.89	0.57	0.94	0.70	0.81	0.149
1.01	0.82	1.00	1.35	0.90	0.93	1.03	1.00	0.93	1.21	1.02	0.145
12.68	12.80	12.63	12.55	12.60	10.66	12.63	12.06	10.70	10.68	12.00	0.074
5.66	4.62	5.76	5.57	5.65	4.18	5.76	5.74	4.65	5.74	5.33	0.107
0.30	0.27	0.34	0.22	0.30	0.27	0.34	0.28	0.32	0.39	0.30	0.148
29.90	26.72	29.46	29.29	28.12	33.53	29.46	28.02	24.83	28.81	28.81	0.074
7.02	6.95	8.11	7.38	7.14	6.16	8.11	9.47	6.76	9.83	7.69	0.146
2.98	2.80	3.26	3.28	3.26	2.81	3.26	2.50	2.42	2.37	2.89	0.121
3.44	3.00	3.87	4.02	3.67	3.30	3.87	2.86	3.02	2.74	3.38	0.130
7.71	8.02	8.68	7.67	6.45	10.92	8.68	8.77	7.08	7.07	8.11	0.147
										Average	0.119

A1.3. Values of y and Z

y										Mean	SD/Mean
.345	.345	.345	.386	.342	.355	.345	.339	.345	.339	0.35	0.038
.363	.343	.324	.339	.386	.343	.324	.348	.343	.348	0.35	0.050
.377	.345	.377	.375	.332	.345	.377	.375	.345	.375	0.36	0.047
.383	.339	.384	.390	.278	.343	.348	.352	.339	.352	0.35	0.087
.362	.344	.362	.360	.362	.322	.362	.368	.344	.368	0.36	0.039
.259	0.26	.269	.275	.260	.267	.269	.285	.264	.285	0.27	0.033
.364	.345	.355	.358	.364	.398	.355	.364	.345	.364	0.36	0.039
.378	.338	.375	.365	.378	.330	.375	.425	.338	.425	0.37	0.084
.373	.344	.375	.375	.372	.340	.375	.360	.344	.360	0.36	0.038
.264	0.24	.260	.250	.264	.235	.260	.230	.235	.230	0.25	0.056
.375	.338	.376	.380	.375	.349	.376	.428	.338	.428	0.38	0.080
.289	.339	.299	.289	.319	.332	.290	.299	.339	.299	0.31	0.064
.369	.345	.380	.365	.383	.356	.380	.375	.345	.375	0.37	0.037
.377	.380	.369	.385	.377	.398	.369	.370	.380	.370	0.38	0.023
.343	.336	0.336	.365	.312	.336	.336	.336	.336	.336	0.34	0.036
.358	.343	.380	.375	.358	.343	.380	.375	.343	.375	0.36	0.041
.305	.320	.285	.285	.305	.342	.285	.260	.320	.260	0.30	0.085
.377	0.37	.326	.360	.354	.398	.326	.380	.370	.380	0.36	0.061
.255	0.28	.246	.246	.242	0.243	.246	.280	.280	.280	0.26	0.065
.383	.347	.380	.380	.387	.323	.380	.375	.347	.375	0.37	0.055
										Average	0.053

Z										Mean	SD/Mean
54.50	55.28	51.66	36.06	55.59	53.48	51.66	50.43	56.17	49.12	51.40	0.114
13.81	17.40	17.82	16.42	11.19	17.24	17.82	16.59	17.40	16.78	16.25	0.124
5.32	10.42	6.45	6.44	8.25	10.30	6.45	5.87	8.72	5.72	7.39	0.243
0.27	0.40	0.28	0.25	0.52	0.35	0.34	0.37	0.41	0.43	0.36	0.217
19.34	23.23	19.69	20.71	19.53	29.00	18.20	17.54	23.52	17.54	20.83	0.162
0.60	0.45	0.46	0.64	0.60	0.44	0.46	0.28	0.54	0.33	0.48	0.232
17.68	21.10	16.62	19.54	18.30	11.82	16.62	18.53	20.51	18.44	17.92	0.138
0.61	0.78	0.54	0.32	0.52	0.96	0.54	0.32	0.68	0.37	0.56	0.345
6.84	9.05	5.83	6.03	6.50	9.26	5.83	6.04	9.05	6.01	7.04	0.197
1.40	1.76	1.49	1.70	1.42	1.80	1.49	1.60	2.01	1.66	1.63	0.112
0.40	0.54	0.41	0.39	0.43	0.56	0.41	0.30	0.54	0.37	0.44	0.185
2.63	1.78	2.52	2.34	2.20	2.11	2.64	2.40	2.03	2.91	2.36	0.135
9.55	13.40	8.25	8.15	8.99	10.86	8.25	7.77	11.21	6.89	9.33	0.200
3.59	4.36	4.06	3.69	3.94	3.68	4.06	4.06	4.39	4.06	3.99	0.065
0.29	0.28	0.45	0.26	0.32	0.32	0.45	0.36	0.33	0.50	0.36	0.219
24.79	28.48	19.25	18.88	23.17	21.82	19.25	18.06	26.47	18.57	21.87	0.160
11.96	11.22	14.19	12.92	12.32	10.52	14.19	15.12	10.92	15.70	12.91	0.134
1.71	2.00	2.53	2.41	2.03	1.56	2.53	2.25	1.72	2.14	2.09	0.158
6.46	6.82	6.55	7.01	7.07	7.07	6.55	5.50	5.34	5.28	6.37	0.107
5.01	8.35	5.67	5.22	4.15	7.65	5.67	5.65	7.37	4.56	5.93	0.223
										Average	0.174

*A2. CIEL*a*b* values for the samples in A1.*

*A2.1. Values of L**

L*										Mean (mL)
81.57	79.39	79.84	76.56	81.62	79.90	79.84	78.52	79.90	77.70	79.48
49.37	48.88	49.01	49.37	48.01	48.88	49.01	49.01	48.88	49.25	48.97
34.23	39.07	37.48	37.23	36.71	39.41	37.48	35.75	35.89	35.30	36.85
3.52	3.61	3.61	3.52	3.52	3.25	3.61	3.25	3.70	3.79	3.54
56.49	55.58	58.41	55.99	56.98	57.85	56.49	55.99	55.89	55.99	56.56
3.16	2.53	2.53	3.61	3.16	2.53	2.53	1.63	3.07	1.90	2.66
54.97	53.60	52.95	54.03	54.09	52.95	52.95	56.09	52.95	55.98	54.06
6.96	6.96	6.14	3.52	5.96	8.22	6.14	4.88	6.05	5.69	6.05
37.37	36.33	34.50	35.00	36.37	36.33	34.50	34.40	36.33	34.31	35.54
6.59	7.05	6.87	7.23	7.23	7.05	6.87	6.50	7.86	6.50	6.97
6.87	6.87	7.05	6.87	5.87	6.77	7.05	5.87	6.87	7.23	6.73
12.48	11.48	12.61	12.61	12.29	12.67	12.61	12.29	12.73	14.17	12.59
42.76	43.94	42.46	41.06	43.36	41.06	42.46	41.06	40.48	38.79	41.74
28.38	28.11	28.75	28.90	28.90	27.30	28.75	28.80	28.22	28.80	28.49
2.80	2.53	3.61	2.53	2.53	2.71	3.61	2.89	2.98	4.06	3.03
62.08	60.62	61.52	60.69	60.43	60.69	61.52	59.57	58.77	60.28	60.62
34.66	35.10	35.77	34.17	35.08	35.34	35.77	35.28	34.64	35.93	35.17
19.39	19.31	19.22	20.83	19.64	19.60	19.22	19.68	17.60	19.06	19.35
21.54	23.07	21.58	22.30	21.69	21.32	21.58	21.02	21.02	20.52	21.56
33.77	35.40	35.60	33.77	31.09	35.71	35.60	35.30	33.31	31.76	34.13

A2.2. Value of a*.

a*										Mean |ma*|
4.68	-6.76	4.60	-9.99	5.93	-11.95	4.60	9.39	-6.80	9.30	7.40
3.22	-2.89	11.65	7.88	-2.50	-2.02	11.65	-1.92	-2.89	-1.93	4.86
3.50	-2.17	3.52	3.92	13.67	0.26	3.52	4.21	-2.05	4.17	4.10
-0.50	-0.11	-0.55	-0.36	5.04	-0.00	1.00	-2.12	-0.11	-2.47	1.23
2.08	-3.49	7.27	-4.35	3.00	3.41	7.08	3.57	-3.50	3.57	4.13
2.76	3.13	1.25	1.41	2.69	2.76	1.25	-0.05	3.54	-0.06	1.89
2.64	-3.06	7.61	-4.89	-3.53	-0.08	7.61	2.68	-3.03	2.67	3.78
-2.86	-0.21	-2.33	-0.30	-2.45	0.81	-2.33	-4.11	-0.18	-4.79	2.04
2.24	-2.32	0.72	0.53	2.40	-1.44	0.72	6.73	-2.32	6.72	2.62
-2.48	-1.08	-2.05	-2.31	1.99	-0.05	-2.05	5.31	-0.06	2.74	2.01
5.85	8.93	5.97	5.23	1.39	5.04	5.97	-1.92	8.93	-2.36	5.16
-12.69	-16.07	-13.81	-2.24	-16.15	-16.55	-12.69	-12.40	-16.81	-13.23	13.26
2.21	-2.10	3.17	8.69	-0.95	-4.79	3.17	5.30	-1.98	5.09	3.75
3.95	-7.71	3.47	0.71	1.55	-10.13	3.47	3.12	-7.73	3.12	4.50
0.18	0.16	-1.68	-1.79	1.27	-0.56	-1.68	-1.15	0.19	-1.61	1.03
3.50	-2.73	4.21	7.13	3.74	22.73	4.21	7.03	-2.66	7.09	6.50
-8.59	-11.22	-3.03	-2.94	-9.22	-20.46	-3.03	10.76	-11.12	10.89	9.13
5.17	2.32	10.69	4.04	8.84	1.17	10.69	-5.17	2.21	-5.08	5.54
3.62	-10.35	10.03	9.17	6.55	2.30	10.03	-4.13	-1.24	-4.07	6.15
1.94	-2.22	2.80	1.54	0.94	20.15	2.80	4.77	-2.13	4.44	4.37

A2.3. Values of b*.

b*										Mean |mb*|
9.42	4.91	9.26	21.21	8.46	7.54	9.26	8.23	4.94	8.15	9.14

12.24	3.34	2.69	6.26	16.69	3.66	2.69	5.26	3.34	5.28	6.14
13.49	3.47	14.26	13.84	6.24	4.41	14.26	13.66	3.27	13.54	10.04
2.21	0.47	2.30	2.53	-1.35	0.64	1.30	0.28	0.49	0.33	1.19
12.54	3.92	15.20	9.09	13.02	-1.36	14.81	15.30	3.94	15.30	10.45
-3.15	-2.14	-2.28	-2.92	-3.10	-1.86	-2.28	-1.23	-2.40	-1.43	2.28
13.25	4.27	11.99	7.92	10.47	23.47	11.99	13.46	4.23	13.44	11.45
3.34	0.82	2.81	1.57	2.86	0.40	2.81	3.87	0.71	4.51	2.37
12.51	2.95	11.68	11.71	12.10	2.27	11.68	10.63	2.95	10.61	8.91
-7.92	-10.79	-8.42	-9.90	-7.04	-11.21	-8.42	-10.15	-11.69	-10.78	9.63
6.10	4.05	6.33	6.26	3.95	3.63	6.33	5.87	4.05	7.22	5.38
-8.69	-3.35	-7.66	-6.29	-5.67	-4.25	-8.58	-7.31	-3.50	-7.80	6.31
12.46	3.87	16.15	14.08	15.25	5.61	16.15	15.40	3.65	14.79	11.74
12.36	7.65	10.33	12.69	11.27	9.96	10.33	10.41	7.67	10.41	10.31
0.61	0.31	-0.22	0.58	-0.22	0.07	-0.22	-0.11	0.36	-0.16	0.29
12.50	4.20	21.42	20.70	12.37	15.19	21.42	20.40	4.10	20.59	15.29
-8.44	-5.66	-12.14	-11.77	-8.66	-3.26	-12.14	-15.15	-5.61	-15.34	9.82
10.93	8.13	3.70	7.35	8.40	12.79	3.70	6.62	7.74	6.51	7.59
-13.28	-12.08	-13.58	-14.12	-15.41	-16.05	-13.58	-10.11	-9.38	-9.98	12.76
14.14	3.65	14.26	13.17	13.89	6.62	14.26	13.85	3.50	12.89	11.02

A.2.4. Value of ΔEab (= $\sqrt{(\boldsymbol{L^* - mL^*})^2 + (\boldsymbol{a^* - ma^*})^2 + (\boldsymbol{b^* - mb^*})^2}$

ΔE^*_{ab}										Mean |mb*|
3.44	4.28	2.82	12.69	2.68	4.84	2.82	2.39	4.26	2.79	4.30
6.32	3.42	7.62	3.05	10.85	3.77	7.62	3.06	3.42	3.06	5.22
4.37	7.20	4.30	3.82	10.30	7.28	4.30	3.79	7.15	3.83	5.63
1.26	1.33	1.30	1.60	3.82	1.37	0.26	1.31	1.33	1.53	1.51
2.93	6.63	5.99	1.49	2.84	9.20	5.26	4.92	6.58	4.92	5.08
1.33	1.25	0.65	1.24	1.25	0.97	0.65	2.36	1.70	2.16	1.36
2.32	7.23	4.02	3.70	1.01	12.63	4.02	3.07	7.35	2.98	4.83
1.56	2.56	0.54	3.17	0.65	3.17	0.54	2.81	2.49	3.51	2.10
4.05	6.02	3.52	3.53	3.31	6.79	3.52	4.61	6.02	4.61	4.60
1.82	1.48	1.22	0.47	2.60	2.52	1.22	3.37	2.98	1.44	1.91
1.01	4.00	1.29	0.89	4.12	1.76	1.29	3.39	4.00	3.39	2.51
2.45	4.23	1.46	11.03	2.97	3.88	2.35	1.36	4.53	2.17	3.64
1.98	8.34	4.51	5.51	4.77	6.26	4.51	4.04	8.38	4.45	5.28
2.12	4.19	1.06	4.49	3.13	5.77	1.06	1.41	4.18	1.41	2.88
0.93	1.00	0.88	0.96	0.56	0.60	0.88	0.25	0.84	1.20	0.81
4.35	11.72	6.61	5.45	4.02	16.23	6.61	5.24	11.98	5.34	7.76
1.56	4.66	6.55	6.57	1.17	13.09	6.55	5.58	4.69	5.85	5.63
3.37	3.26	6.46	2.11	3.42	6.80	6.46	1.08	3.77	1.21	3.79
2.58	4.52	3.97	3.40	2.69	5.07	3.97	3.37	5.99	3.62	3.92
3.97	7.78	3.88	3.58	5.41	16.45	3.88	3.08	7.89	3.02	5.89
									Average	**3.93**

Appendix A3. Colour measurement of mobile phones repeated 8 times.

A3.1 Measurements for iPhone6S

1			2			3			4		
Y	X	y	Y	X	y	Y	X	y	Y	X	y
493	.306	.337	498	.306	.343	487	.306	.337	499	.343	.306
207	.306	.338	213	.306	.322	202	.306	.338	208	.322	.307
123	.305	.336	119	.305	.383	143	.305	.337	154	.383	.306
33.3	.309	.329	32.6	.309	.332	32.2	.309	.333	33.3	.332	.309
280	.306	.336	278	.306	.389	274	.307	.323	279	.389	.306
41.5	.307	.339	41.0	.307	.339	49.3	.307	.339	40.6	.339	.307
249	.304	.334	265	.304	.323	239	.304	.334	249	.323	.304
48.0	.305	.330	43.9	.305	.329	47.3	.305	.330	47.6	.329	.305
139	.305	.335	168	.305	.305	138.7	.305	.334	141	.305	.305
24.3	.372	.335	22.9	.372	.335	22.6	.371	.335	22.9	.335	.370
49.0	.307	.330	43.6	.307	.333	43.7	.307	.330	48.76	.333	.372
25.0	.370	.329	22.9	.370	.321	22.7	.370	.326	22.0	.321	.307
168	.304	.334	185	.304	.337	167	.304	.333	148	.337	.304
103	.305	.334	100	.305	.343	108	.305	.334	101	.343	.305
27.5	.305	.322	27.5	.305	.310	22.87	.305	.319	25.6	.310	.305
327	.304	.335	327	.304	.323	319	.304	.335	328	.323	.304
8.52	.303	.290	8.76	.303	.365	7.88	.303	.376	8.76	.365	.303
77.5	.306	.334	75.7	.306	.311	71.6	.306	.334	77.6	.311	.304
16.7	.311	.329	15.2	.311	.354	15.6	.310	.310	16.8	.354	.312

5			6			7			8		
Y	X	y	Y	X	y	Y	X	y	Y	X	y
487	.306	.337	493	.306	.337	493	.306	.337	493	.306	.337
202	.306	.338	207	.306	.338	207	.306	.338	207	.306	.338
143	.305	.336	123	.305	.336	123	.305	.336	123	.305	.336
33.3	.309	.329	33.3	.309	.329	33.3	.309	.329	33.3	.309	.329
279	.306	.336	280	.306	.336	280	.306	.336	280	.306	.336
40.6	.307	.339	41.5	.307	.339	41.5	.307	.339	41.5	.307	.339
249	.304	.334	249	.304	.334	249	.304	.334	249	.304	.334
47.6	.305	.330	48.0	.305	.330	48.0	.305	.330	48.0	.305	.330
141	.305	.335	139	.305	.335	139	.305	.335	138.7	.305	.334
22.9	.372	.335	24.3	.372	.335	24.3	.372	.335	22.6	.371	.335
48.76	.307	.330	49.0	.307	.330	49.0	.307	.330	43.7	.307	.330
22.0	.370	.329	25.0	.370	.329	25.0	.370	.329	22.7	.370	.326
148	.304	.334	168	.304	.334	168	.304	.334	167	.304	.333

101	.305	.334	103	.305	.334	103	.305	.334	108	.305	.334
25.6	.305	.322	27.5	.305	.322	27.5	.305	.322	22.87	.305	.319
319	.304	.335	327	.304	.335	327	.304	.335	319	.304	.335
7.88	.303	.290	8.52	.303	.290	8.52	.303	.290	7.88	.303	.376
77.5	.306	.334	75.7	.306	.311	71.6	.306	.334	77.6	.311	.304
16.7	.311	.329	15.2	.311	.354	15.6	.310	.310	16.8	.354	.312

A3.2 Measurements for Motorola

1			2			3			4		
Y	x	y	Y	x	y	Y	x	y	Y	x	y
493	0.306	0.337	492	0.305	0.336	493	0.306	0.335	493	0.306	0.337
207	0.306	0.338	208	0.306	0.338	207	0.306	0.338	208	0.305	0.338
123	0.305	0.336	123	0.305	0.339	120	0.306	0.337	123	0.305	0.336
33.3	0.309	0.329	33.6	0.309	0.329	33.4	0.305	0.33	33.9	0.305	0.337
280	0.306	0.336	282	0.306	0.335	280	0.306	0.335	283	0.306	0.335
41.5	0.307	0.339	41	0.306	0.333	41	0.306	0.34	41	0.306	0.333
249	0.304	0.334	249	0.305	0.34	247	0.305	0.333	247	0.306	0.333
48	0.305	0.33	48	0.305	0.333	47.8	0.305	0.34	47.3	0.306	0.336
139	0.305	0.335	138	0.305	0.334	139	0.309	0.333	139	0.305	0.336
24.3	0.372	0.335	24.7	0.37	0.33	24.6	0.371	0.334	24.8	0.307	0.334
49	0.307	0.33	49.4	0.308	0.332	49	0.308	335	49.4	0.372	0.335
25	0.37	0.329	25.2	0.368	0.335	25	0.367	0.334	25.2	0.362	0.33
168	0.304	0.334	168	0.307	0.33	169	0.369	0.333	168	0.305	0.334
103	0.305	0.334	102	308	0.33	103	0.303	0.33	101	0.303	0.33
27.5	0.305	0.322	27.4	0.305	0.32	27.5	0.305	0.332	27.4	0.306	0.302
327	0.304	0.335	324	0.303	0.334	327	0.308	0.33	327	0.305	0.33
8.52	0.303	0.29	8.45	0.303	0.302	8.5	0.307	0.32	8.5	0.307	0.33
77.5	0.306	0.334	78.2	0.305	0.32	77.8	0.305	0.33	77.4	0.305	0.32
26.7	0.311	0.329	25.8	0.31	0.33	26.8	0.305	0.334	26.5	0.306	0.332
119	0.304	0.333	120	0.305	0.338	118	0.31	0.32	116	0.303	0.335

A3.3 Measurements for Samsung S6

1			2			3			4			5		
Y	x	y	Y	x	y	Y	x	y	Y	x	y	Y	x	y
177	0.318	0.363	176	0.318	0.363	175	0.318	0.363	176	0.318	0.363	177	0.318	0.363
107	0.317	0.363	105	0.317	0.363	107	0.317	0.365	107	0.317	0.363	107	0.317	0.363
101	0.322	0.351	100	0.322	0.351	101	0.321	0.352	102	0.322	0.351	101	0.322	0.351

15.2	0.324	0.35	15.3	0.323	0.35	15.4	0.324	0.35	15.2	0.324	0.35	15.2	0.324	0.35
69.6	0.325	0.352	69.6	0.325	0.352	69.4	0.325	0.352	69.6	0.325	0.352	69.6	0.325	0.352
57.9	0.323	0.347	57.9	0.323	0.347	57.7	0.323	0.347	57.8	0.323	0.347	57.9	0.323	0.347
53.4	0.324	0.348	53.4	0.324	0.348	53.2	0.322	0.348	53.3	0.324	0.348	53.4	0.324	0.348
51.2	0.325	0.344	51.2	0.325	0.344	51.1	0.325	0.344	51.2	0.325	0.344	51.2	0.325	0.344
49.4	0.324	0.346	49.4	0.323	0.346	49.4	0.324	0.345	49.4	0.324	0.346	49.4	0.324	0.346
48.6	0.325	0.342	48.6	0.325	0.342	48.6	0.322	0.343	48.3	0.325	0.342	48.6	0.325	0.342
49.8	0.325	0.348	49.7	0.324	0.348	49.1	0.325	0.348	49.8	0.325	0.348	49.8	0.325	0.348
36.7	0.326	0.34	36.2	0.326	0.34	36.7	0.325	0.342	36.7	0.326	0.34	36.7	0.326	0.34
51.4	0.324	0.348	51.2	0.324	0.348	51.4	0.322	0.348	51.4	0.324	0.348	51.4	0.324	0.348
46.5	0.324	0.348	46.5	0.323	0.349	46.3	0.324	0.349	46.5	0.324	0.348	46.5	0.324	0.348
71.2	0.319	0.351	71.1	0.319	0.351	71.2	0.317	0.35	71.2	0.319	0.351	71.2	0.319	0.351
80.3	0.315	0.355	80.1	0.315	0.356	80.3	0.316	0.354	80.3	0.315	0.355	80.3	0.315	0.355
75.4	0.316	0.356	75.3	0.316	0.355	75.4	0.316	0.356	75.4	0.316	0.356	75.4	0.316	0.356
68.4	0.316	0.352	68.4	0.316	0.352	68.2	0.316	0.351	68.4	0.316	0.352	68.4	0.316	0.352
62.4	0.319	0.352	62.2	0.319	0.351	62.1	0.318	0.352	62.4	0.319	0.352	62.4	0.319	0.352
53.7	0.321	0.349	53.3	0.321	0.349	53.4	0.321	0.348	53.7	0.321	0.349	53.7	0.321	0.349

A3.4 Measurements for iPhone10

1			2			3			4			5		
Y	x	y	Y	x	y	Y	x	y	Y	x	y	Y	x	y
173	0.344	0.359	174	0.344	0.359	171	0.344	0.35	173	0.341	0.356	169	0.343	0.358
174	0.345	0.36	170	0.345	0.36	170	0.345	0.362	165	0.345	0.359	172	0.345	0.361
104	0.345	0.351	101	0.345	0.351	99.98	0.345	0.355	100	0.345	0.353	103	0.341	0.352
104	0.345	0.358	104	0.345	0.358	101	0.345	0.352	102	0.346	0.355	101	0.345	0.355
52.1	0.345	0.362	51	0.345	0.362	50	0.344	0.355	52	0.35	0.361	51	0.344	0.361
41.4	0.346	0.358	40	0.346	0.358	42	0.345	0.352	41	0.342	0.358	42.8	0.346	0.359
19.9	0.354	0.362	20.2	0.354	0.362	20.2	0.354	0.36	18.9	0.352	0.361	19.2	0.351	0.362
16.4	0.352	0.352	20.8	0.352	0.352	17.8	0.352	0.354	16.8	0.358	0.355	18	0.35	0.353
6.41	0.36	0.363	6.21	0.36	0.363	4.48	0.362	0.361	5.89	0.358	0.361	6.41	0.361	0.363
19.2	0.355	0.332	19	0.355	0.332	22	0.35	0.338	21	0.352	0.332	19	0.352	0.341
2.07	0.344	0.359	4.01	0.344	0.359	4.08	0.342	0.353	2.1	0.34	0.363	2.07	0.344	0.361
21.5	0.355	0.341	26	0.355	0.341	24	0.351	0.345	22.8	0.352	0.342	21.3	0.353	0.345
20.3	0.349	0.352	22.7	0.349	0.352	24.7	0.34	0.358	20.8	0.351	0.355	20.6	0.351	0.352
28.3	0.35	0.352	24.9	0.35	0.352	28.1	0.353	0.351	28.9	0.352	0.352	26.4	0.35	0.351
86.4	0.342	0.361	88	0.342	0.361	86	0.344	0.358	85	0.345	0.361	88.8	0.344	0.363
145	0.344	0.359	142	0.344	0.359	144	0.345	0.351	142	0.341	0.361	145.5	0.34	0.359
100	0.34	0.366	101.1	0.34	0.366	99.9	0.346	0.361	99	0.344	0.366	101	0.342	0.363
90.8	0.344	0.358	90.5	0.344	0.358	90.1	0.358	0.359	89.9	0.341	0.355	90.3	0.343	0.352

67.4	0.346	0.355	64	0.346	0.355	66.7	0.344	0.351	66.6	0.342	0.352	65	0.345	0.354
29.7	0.346	0.353	27	0.346	0.353	29.4	0.346	0.355	28.8	0.344	0.357	29.6	0.342	0.351

Appendix A4. The steps of calculation of CIECAM.

7. The steps of calculation of CIECAM02 model.

1. Firstly, the measurement using a colour meter for luminance, reference white, background, test colour samples take place to obtain L_A, $L_{A\text{-}bg}$, and X, Y, Z values.
2. View conditions and notations where λ is newly introduced factor in the CAMcc model for the calculation of simultaneous contrast.

Surround	F	C	Nc
Average	1.0	0.69	1.0
Dim	0.9	0.59	0.95
Dark	0.8	0.525	0.8
Luminous computer monitor	0.2	0.41	0.80

L_A	Luminance of reference white in cd/m^2
$L_{A\text{-}bg}$	Luminance of background in cd/m^2
Y_b	Y value for background ranging within [1,100].
Y_w	Y value for reference white and close to 100.

$$k = \frac{1}{5L_A + 1}$$

$$F_L = 0.2k^4(5L_A) + 0.1(1 - k^4)^2(5L_A)^{1/3}$$

$$n = \frac{Y_b}{Y_w}$$

$$N_{bb} = N_{cb} = 0.725(\frac{1}{n})^{0.2}$$

$$z = 1.48 + \sqrt{n}$$

3. Chromatic adaption

$$\begin{bmatrix} R \\ G \\ B \end{bmatrix} = M_{CAT02} \begin{bmatrix} X \\ Y \\ Z \end{bmatrix} \quad \text{(A.1)}$$

$$M_{CAT02} = \begin{bmatrix} 0.7328 & 0.4296 & 0.1624 \\ 0.7036 & 1.6975 & 0.0061 \\ 0.0030 & 0.0136 & 0.9834 \end{bmatrix} \quad \text{(A.2)}$$

$$D = F(1 - \frac{1}{3.6} e^{-\frac{L_a+42}{92}} \quad \text{(A.3)}$$

$$R_c = R\left[D\frac{Y_b}{R_b}\frac{R_w}{Y_w} + 1 - D\right] \quad \text{(A.4)}$$

$$G_c = G\left[D\frac{Y_b}{G_b}\frac{G_w}{Y_w} + 1 - D\right] \quad \text{(A.5)}$$

$$B_c = B\left[D\frac{Y_b}{B_b}\frac{B_w}{Y_w} + 1 - D\right] \quad \text{(A.6)}$$

$$\begin{bmatrix} R' \\ G' \\ B' \end{bmatrix} = M_H M_{CAT02}^{-1} \begin{bmatrix} R_c \\ G_c \\ B_c \end{bmatrix} \quad \text{(A.7)}$$

$$M_{CAT02}^{-1} = \begin{bmatrix} 1.0961 & 0.2788 & 0.1827 \\ 0.4543 & 0.4735 & 0.0720 \\ 0.0009 & 0.0056 & 1.0153 \end{bmatrix} \quad \text{(A.8)}$$

$$M_H = \begin{bmatrix} 0.3897 & 0.6889 & 0.0786 \\ 0.2298 & 1.1834 & 0.0464 \\ 0.0000 & 0.0000 & 1.0000 \end{bmatrix} \quad \text{(A.9)}$$

4. Non-linear Response Compression

$$R'_a = \frac{400\left(\frac{F_L R'}{100}\right)^{0.42}}{27.13+\left(\frac{F_L R'}{100}\right)^{0.42}} + 0.1 \quad \text{(A.10)}$$

$$G'_a = \frac{400\left(\frac{F_L G'}{100}\right)^{0.42}}{27.13+\left(\frac{F_L G'}{100}\right)^{0.42}} + 0.1 \quad \text{(A.11)}$$

$$B'_a = \frac{400\left(\frac{F_L B}{100}\right)^{0.42}}{27.13+\left(\frac{F_L B'}{100}\right)^{0.42}} + 0.1 \quad \text{(A.12)}$$

5. Perceptual attribute correlates

$$a = R'_a - \frac{12G'_a}{11} + \frac{B'_a}{11} \quad \text{(A.13)}$$

$$b = \frac{1}{9}(R'_a + G'_a - 2B'_a) \quad \text{(A.14)}$$

Hue angle:

$$h = tan^{-1}(\frac{b}{a}) \tag{A.15}$$

Eccentricity factor:

$$e_t = \left[\frac{12500}{13} N_c N_{cb}\right]\left[\cos\left(h\frac{\pi}{180} + 2\right) + 3.8\right] \tag{A.16}$$

$$t = \frac{50\left(a^2+b^2\right)^{\frac{1}{2}} 100 e_t \left(\frac{10}{13}\right) N_c N_{cb}}{R'_a + G'_a + \frac{21}{20} B'_a} \tag{A.17}$$

Hue response:

$$H = H_i + \frac{\frac{100(h-h_i)}{e_i}}{\frac{h-h_i}{e_i} + \frac{h_{i+1}-h}{e_{i+1}}} \tag{A.18}$$

where $h_i \leq h < h_{i+1}$ and if $h > h_5$, $h = h - 360$.

	Red	**Yellow**	**Green**	**Blue**	**Red**
i	1	2	3	4	5
h_i	20.14	90	164.25	237.53	380.14
e_i	0.8	0.7	1.0	1.2	0.8
H_i	0	100	200	300	400

Achromatic Response:

$$A = \left[2R'_a + G'_a + \left(\frac{1}{20}\right) B'_a - 0.305\right] N_{bb} \tag{A.19}$$

Lightness:

$$J = 100(\frac{A}{A_w})^{cz} \tag{A.20}$$

where A_w is the A value for reference white.

Brightness:

$$Q = \frac{4}{c}\left(\frac{J}{100}\right)^{0.5}(A_w + 4)F_L^{0.25} \quad \text{(A.21)}$$

where A_w is the A value for reference white.

Chroma:

$$C = t^{0.9}\left(\frac{J}{100}\right)^{0.5}(1.64 - 0.29^n)^{0.73} \quad \text{(A.22)}$$

Colourfulness:

$$M = CF_L{}^{1/4} \quad \text{(A.23)}$$

Saturation:

$$s = 100\sqrt{\frac{M}{Q}} \quad \text{(A.24)}$$

Appendix A5. Demonstrations of lightness enhancement for iPhones with COVID19 x-ray images. Arrows point to COVID features. In theory, enhanced figure (graph (d)) should match (a) that is original image presented in the LCD monitor.

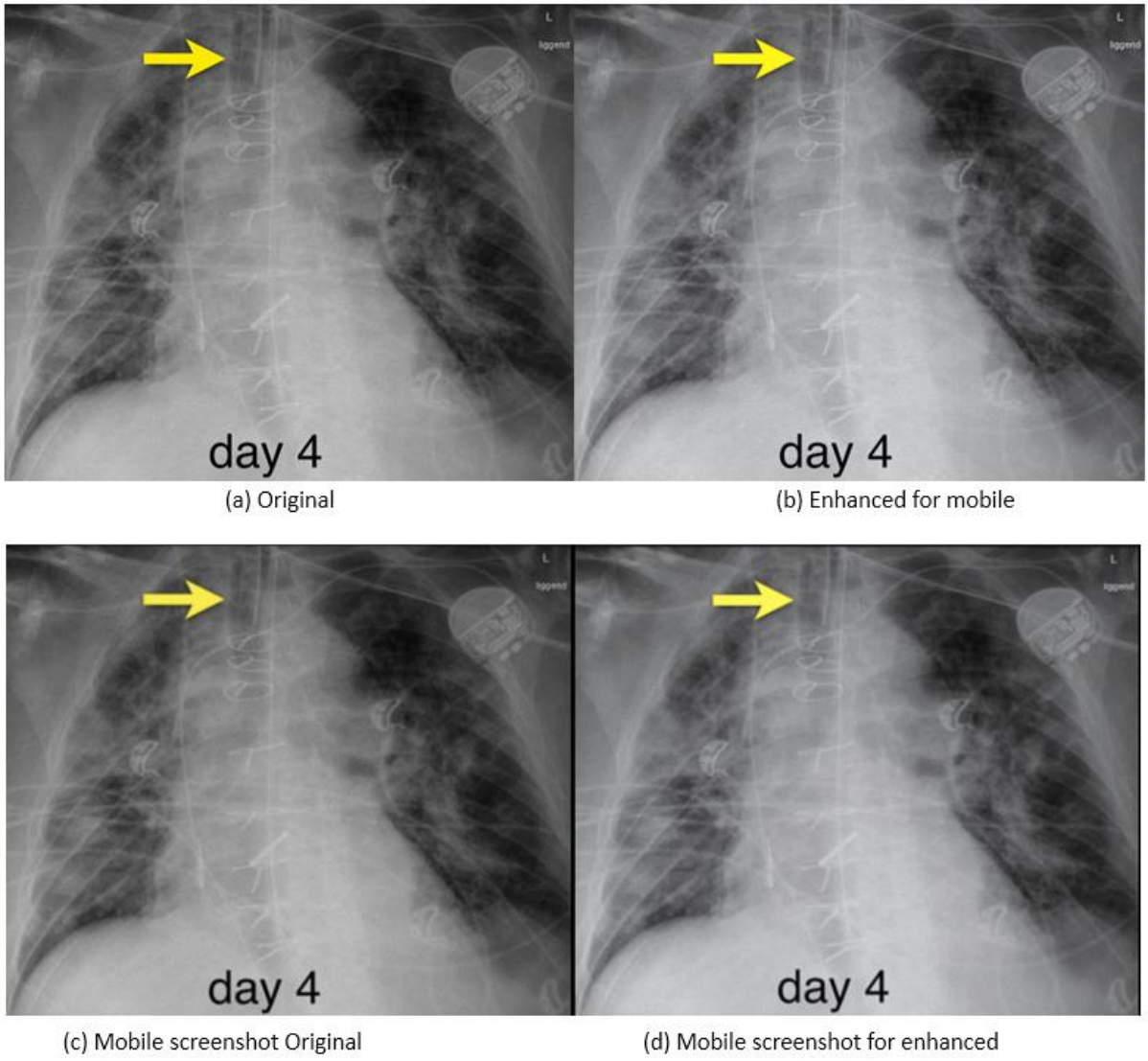

(a) Original (b) Enhanced for mobile

(c) Mobile screenshot Original (d) Mobile screenshot for enhanced

Figure A5.1.

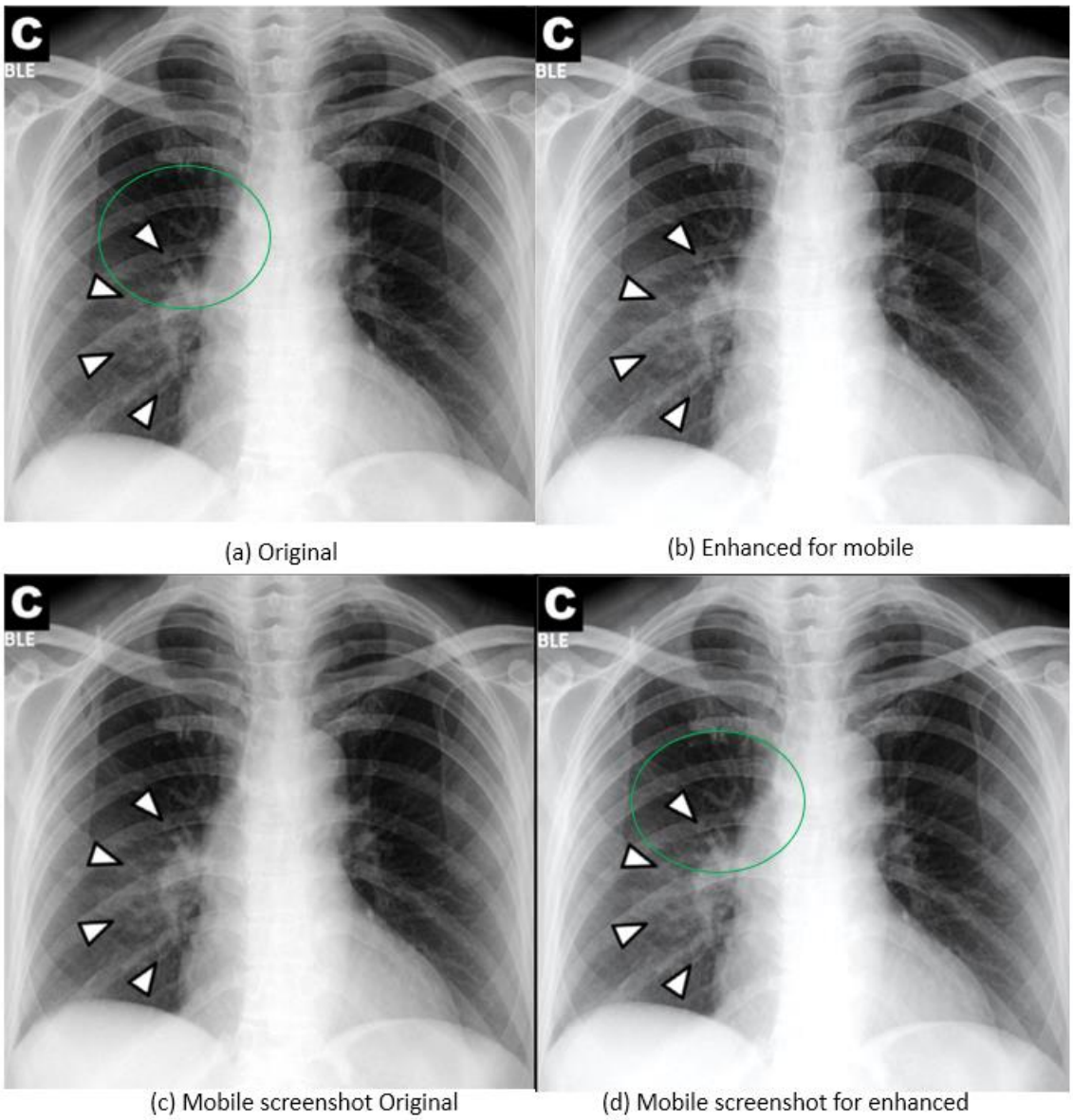

Figure A5.2. iPhone6S

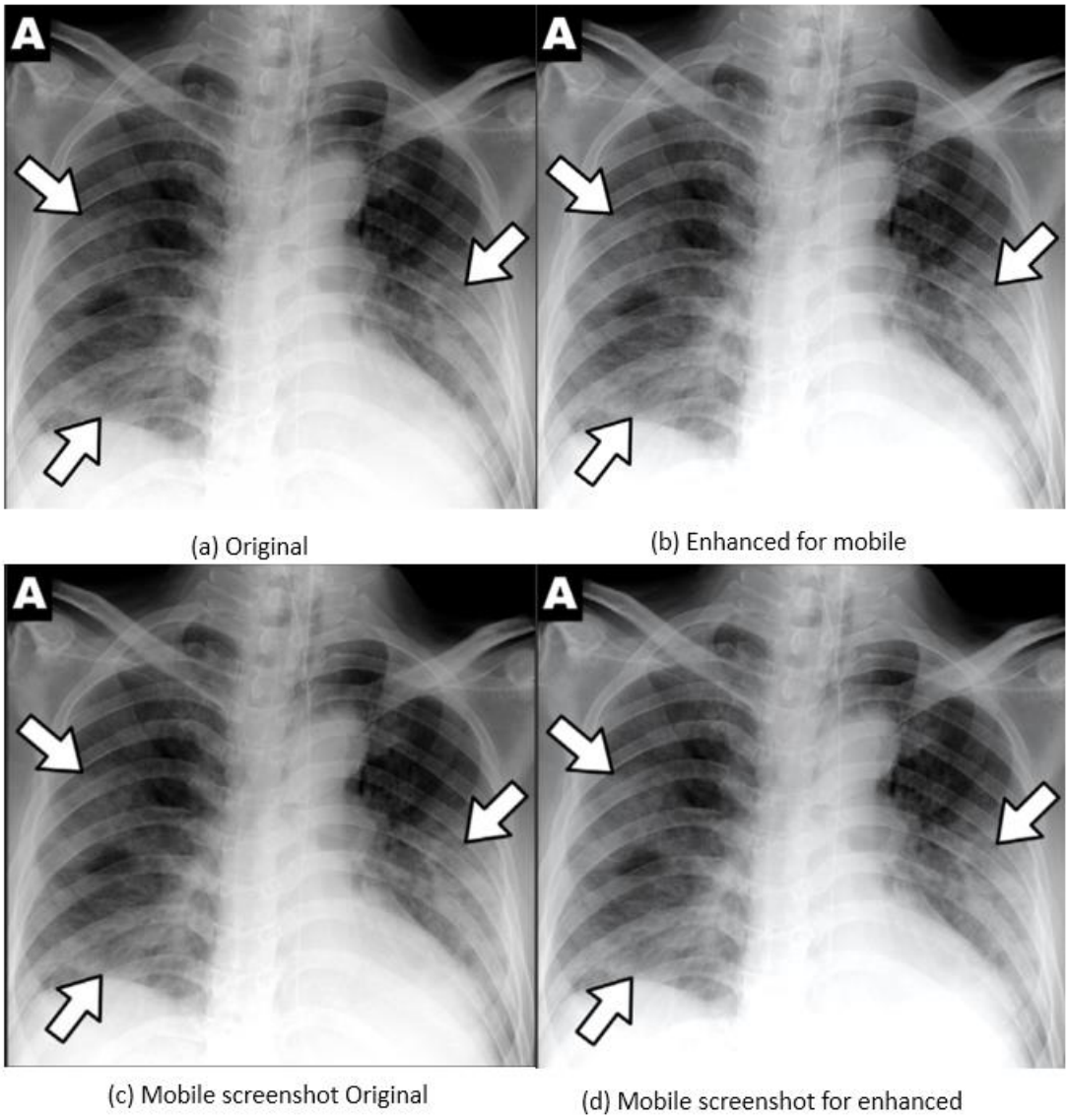

Figure A5.3. iPhone10

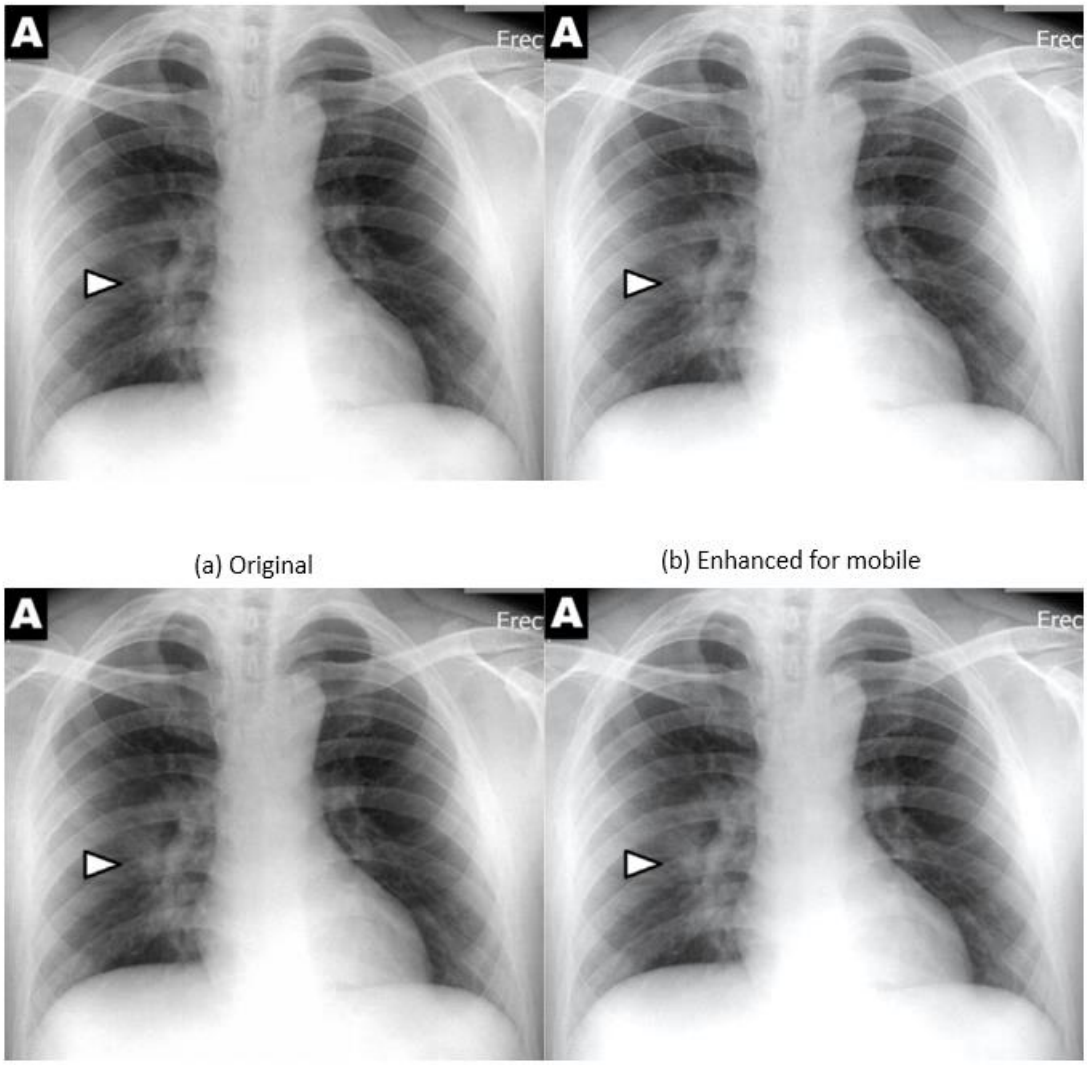

(a) Original

(b) Enhanced for mobile

(c) Mobile screenshot Original

(d) Mobile screenshot for enhanced

Figure A5.4. iPhone 13 Pro.

(a) Original (b) Enhanced Mobile

(c) Original Mobile screenshot (d) Enhanced Mobile screenshot

Figure A5.5

A6. MATLAB code applied to convert RGB to XYZ

```
function xg_get_M_4RGB2XYZ()

rgb0 = double(textread('24-checker-RGB.txt'));
xyz = double(textread('24-checker-XYZ.txt'));

rgb(:,1:3) = rgb0(:,1:3);

R = rgb(:,1);  %y=ground truth, for model = fitcsvm(X,Y)
X = xyz;

sz = [size(R), size(X)]
% XYZ = RGB * M
%opts.POSDEF = true;
[M, dim] = linsolve(rgb,xyz)

R1 = [xyz,rgb * M];
err1 = xyz -rgb*M
```

A7. Submitted paper to AIC2023

MEDICAL IMAGE ENHANCEMENT FOR MOBILE PHONE VIEWING BY APPLYING COLOUR APPEARANCE MODEL CIECAM

Monalisa Soni, Shahedur Rahman, Xiaohong Gao *

Computer Science Department
Middlesex University
London, UK

*Corresponding author: x.gao@mdx.ac.uk

Keywords: Color appearance model CIECAM, mobile phone viewing, medical images, DICOM, grayscale standard display function (GSDF)

Background:
To display a medical image across varying computer monitors, DICOM introduces a grey-scale standard display function (GSDF) to ensure that all monitors are calibrated to the same brightness level, e.g. D65. However, most smart phones do not facilitate this mechanism. This study investigates the feasibility of using a mobile phone to display medical images. As such, colour appearance model CIECAM/CAM16 is applied to enhance displayed medical images in order to entail all the important features depicted in a phone in full. Since most of radiological images are in grey level, this work focuses on the lightness level of an image. Towards this end, a series of psychophysical experiments are conducted on both a LCD monitor and an iphone-6S. These data are then applied to find the right parameters for CIECAM to model these two display platforms. As a result, for prediction of lightness on a mobile phone, the parameter c that indicates the impact of surrounding, should be adjusted to be 0.55 from the original 0.59 in order to produce the best fitting. The evaluation on medical images illustrates clearer patterns on the enhanced images. Future work will include more smartphones as well as the other colour attributes in addition to brightness. Hence This research aims to investigate the feasibility of predicting mobiles' colour behaviour using a standard colour appearance model, CIECAM, to provide a GSDF-equivalent function for smart phones to complement the existing practice.

Experimental:
A series of psychophysical experiments are conducted to estimate the viewing differences when a grey sample presented on both a monitor and an iPhone. In these experiment, a 15" LCD monitor (Dell Latitude E5450 Laptop running windows 10 OS) with resolution of 1366x768 is utilised as well as an iPhone 6S. Twenty test samples are selected trying to cover wider range of brightness. Fourteen observers (7 males and 7 females) with normal colour vision are recruited in this preliminary experiment, who are aged between 19 and 33 with varying professional background (research students, IT professionals, staff). All of them perform one or more experiments after initial training. Before each experiment, the LCD laptop monitor is calibrated to D65 (average daylight) using ColorMunki Smile software. For the iPhone 6S, the brightness is set to the maximum on each phone.

Results:
The result shows a large discrepancy (>20%) occurs on the samples in the middle lightness range, e.g. a lightness of 50% is perceived as 73% on the iPhone. This phenomenon will be further investigated in the future by including more test samples in this range. In general, for medium grey samples, they appear brighter on iPhone-6S than on LCD monitor. To evaluate the perceived differences between two media, CIE colour appearance model CIECAM is applied to predict observers' perception. It appears that parameter c needs to be adjusted for mobile phones in this study. For iPhone6S, the following parameter setting delivers the best results where $c = 0.55$, $Nc = 0.9$, $F = 0.9$, $s = 1$.

Conclusion:
This study investigates the feasibility of applying CIECAM/CAM16 model to enhance medical images to be viewed on smartphones. Psychophysical experiments are conducted to investigate the differences when observers are

viewing lightness between computer monitors and mobile phones. Then these experimental results are applied to enhance CIECAM model by finding the best parameter of c value. The result looks very promising. Future work will include more mobiles and will also study coloured medical images.